



UNIL | Université de Lausanne

Unicentre

CH-1015 Lausanne

<http://serval.unil.ch>

Year : 2013

Molecular genetics of ocular diseases

Venturini Giulia

Venturini Giulia, 2013, Molecular genetics of ocular diseases

Originally published at : Thesis, University of Lausanne

Posted at the University of Lausanne Open Archive.

<http://serval.unil.ch>

Droits d'auteur

L'Université de Lausanne attire expressément l'attention des utilisateurs sur le fait que tous les documents publiés dans l'Archive SERVAL sont protégés par le droit d'auteur, conformément à la loi fédérale sur le droit d'auteur et les droits voisins (LDA). A ce titre, il est indispensable d'obtenir le consentement préalable de l'auteur et/ou de l'éditeur avant toute utilisation d'une oeuvre ou d'une partie d'une oeuvre ne relevant pas d'une utilisation à des fins personnelles au sens de la LDA (art. 19, al. 1 lettre a). A défaut, tout contrevenant s'expose aux sanctions prévues par cette loi. Nous déclinons toute responsabilité en la matière.

Copyright

The University of Lausanne expressly draws the attention of users to the fact that all documents published in the SERVAL Archive are protected by copyright in accordance with federal law on copyright and similar rights (LDA). Accordingly it is indispensable to obtain prior consent from the author and/or publisher before any use of a work or part of a work for purposes other than personal use within the meaning of LDA (art. 19, para. 1 letter a). Failure to do so will expose offenders to the sanctions laid down by this law. We accept no liability in this respect.



UNIL | Université de Lausanne

Faculté de biologie
et de médecine

Département de Génétique Médicale

Molecular genetics of ocular diseases

Thèse de doctorat ès sciences de la vie (PhD)

Présentée à la Faculté de Biologie et de Médecine de l'Université de Lausanne

Par

Giulia Venturini

Diplômée en Biotechnologie Médicale
Université de Florence, Italie

Jury

Prof. Christian Widmann, Président
Dr. Carlo Rivolta, Directeur de thèse
Dr. Carmen Ayuso, Expert
Prof. Sandro Banfi, Expert

LAUSANNE 2013

Imprimatur

Vu le rapport présenté par le jury d'examen, composé de

<i>Président</i>	Monsieur Prof. Christian Widmann
<i>Directeur de thèse</i>	Monsieur Prof. Carlo Rivolta
<i>Experts</i>	Madame Dr Carmen Ayuso
	Monsieur Prof. Sandro Banfi

le Conseil de Faculté autorise l'impression de la thèse de

Madame Giulia Venturini

master en biotechnologie médicale de l' Université de Florence, Italie

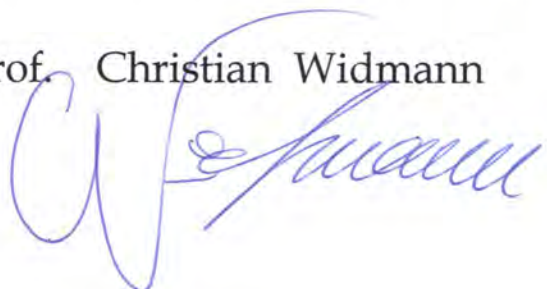
intitulée

Molecular genetics of ocular diseases

Lausanne, le 12 juillet 2013

pour Le Doyen
de la Faculté de Biologie et de Médecine

Prof. Christian Widmann



Merci

Ce travail de thèse a été réalisé entre Février 2009 et Juin 2013 au sein du Département de Génétique Médicale de l'Université de Lausanne, dans le groupe du Dr. Carlo Rivolta.

Je voudrais d'abord remercier le Dr. Carlo Rivolta de m'avoir accueillie dans son groupe de recherche et de m'avoir donnée la confiance nécessaire pour mener indépendamment les projets de recherche dans lesquels j'ai été impliquée. Je tiens également à remercier tous les membres passés et présents de son équipe de recherche, Alessandro, Paola, Hanna, Adri, Goranka, Laurent, Natacha, Petra, Stephanie, Alexandra, Koji, Pietro, Kostas, et Rosanna, pour avoir créé une ambiance si agréable et pour avoir contribué chacun différemment à la réussite de ma thèse. Merci à tous les autres membres du Département de Génétique Médicale et en particulier à Hanna, Chrysanthi, Estelle et Nadya pour leur amitié et leur soutien au cours de ces années.

Je tiens également à remercier le Dr. Eliot L. Berson du Massachussets Eye and Ear à Boston, une personne d'une grande expérience et disponibilité, avec qui cela a été un plaisir de travailler.

Merci au Dr. Alexandre Moulin de l'Hôpital Ophtalmique Jules-Gonin à Lausanne qui m'a appris beaucoup de choses sur les tumeurs de l'œil et avec qui il a toujours été intéressant de discuter.

Merci également au Professeur Shomi S. Bhattacharya et ses Post-Doctorants Anna M. Rose et Amna Z. Shah de l'University College à Londres pour leur contribution au projet de PRPF31.

Je remercie également les Professeurs C. Widmann et S. Banfi ainsi que le Dr. C. Ayuso pour leur participation à mon jury de thèse.

Mes plus grands remerciements vont à mes parents et à ma soeur, qui m'ont toujours encouragée afin d'atteindre mes objectifs.

Merci à mes amis de Florence, Sara, Anna, Susy, Gine, Caro, Ire, Silvia, Giulia et Cate, et tous les amis que j'ai rencontré à Lausanne, en particulier Francesca, Loredana, Anna, Sev & Lolo, Carmen & Alberto, Vlasta, Hadi, Caroline, Stefano, Danilo, avec qui j'ai passé de bons moments.

Enfin, merci à l'amour de ma vie, Luca, pour son soutien inconditionnel.

Abstract

The eye is a complex organ, which provides one of our most important senses, sight. The retina is the neuronal component of the eye and represents the connection with the central nervous system for the transmission of the information that leads to image processing.

Retinitis pigmentosa (RP) is one of the most common forms of inherited retinal degeneration, in which the primary death of rods, resulting in night blindness, is always followed by the loss of cones, which leads to legal blindness. Clinical and genetic heterogeneity in retinitis pigmentosa is not only due to different mutations in different genes, but also to different effects of the same mutation in different individuals, sometimes even within the same family.

My thesis work has been mainly focused on an autosomal dominant form of RP linked to mutations in the *PRPF31* gene, which often shows reduced penetrance. Our study has led to the identification of the major regulator of the penetrance of *PRPF31* mutations, the CNOT3 protein, and to the characterization of its mechanism of action.

Following the same rationale of investigating molecular mechanisms that are responsible for clinical and genetic heterogeneity of retinitis pigmentosa, we studied a recessive form of the disease associated with mutations in the recently-identified gene *FAM161A*, where mutations in the same gene give rise to variable clinical manifestations. Our data have increased the knowledge of the relationship between genotype and phenotype in this form of the disease.

Whole genome sequencing technique was also tested as a strategy for disease gene identification in unrelated patients with recessive retinitis pigmentosa and proved to be effective in identifying disease-causing variants that might have otherwise failed to be detected with other screening methods.

Finally, for the first time we reported a choroidal tumor among the clinical manifestations of *PTEN* hamartoma tumor syndrome, a genetic disorder caused by germline mutations of the tumor suppressor gene *PTEN*. Our study has highlighted the heterogeneity of this choroidal tumor, showing that genetic and/or epigenetic alterations in different genes may contribute to the tumor development and growth.

Résumé

L'œil est un organe complexe, à l'origine d'un de nos sens les plus importants, la vue. La rétine est la composante neuronale de l'œil qui constitue la connexion avec le système nerveux central pour la transmission de l'information et qui conduit à la formation des images.

La rétinite pigmentaire (RP) est une des formes les plus courantes de dégénérescence rétinienne héréditaire, dans laquelle la mort primaire de bâtonnets, entraînant la cécité nocturne, est toujours suivie par la perte de cônes qui conduit à la cécité complète. L'hétérogénéité clinique et génétique dans la rétinite pigmentaire n'est pas seulement due aux différentes mutations dans des gènes différents, mais aussi à des effets différents de la même mutation chez des individus différents, parfois même dans la même famille.

Mon travail de thèse s'est principalement axé sur une forme autosomique dominante de RP liée à des mutations dans le gène *PRPF31*, associées souvent à une pénétrance réduite, me conduisant à l'identification et à la caractérisation du mécanisme d'action du régulateur principal de la pénétrance des mutations: la protéine CNOT3.

Dans la même logique d'étude des mécanismes moléculaires responsables de l'hétérogénéité clinique et génétique de la RP, nous avons étudié une forme récessive de la maladie associée à des mutations dans le gène récemment identifié *FAM161A*, dont les mutations dans le même gène donnent lieu à des manifestations cliniques différentes. Nos données ont ainsi accru la connaissance de la relation entre le génotype et le phénotype dans cette forme de maladie.

La technique de séquençage du génome entier a été ensuite testée en tant que stratégie pour l'identification du gène de la maladie chez les patients atteints de RP récessive. Cette approche a montré son efficacité dans l'identification de variantes pathologiques qui n'auraient pu être détectées avec d'autres méthodes de dépistage.

Enfin, pour la première fois, nous avons identifié une tumeur choroïdienne parmi les manifestations cliniques du *PTEN* hamartoma tumor syndrome, une maladie génétique causée par des mutations germinales du gène suppresseur de tumeur *PTEN*. Notre étude a mis en évidence l'hétérogénéité de cette tumeur choroïdienne, montrant que les altérations génétiques et/ou épigénétiques dans les différents gènes peuvent contribuer au développement et à la croissance tumorale.

Table of contents

Table of contents	3
Chapter 1	5
Introduction	5
1.1 <i>Anatomy and physiology of the human eye</i>	6
1.1.1 <i>General anatomy of the eye</i>	6
1.1.2 <i>Physiological processes in the eye</i>	10
1.2 <i>Inherited and multifactorial forms of photoreceptor degeneration</i>	13
1.3 <i>Retinitis pigmentosa</i>	16
1.3.1 <i>Clinical and pathological features</i>	16
1.3.2 <i>Genetic causes</i>	18
1.3.3 <i>Therapeutic approaches</i>	20
1.4 <i>Clinical and genetic heterogeneity in retinitis pigmentosa</i>	23
1.4.1 <i>Autosomal dominant forms with reduced penetrance</i>	23
1.4.2 <i>Autosomal recessive forms</i>	28
1.5 <i>Genomics technologies and disease gene identification strategies</i>	31
References	33
Chapter 2	39
<i>CNOT3 is a modifier of PRPF31 mutations in retinitis pigmentosa</i>	39
with incomplete penetrance	39
2.1 <i>Additional experiments (unpublished results)</i>	53
2.1.1 <i>CNOT3 mRNA expression in two other families with PRPF31-linked autosomal dominant retinitis pigmentosa showing incomplete penetrance</i>	54
2.1.2 <i>CNOT3 polymorphic alleles in an additional pedigree of PRPF31-linked autosomal dominant retinitis pigmentosa showing incomplete penetrance</i>	56
2.1.3 <i>microRNA expression analysis in the asymptomatic and affected individuals of the RP856/AD5 family</i>	57
2.1.4 <i>Expression of other splicing factors in families with PRPF31-linked autosomal dominant retinitis pigmentosa showing incomplete penetrance</i>	59
2.1.5 <i>Effect of CNOT3 on the transcription of other splicing factors</i>	60
2.1.6 <i>CNOT3 binding to the promoter of the other splicing factors</i>	62
2.1.7 <i>CNOT2 expression in the RP856/AD5 family and effect of CNOT2 on PRPF31 transcription</i>	63
References	64
Chapter 3	65
<i>FAM161A mutations in patients with early-onset retinitis pigmentosa</i>	65
in North America	65
Introduction	68
Methods	69
Results	70
Discussion	72
References	73
Chapter 4	78
A 353-bp Alu insertion in <i>MAK</i> is a prevalent cause of	78
recessive retinitis pigmentosa in North American Jewish patients	78
Introduction	81
Methods	82
Results	83
Discussion	84
References	86

Chapter 5	90
Genome-wide sequencing to identify disease-causing mutations.....	90
in patients with recessive retinitis pigmentosa.....	90
Introduction.....	93
Methods.....	94
Results.....	96
Discussion.....	99
References.....	101
Chapter 6	106
Clinicopathologic and molecular analysis of a choroidal pigmented schwannoma in the context of a <i>PTEN</i> hamartoma tumor syndrome.....	106
Chapter 7	119
Discussion.....	119
References.....	124
Other collaborations	126
Abbreviations	127

Introduction

The eye is a complex organ composed of different tissues and cell types that work in a coordinated manner to provide one of our most vital senses, sight.

The retina is an essential component of the eye, since it represents the connection with the central nervous system for the transmission of information that leads to image processing.

Among the neuronal cells that make up the retina, photoreceptors are the photosensitive cells that respond to different wavelengths of light providing both colour vision and vision in the dark. Despite reduction in the number of photoreceptor cells is a physiological process at old age, progressive death of these cells may be associated with hereditary degenerative disorders of the retina.

The first chapter summarizes the anatomical organization of the various tissues in the eye with particular emphasis to the retina.

Inherited forms of photoreceptor degeneration are introduced, and clinical and genetic features of one of the most common form, called retinitis pigmentosa, are described.

Autosomal dominant retinitis pigmentosa with reduced penetrance linked to mutations in the gene *PRPF31* is introduced in order to facilitate comprehension of chapter 2, which covers the main results obtained during my thesis work.

Then, recessive forms of the disease associated with mutations in the recently identified genes *FAM161A* and *MAK* are presented in order to prepare for chapters 3 and 4.

Finally, technical advances in massively parallel sequencing are discussed, with a particular emphasis to whole genome sequencing technique that has been used in chapter 5 as a strategy for disease gene identification in retinitis pigmentosa patients.

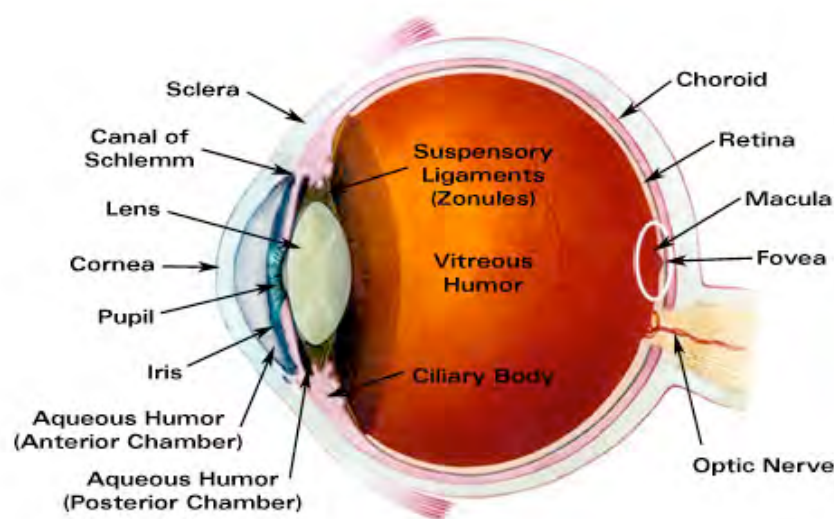
1.1 Anatomy and physiology of the human eye

1.1.1 General anatomy of the eye

The eye is one of the most perfect and complex organ of the human body. Its function is to process the light that is emitted or reflected from the surroundings objects allowing us to perceive the shapes and colours of objects.

In the human eye we can distinguish three different anatomical structures, called tunics [1-2] (Figure 1):

- The fibrous tunic is the outermost layer, which is composed by the cornea and the sclera. The cornea is a transparent layer, while the sclera is a collagen-rich connective tissue, which gives the white colour to the eye and supports the eyeball shape.
- The vascular tunic is the central layer, which is formed by the choroid, the ciliary body and the iris. The choroid is a connective tissue that provides nourishment and oxygen to the retinal cells. The ciliary body is responsible for the production of the aqueous humor, which is vital for the maintenance of normal intraocular pressure and to bring nutrients to the lens and the cornea. The iris is the diaphragm of the eye, with the pupil being its central opening; it also regulates the flow of fluid inside the eye.
- The nervous tunic is the innermost layer, which is constituted by the retina, the essential component of the eye for the process of photoreception.



Source: www.laramyk.com

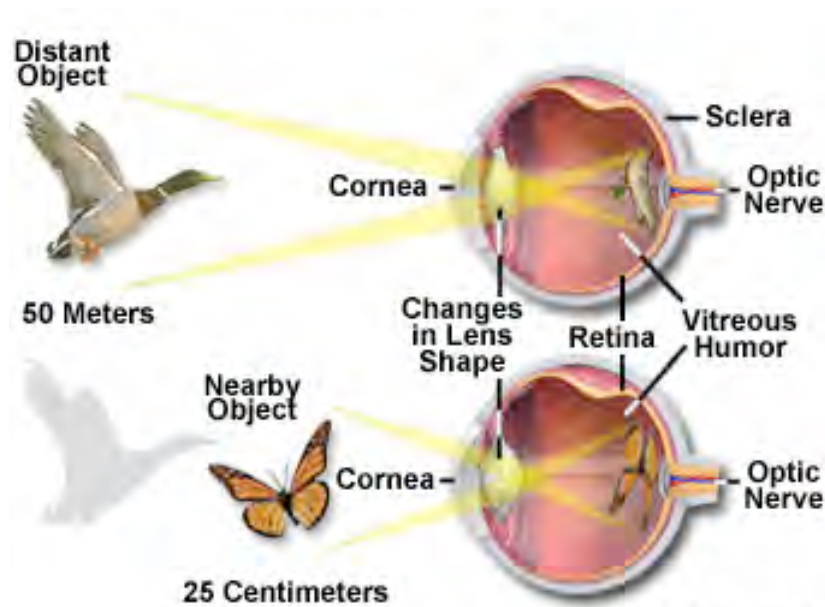
Figure 1. *Simplified anatomy of the human eye.*

The shape of the eye is not exactly that of a sphere, but rather that of two combined spheres, a smaller and more curved one at the front and a larger and less curved one in the back.

The anterior part of the eye is constituted by the cornea, the iris, the ciliary body and the lens, while the posterior part is composed by the vitreous humor, the retina, the choroid, and the optic nerve (Figure 1).

The size of the eye is rather constant, varying only 1-2 millimetres among humans; the average vertical diameter of a human eye is 24 millimetres, which is usually smaller than the transverse diameter.

The lens is a transparent avascular structure that is semi-permeable to water and electrolytes. Since the depth of field of the mammalian eye is limited, the curvature of the lens needs to be adjusted so that, in order to focus on nearby objects, the lens becomes thicker and rounder, while for distant objects it gets flatter. This process is known as accommodation, and the ability of the lens to accommodate for near objects decreases with age [2] (Figure 2).



Source: zeiss-campus.magnet.fsu.edu

Figure 2. Accommodation of the human eye.

Light coming from an object first encounters the cornea, which allows light to enter the eye and to proceed through the pupil that can adapt to different intensities of light by changing its dimensions; in case of bright light the pupil gets smaller, while it dilates in dark conditions. Behind the pupil the

light waves converge on the lens, where the image is turned backwards and upside-down (Figure 2). Through the vitreous humor, a transparent gel that constitutes almost the 80% of the total volume of the eye, the light finally is focused on the retina. Within the different retina layers light is processed into electric signals that are then sent through the optic nerve to the occipital cortex of the brain, where they are elaborated as a visual image.

The retina is the innermost tissue of the eyeball, which surrounds the vitreous cavity and is protected and kept in its correct location by the sclera and the cornea.

It is the neural tissue of the eye and actually a component of the central nervous system despite its peripheral location [3].

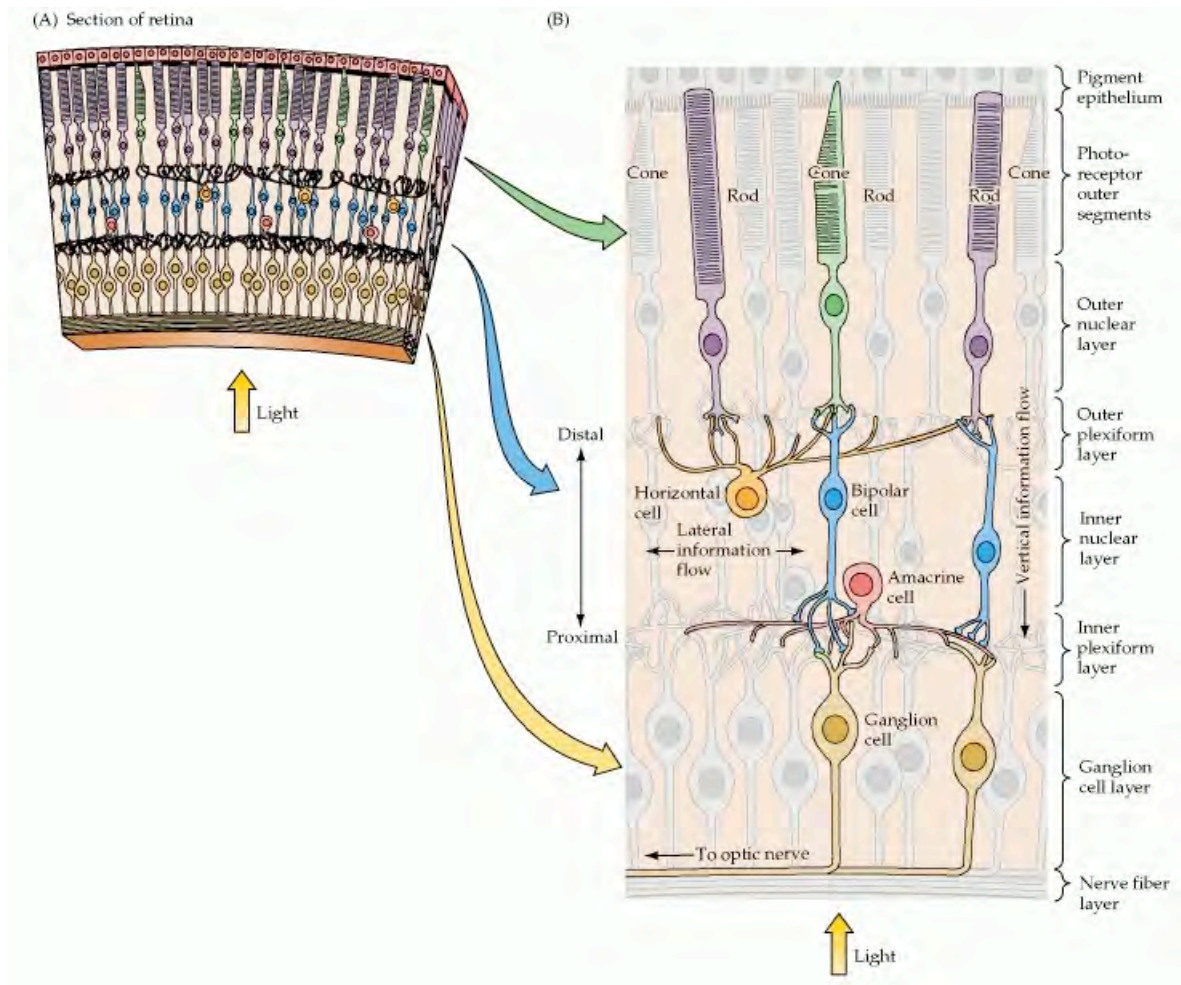
In the retina we can distinguish five major types of neurons: photoreceptors, bipolar cells, amacrine cells, horizontal cells and ganglion cells.

Retinal neurons are arranged in parallel layers, three of which consist of neuronal-cell bodies and two are synaptic layers (Figure 3):

- The outer nuclear layer (ONL) contains the nuclei of photoreceptor cells.
- The outer plexiform layer (OPL) is where photoreceptors interact with bipolar and horizontal cells.
- The inner nuclear layer (INL) contains the nuclei of amacrine, horizontal and bipolar cells.
- The inner plexiform layer (IPL) is where bipolar and amacrine cells interact with synapses of ganglion cells.
- The ganglion cell layer (GCL) contains the nuclei of ganglion cells.
- The nerve fiber layer (NFL) is where there are the axons of ganglion cells.

Overlying all these layers there is the retinal pigment epithelium (RPE), which is composed of hexagonal cells interacting with the choroid on one side and with photoreceptors on the other.

The RPE provides nourishment and support to the photoreceptors, as well as eliminates their metabolic wastes by phagocytosis. The latter represents a major task considering that photoreceptor discs in their outer segment are replaced every 12 days [3]. In addition, the RPE is even able to regenerate the photopigments (the pigments involved in photoreception) after they have been exposed to light [3].



Source: Purves *et al.* [3]

Figure 3. Cross section of the retina with the retinal layers.

In the retina of most vertebrates there are two types of photoreceptor cells, rods and cones, which are structurally similar, but respond to different light intensities and are differentially distributed in the retina.

Both cells have an outer segment where photopigments are accumulated within membranous discs and which is in contact with the RPE, and an inner segment, which contains the cell nucleus, and from where the synapses that then make contacts with bipolar and horizontal cells derive [3].

Cones are mainly located in the fovea, a dip in the macula (the central part of the retina), directly behind the lens, which is responsible for sharp central vision due to the largest concentration of cones there. Rods are not present in the fovea, but are mostly distributed at the outer edges of the retina.

There are three different types of cones (S, M, and L cones) that respond to different wavelengths of light to provide colour vision.

Higher visual acuity of cone cells depends on the fact that each of them makes contact with a single bipolar cell, while several rod cells interact with a single bipolar cell (Figure 3).

Rods are conversely highly more sensitive than cones to photons of light and are responsible for vision in dark conditions, but do not provide colour vision.

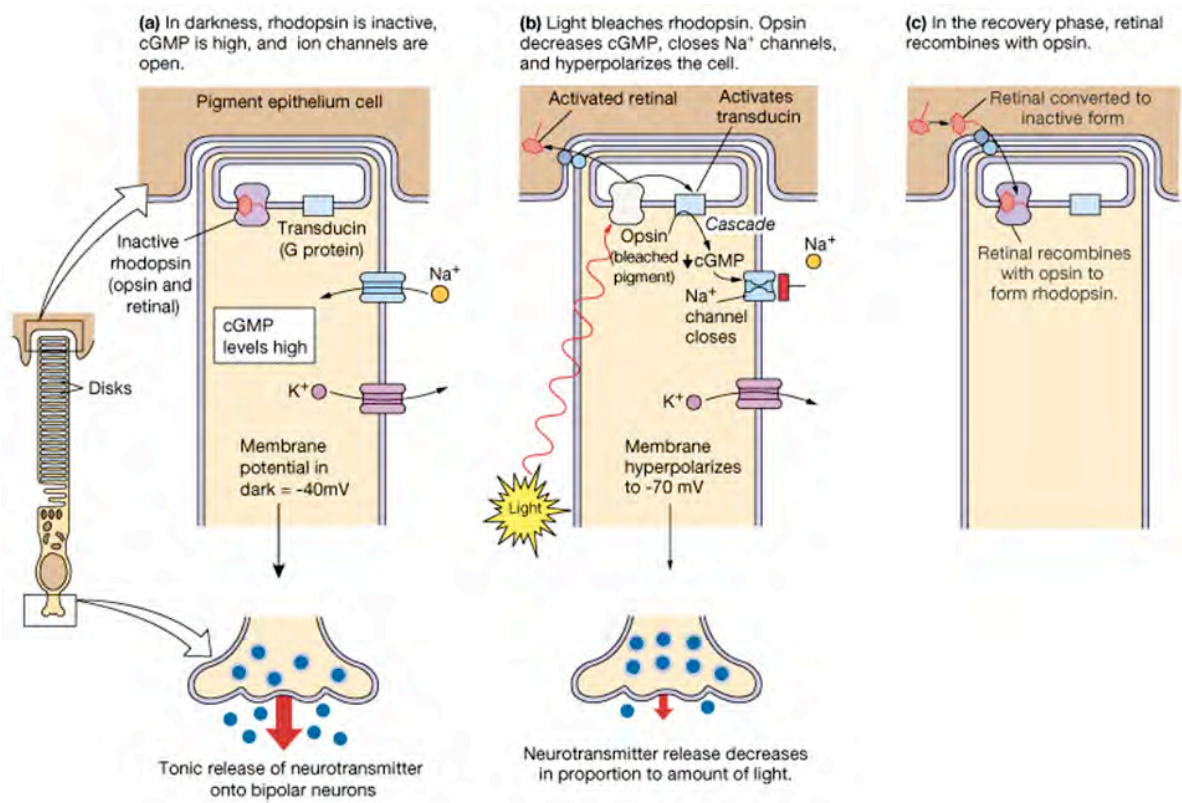
In the human retina there is also a third small class of photosensitive cells, represented by the intrinsically photosensitive retinal ganglion cells (ipRGCs). Unlike photoreceptors, they are probably not involved in vision, but regulate circadian rhythms of light-dark cycles, control the pupillary light responsiveness, and the light-regulated melatonin release by the pineal gland [4].

1.1.2 Physiological processes in the eye

The process through which the light is converted into biological signals within the retina is called phototransduction. In daylight conditions photoreceptors respond to light thanks to the photopigments they contain in their outer segment discs [5] (Figure 4).

These molecules are constituted by a cell membrane protein, called opsin, and the retinal, a chromophore derived from vitamin A that is reversibly bound to it. In both rods and cones the chromophore is the same but the protein moiety changes. Rod photopigment is called rhodopsin, while cones have three different opsins that are able to absorb light with short, medium and long wavelengths.

Light isomerizes the retinal from an 11-*cis* to an all-*trans* conformation, leading to separation of the retinal from the opsin. Through the activation of a cascade of proteins, the second messenger cyclic guanosine monophosphate (cGMP) is hydrolyzed, the ion channels on the photoreceptor membranes are closed, thus the membrane hyperpolarizes to -70mV, leading to a decrease in the release of the neurotransmitter glutamate [5-6] (Figure 4).



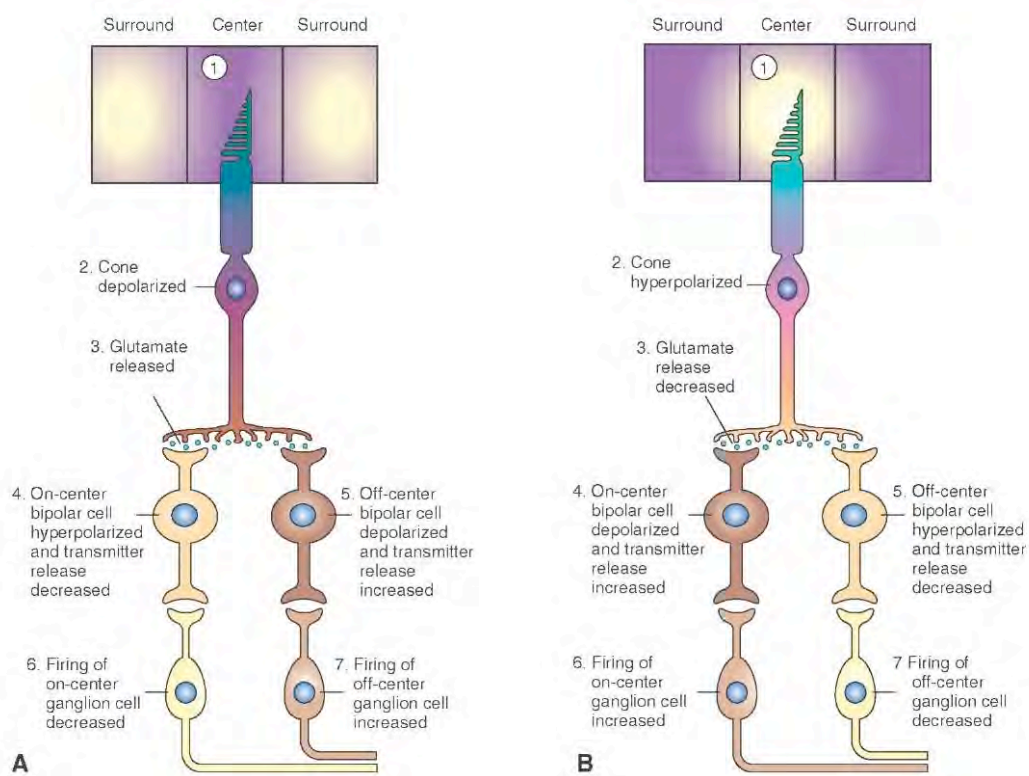
Source: faculty.pasadena.edu

Figure 4. Phototransduction in rods.

Subsequently, the all-*trans* retinal and the intermediate of opsin are transformed back into 11-*cis* retinal and opsin (Figure 4).

Conversely, under dark conditions, the cGMP is accumulated in the discs of photoreceptor cells where it allows the influx of cations, especially sodium, through the ion channels, which in turn leads to a constant release of glutamate onto bipolar neurons [7] (Figures 4 and 5).

The main route through which information passes from the photoreceptors to the optic nerve is the direct contact between three types of neurons (photoreceptors to bipolar cells to ganglion cells) [3] (Figure 3). Bipolar cells respond to the chemical signal coming from the photoreceptors through different glutamate receptors [7] (Figure 5). The OFF-center bipolar cells have excitatory synapses with photoreceptor cells, while the ON-center bipolar cells have inhibitory synapses. These parallel bipolar cell channels allow us to perceive the contrast between images and their background [7].



Source: what-when-how.com/neuroscience

Figure 5. Response properties of bipolar and ganglion cells to light and dark conditions.

Two types of ganglion cells communicate with ON- and OFF-center bipolar cells: the ON-center ganglion cells that are activated by light targeting the center of their receptive field and the OFF-center ganglion cells that are activated by light targeting the periphery of their receptive field [7] (Figure 5).

Lateral interactions within the retina are indeed mediated by two other types of neurons, the horizontal and amacrine cells, whose cell bodies are located in the INL [3] (Figure 3).

The axon terminals of horizontal cells interact with photoreceptor cells, producing a surround effect that enhances brighter contrast depending on the background (Figure 3).

Amacrine cells make contacts with bipolar and ganglion cells, providing not only lateral but also vertical connections between cells (Figure 3).

1.2 Inherited and multifactorial forms of photoreceptor degeneration

In the retina of a healthy individual loss of photoreceptor cells with age is a physiological mechanism, with an average of 30% of cell death in a 80-year-old person [8].

Pathological photoreceptor degeneration indeed can be considered as a complex trait, since it is caused not only by mutations in different genes, but also by the contribution of environmental factors [9].

Despite not being a homogeneous group of diseases, photoreceptor degenerations have in common that the primary or secondary event leading to loss of vision is the premature death of photoreceptor cells [9].

Inherited forms of photoreceptor degeneration (except AMD) are usually monogenic and rare disorders (minor allele frequency < 0.01), having an average prevalence of 1/3000 individual (reviewed in [9]).

Retinitis pigmentosa (RP) is the most common type of retinal degeneration, affecting approximately 1/4000 individual worldwide (reviewed in [10-12]). It is a clinically and genetically highly heterogeneous disease, whose initial feature is poor night vision due to rod dysfunction in early or middle life, which invariably leads to a secondary cone dysfunction.

Leber congenital amaurosis (LCA) is the most severe form of retinal degeneration, with photoreceptors that are lost within the first years of life, or are already dead at birth. Different mutations in genes that cause LCA can also be responsible for the pathogenesis of RP and other retinal dystrophies, depending on the severity of the variants.

Cone degenerations are not uncommon forms in which all three types of cones are lost, while rods are preserved. The end stage of the disease is rod monochromacy, known as achromatopsia, that is when exclusively rods mediate vision.

Cone-rod degenerations are characterized by the primary degeneration of cones, followed by the secondary loss of rods. Retinal pigment deposits are present predominantly in the macula. Decreased visual acuity and colour vision defects appear in the early stages, followed by loss of the peripheral vision and night blindness in the later stages. The clinical course of the disease is usually more severe and rapid than the one observed in rod-cone degenerations.

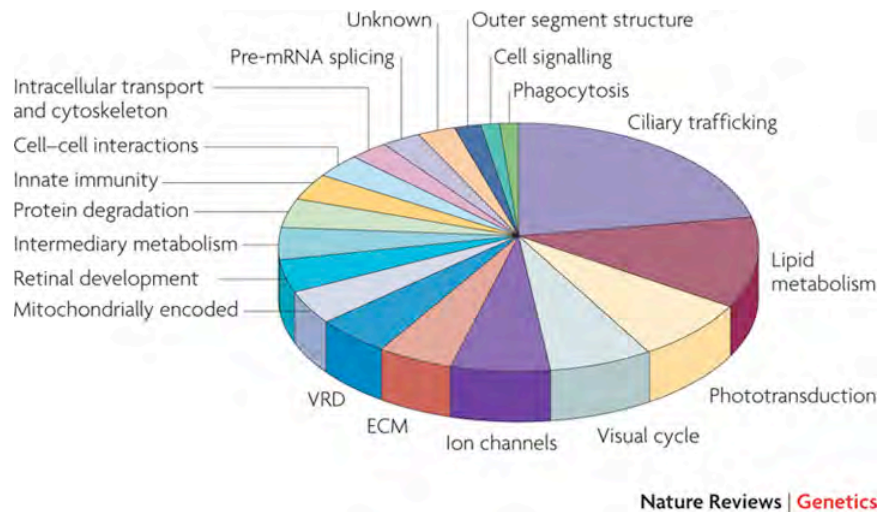
Inherited macular degenerations represent a large number of relatively rare retinal degenerations that affect photoreceptor cells in the macula. They usually occur at early to middle age and are characterized by gradual loss of visual acuity, colour vision and contrast sensitivity [13].

Inherited retinal degenerations can occur alone or even in the context of more complex syndromes that present extra-ocular manifestations.

Usher syndrome is the most frequent form of syndromic retinitis pigmentosa, where early or congenital hearing impairment is associated with early onset RP [11, 14]. According to the type of mutation, some genes that cause Usher syndrome can cause either only retinitis pigmentosa or hearing loss [15-16].

Bardet-Biedl syndrome is another syndromic form of RP, whose clinical features, such as obesity, polydactyly, hypogenitalism, cognitive impairment, and renal disease, are variably associated with retinitis pigmentosa. The inheritance pattern is usually autosomal recessive, even if in some families compound heterozygosis or homozygosis at one gene locus has been found together with a heterozygous mutation at a second gene locus, which is indicative of triallelic-digenism (reviewed in [11, 17]).

Most of the genes that contribute to the inherited forms of photoreceptor degeneration account only for a small fraction of cases and these are essential genes not only for photoreceptor-specific functions, such as the visual cycle and phototransduction, but also for general cellular functions, such as mRNA splicing, protein degradation, and many others (Figure 6).



Source: Wright, A.F. *et al* [9]

Figure 6. Pathways responsible for photoreceptor degeneration.

Among the multifactorial form of photoreceptor degeneration *age-related macular degeneration* (AMD) represents the leading cause of blindness in the Western countries, with a prevalence that rises exponentially with age [9]. Typical features of the disease are lipid and protein deposits, called drusen of the macula, that lead to macula degeneration. There are two distinct manifestations of the disease, a dry form and a wet form due to abnormal blood vessels into the macula. Several studies have shown that AMD is a complex trait, with multiple susceptibility genes and environmental factors that could contribute to the risk of developing the disease, but monogenic forms could be rare (reviewed in [9]).

1.3 Retinitis pigmentosa

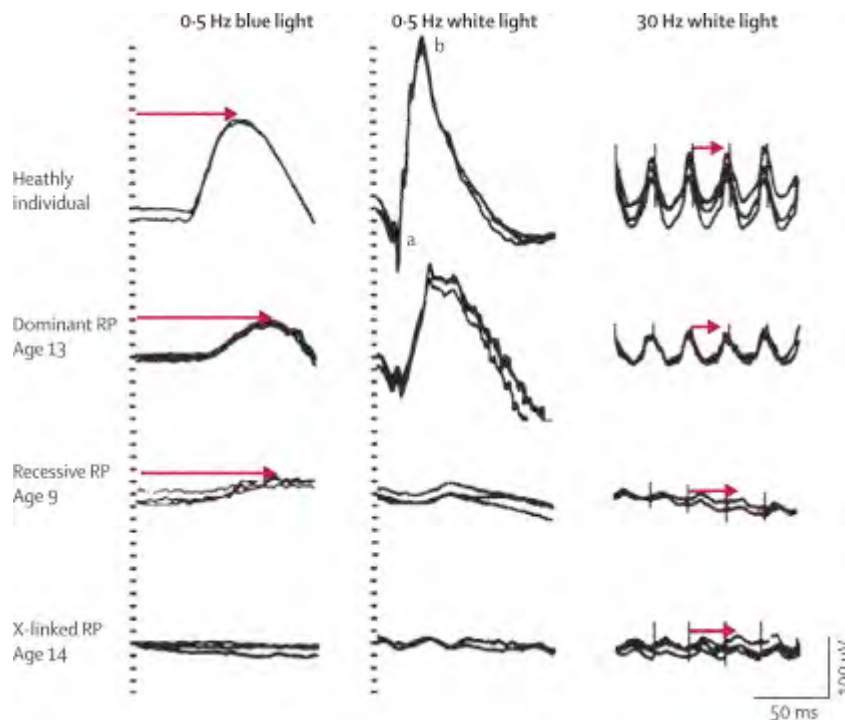
1.3.1 Clinical and pathological features

Retinitis pigmentosa is the most common inherited form of photoreceptor degeneration, which is characterized by pigmented deposits in the periphery of the retina, and by a primary degeneration of rod photoreceptors.

The course of the disease often involves several decades, even if there are exceptional cases of rapid evolution or of very slow progression of the disease.

The electroretinogram (ERG) is a powerful tool to measure the electrical responses of the retina to standardized stimuli (flashes of light), and it is routinely used for the diagnosis of various retinal diseases, included RP [18]. A single dim blue light flash stimulates a rod response, a single brighter white light flash stimulates a rod-cone response, and a flickering white light stimulus enhances a cone response. With single flashes of white light there is first a hyperpolarization of the photoreceptors (represented by the a wave), followed by the depolarization of the same cells (represented by the b wave) (Figure 7). Patients with retinitis pigmentosa show reduced amplitude of both rod and cone responses, as well as a delayed timing [19] (Figure 7). The clinical usefulness of ERG for RP patients is not only in detecting individuals with retinitis pigmentosa within a family, but especially in identifying healthy relatives of affected subjects. The results obtained from studies of siblings in families with RP show that ERG results follow Mendel's law of inheritance [12].

Optical coherence tomography is another technique that can be useful for evaluating the retinal morphology, in particular to look at the photoreceptor cell layer without being invasive [20]. Usually the remaining photoreceptors in RP patients present a shorter outer segment but have an intact cell body. Despite being reduced in cell number and having a reduced quantity of visual pigments they are therefore still functional [12].



Source: Hartong, D.T. *et al* [11]

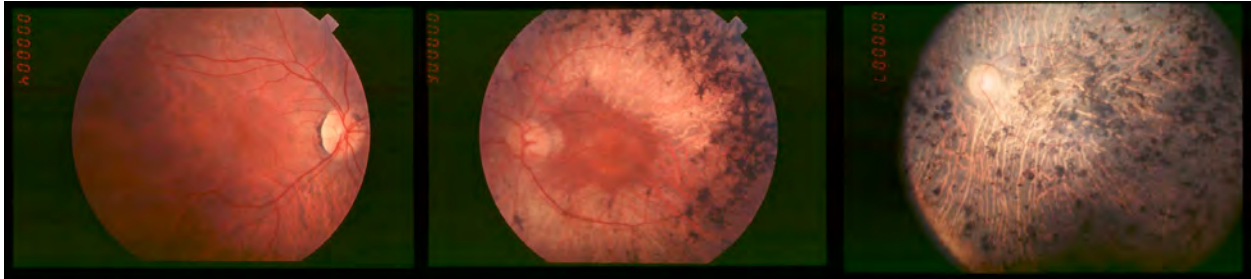
Figure 7. ERG responses in a healthy individual and in RP patients with different mode of inheritance.

In *early RP stages* patients first complain about night blindness, and ERG could reveal decreased amplitude of the b-wave that originates in retinal cells that are post-synaptic to the photoreceptors under low light conditions (the so called scotopic vision) [10, 12]. Anomalies in ERG responses can even be detected years before the onset of clinical symptoms [12].

In this early phase of the disease, retinal pigments are usually not yet present, and visual acuity and colour vision are normal [11-12] (Figure 8).

In *mid RP stages* patients experience the loss of peripheral visual field in daylight conditions, a reduction in cone sensitivity, and possibly macular involvement (i.e. macular edema) [12]. Cataracts is often present, together with refractive errors, like myopia and astigmatism [12]. Bone-spicule-shaped pigment deposits appear at this stage in the mid periphery, along with atrophy of the retina, and can be revealed by fundus examination [10-11] (Figure 8). These pigment deposits originate from the retinal pigment epithelium that invades the neural retina in response to photoreceptor cell

death [11]. ERG at this stage does not record any response from rods in scotopic conditions, while cone responses are hypovolted [10].



Source: Hamel, C. [10]

Figure 8. *Fundus examination of an RP patient, from early to mid and end stage (panels from the left to the right).*

In *end RP stages* peripheral vision is completely lost (classical tunnel vision) and fundus examination shows that pigmentation has invaded even the center of the retina, retinal vessels became thin and the optic disc is pale [10-12] (Figure 8). At this stage ERG is unrecordable.

Visual acuity may be normal even in the later stages of the disease, when only a small part of the visual field is preserved and ERG amplitudes are very low, or can be lost very early [11].

1.3.2 Genetic causes

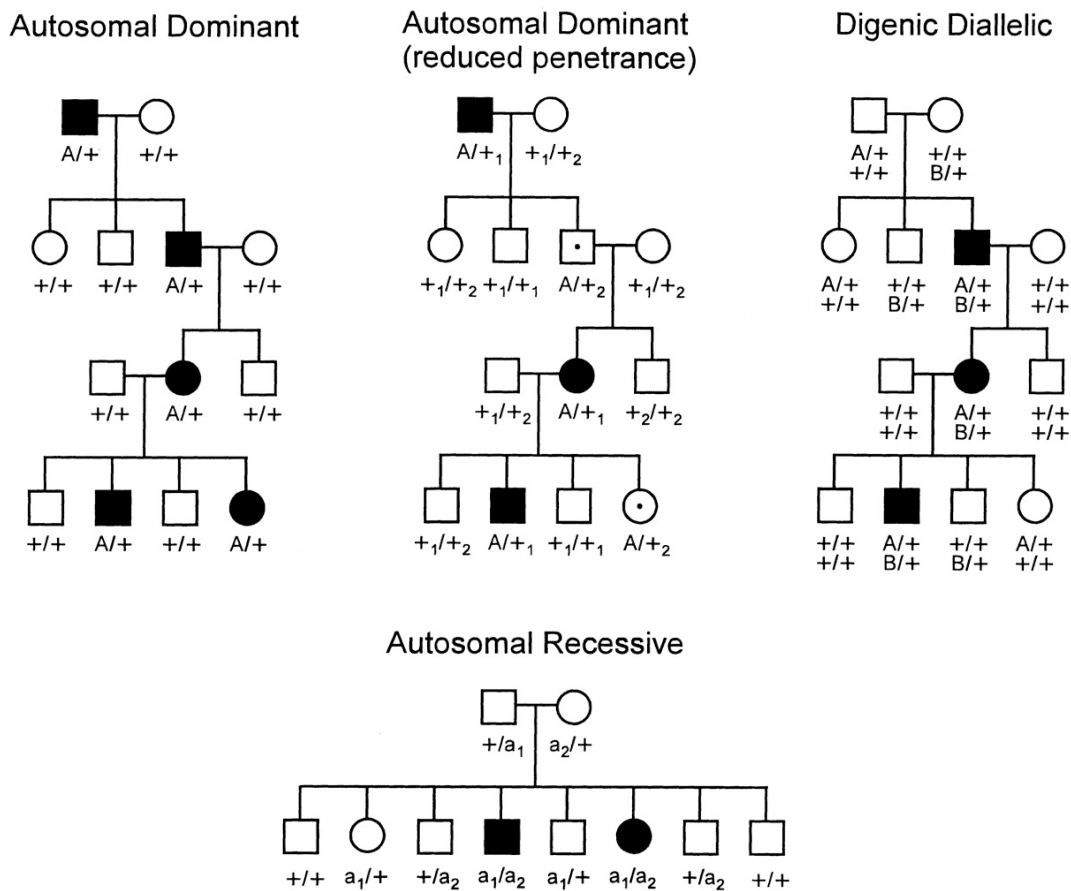
Non-syndromic forms of RP are usually monogenic disorders that are transmitted by classical inheritance patterns (reviewed in [17]) (Figure 9):

- *Autosomal dominant* forms are the mildest, and can present variable penetrance and expressivity in the forms linked to mutations in *PAP-1*, *PRPF31*, *PRPF8*, *BRR2*, and *RPI* genes [21-23].
- *Autosomal recessive* forms are usually more severe and appear earlier, often during the first decade of life.
- *X-linked* forms are frequently associated with myopia and start early in life [10]. The way of inheritance is mostly recessive, but they can also be inherited in a dominant way, characterized by the presence of affected females [10]. ERG testing can help to identify female carriers of X-linked retinitis pigmentosa, since ERGs from obligate carriers are

reduced in amplitude or delayed in implicit time or both [24]. Being able to distinguish X-linked forms from recessive forms of the disease has important clinical implications, since males affected by X-linked RP become legally blind by ages 30-45, while males with recessive forms are usually legally blind by ages 45-60 [12].

- *Digenic-diallelic* forms are characterized by the presence of affected individuals that are heterozygous for mutations in two unlinked genes. The way of inheritance resembles in the first affected generation a recessive pattern, while in the subsequent generations mimics a dominant pattern with a 25% risk of affected offspring [25]. The first example of digenic inheritance in RP was that of *RDS* and *ROM1* genes [25].

Among non-syndromic cases dominant RP represents roughly 30% of the cases, recessive RP 20% of the cases, and X-linked RP 15% of the cases. The remaining cases are mostly isolate or *de novo* mutations (reviewed in [26]).



Source: modified from Rivolta C. *et al.* [17]

Figure 9. Retinitis pigmentosa mode of inheritance.

Most genes involved in the pathogenesis of RP cause exclusively one genetic subtype of the disease, but some others, like the transcription factor *NRL*, can be responsible for both dominant and recessive forms of RP [27-28].

The majority of genes that cause RP are responsible only for a minority of cases, with the exception of *RHO*, which was the first RP gene to be identified [29-30], that accounts for about 25% of dominant RP cases in the U.S., *USH2A*, which causes about 20% of recessive RP cases, and *RPGR*, which alone explains about 70% of X-linked RP cases [11].

To date, according to RetNet – the Retinal Information Network (<https://sph.uth.edu/retnet/>, last updated February 2013), there are 50 genes and loci that have been shown to be responsible for non-syndromic RP, including 19 genes/loci for autosomal dominant, 26 for autosomal recessive, and 5 for X-linked forms. Most of the genes are appointed to photoreceptor-specific functions, but there are also others that are essential for more general cellular functions, suggesting that photoreceptors may have a higher metabolic requirement compared to other cell types in order to elicit their functions [31]. The high energy consumption of the photoreceptor cells may require an intense mRNA and protein synthesis, thus if one of these cellular mechanisms stops functioning at full capacity the photoreceptors undergo apoptosis.

The genes that have been associated with the pathogenesis of RP to date account only for about 50-60% of the cases, suggesting that there is still much to do to discover the missing genetic causes of the disease. There can be several explanations for such a percentage of unsolved cases: first, novel mutations in known RP genes, as well as genomic rearrangements or deletions, could fail to be detected by conventional screening approaches; second, there are for sure additional unknown RP genes that will be possibly identified within the next years by high-throughput sequencing techniques. Discover the genetic causes of such a heterogeneous disease will help not only for family counselling and to assess the risk of recurrence, but also in view of gene-specific therapies to be developed.

1.3.3 Therapeutic approaches

Different therapeutic strategies are aiming to slow the progression of the disease or even restore vision to patients: 1) nutritional treatments; 2) gene-specific approaches; 3) treatments that affect secondary biochemical pathways; 4) transplantation; 5) implanted electrical devices.

Clinical trials to assess the effectiveness of strategies based on supplementation of vitamin A to patients affected by different forms of RP revealed so far a slower decline in cone ERG amplitudes and a slower loss of visual field in patients who followed the diet compared to those who did not take the supplement [32-34]. Based on these findings some doctors recommend to adult patients in the early or mid stages of the disease a daily dose of oral vitamin A (retinyl palmitate 15000 IU/d). Toxic effects due to the supplementation in the diet of vitamin A have been reported; in particular the treatment can increase the risk of birth defects in pregnant women and of fractures in older individuals [35-37].

Additional nutritional treatment for RP is docosahexaenoic acid (DHA), an omega-3 fatty acid that is highly present in oily fish and in the photoreceptor cell membranes. Despite initial studies did not show a clear benefit with this treatment, following studies in larger cohorts of patients could show that a combined vitamin A and omega-3-rich diet can not only slow the rate of decline of ERG and visual field, but also retain visual acuity [34, 38-40]. Omega-3 can help the delivery of vitamin A from rods to cones via Müller cells, providing a possible explanation of how combination of vitamin A and omega-3-rich diet can rescue the remaining cones in patient with RP [41].

Gene-specific therapeutic approaches are highly depending on the type of mutation to be targeted. Null mutations are usually responsible for the recessive forms of the disease and represent the ideal target for gene-replacement since the normal copy of the gene is lost. Mutations that are responsible for dominantly inherited forms are typically producing an aberrant transcript that can be toxic for the cell; in such cases one strategy is to reduce or eliminate the expression of the mutant copy of the gene. In several animal models with dominant and recessive forms of RP gene-replacement and silencing were shown to be effective strategies to restore vision, but there are still many difficulties before these techniques can be applied to humans (reviewed in [42-45]). One limitation is that patients may have lost all or almost all rod cells, therefore the therapeutic approach would be rather aiming at the preservation of the few remaining cone cells. Gene-therapy looks particularly promising in the treatment of one form of Leber's congenital amaurosis (LCA), which is caused by recessive mutations in the *RPE65* gene, a retinal isomerase involved in the phototransduction cascade. Proof of concept that gene-therapy could represent an effective strategy for the treatment of this form of the disease came from studies in the Briard dog, a naturally occurring animal model for *RPE65*-linked form of LCA [46-50]. Later, independent clinical trials in humans, performed by subretinal delivery of a recombinant adeno-associated virus carrying *RPE65* complementary DNA (cDNA) in patients with severely advanced LCA, could show an improvement in visual function and no detectable side effects in the short term [51-53].

Neurotrophic factors are proteins that are responsible for the growth and survival of developing neurons and the maintenance of mature neurons. In the treatment of retinal degenerative diseases they represent a therapeutic approach that is independent of the aetiology of the disease. Their effect is to protect the integrity of photoreceptors by preserving their environment. In RP animal models several factors that can slow photoreceptor death by acting on secondary biochemical pathways have been identified (reviewed in [54-55]). Basic fibroblast-derived growth factor (bFGF) has been extensively investigated since the nineties, but has never been introduced in the clinic because of the problems related to its delivery to the retina and to side-effects [54]. Ciliary neurotrophic factor (CNTF) has been shown to reduce photoreceptor degeneration in RP animal models [56]. The first phase of a clinical trial in patients was well tolerated [57], although it has not yet been proven that the treatment is improving photoreceptor function in patients with RP [58].

Transplantation of retinal pigment epithelial cells, photoreceptors, or stem cells looks at the moment a very promising approach to treat retinal degenerations [59-62].

Implanted devices to electrically stimulate the retina have been developed and tested in animals and humans. Recently, the U.S. Food and Drug Administration has approved the first artificial retinal implant to help restore vision in people affected by RP [63].

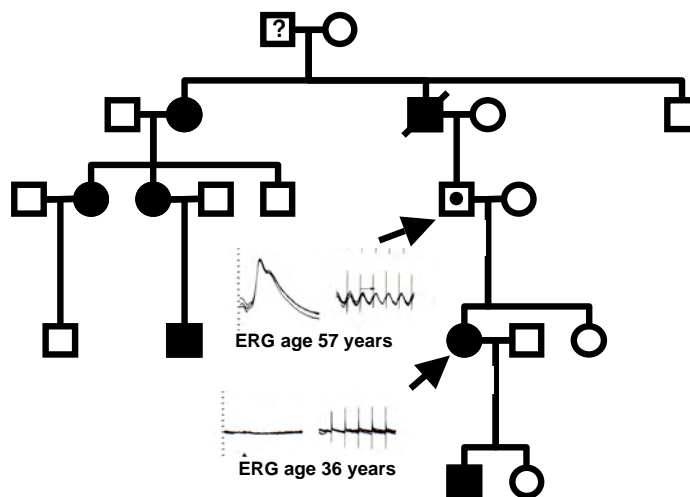
1.4 Clinical and genetic heterogeneity in retinitis pigmentosa

Clinical and genetic heterogeneity in retinitis pigmentosa is not only due to different mutations in different genes, but also to different effects of the same mutation in different individuals, sometimes even within the same family [12, 26].

1.4.1 Autosomal dominant forms with reduced penetrance

In medical genetics, penetrance refers to the proportion of individuals with a particular variant of a gene that develops the clinical manifestation of the disease.

Transmission of the disease through at least three consecutive generations in a branch of a family is a prerequisite for the autosomal dominant forms of retinitis pigmentosa. Skipping of symptoms in one or two generations has been early described in some families with autosomal dominant RP (adRP), indicating reduced penetrance [64-67]. Asymptomatic obligate carriers show no impaired vision and normal to slightly reduced electroretinographic recordings, and remain unaffected even after many years of follow-up [64-65] (Figure 10).



Source: Adapted from Berson and Simonoff [65]

Figure 10. In some pedigrees autosomal dominant RP displays reduced penetrance.

The asymptomatic individual is represented by the black dot. ERG of the affected patient is flat, whereas the asymptomatic patient shows an ERG only reduced in amplitude.

A clinical feature of the dominant forms of RP showing incomplete penetrance is that the affected individuals of such families show, together with an early involvement of the rod cells, a delayed in implicit time of the cone system [64]; since their visual field is still preserved and they retain a good visual acuity this abnormality probably derives from an abnormal function of the extrafoveal cones [65].

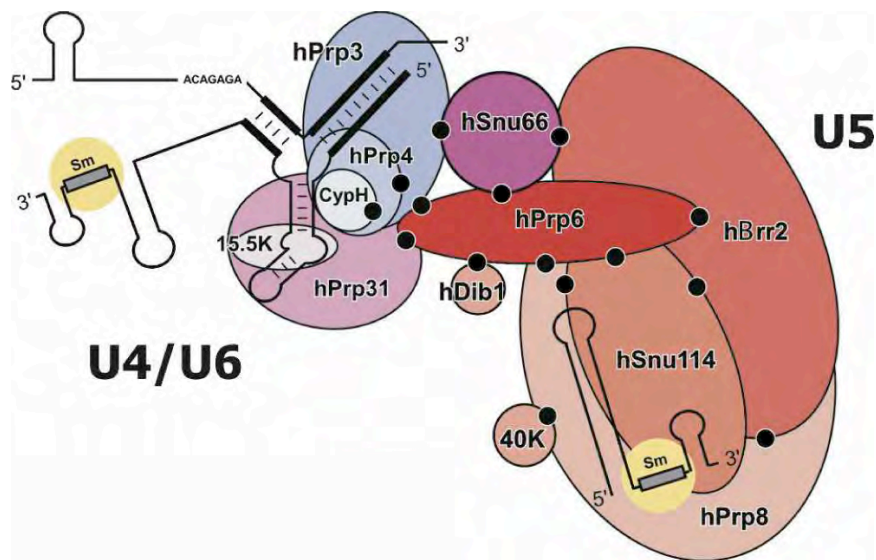
Linkage analysis in families with dominant RP with reduced penetrance showed an association of the responsible disease gene, called RP11, with markers within chromosome 19q13.4 [68-71].

Patients from these pedigrees show bimodal expressivity defined by the presence of complete asymptomatic individuals who have both affected parents and affected children [72-73].

In 2001, mutations in the gene *PRPF31*, homologous to *Saccharomyces cerevisiae* pre-mRNA splicing gene Prp31 [74], were reported in families with autosomal dominant RP linked to the RP11 locus [75].

The *PRPF31* gene comprises 14 exons and encodes a protein of 499 amino acids, among which a nuclear localization signal and a Nop domain (a ribonucleoprotein binding module, exhibiting RNA and protein binding surfaces) have been identified. As demonstrated by PCR analysis of cDNAs from a variety of normal tissues and in agreement with data from the EST database (<http://www.ncbi.nlm.nih.gov/unigene>), *PRPF31* is ubiquitously expressed in the human body [76]. As previously mentioned, *PRPF31* encodes for a protein that is a component of an essential cell machinery, the spliceosome. Removal of intron sequences by splicing occurs by two sequential *trans*-esterification reactions that are catalyzed by the components of this large RNA-protein complex [77].

The formation of the major spliceosome complex involves the stepwise assembly of four small nuclear ribonucleoprotein particles (snRNP U1, U2, U4/U6, and U5) and many non-snRNP splicing factors on a pre-mRNA. The U4/U6.U5 tri-snRNP is one of the major components of the spliceosome. Three splicing factors (PRPF3, PRPF8, and PRPF31), whose mutations have been associated with adRP, were shown by yeast two-hybrid screening to be part of the tri-snRNP complex [78] (Figure 11). PRPF31 is a critical component of the spliceosome for the formation and the stability of the tri-snRNP [79-80], in addition to being essential for cell survival, as demonstrated by repressing its expression by RNAi, which finally leads to cell death by apoptosis [81]. In the U4/U6 di-snRNP it binds to the U4 snRNA [82] and forms a bridge between this di-snRNP and the U5 snRNP by specifically interacting with the U5-specific protein, PRPF6 [79] (Figure 11).



Source: Liu *et al.* [78]

Figure 11. Schematic representation of the tri-snRNP composition. Black dots indicate interactions.

PRPF31-linked autosomal dominant RP accounts for about 5% of adRP cases [11, 83] and, so far, the prevalence of frameshift mutations suggests that the pathophysiological basis of adRP linked to this locus is the functional loss of one allele, resulting in haploinsufficiency [84-87].

To date, over 40 mutations have been identified (reviewed in [85]), including frameshift, nonsense, missense, and splice site mutations, and recently even a single-base pair mutation in the promoter region of *PRPF31* has been described [88].

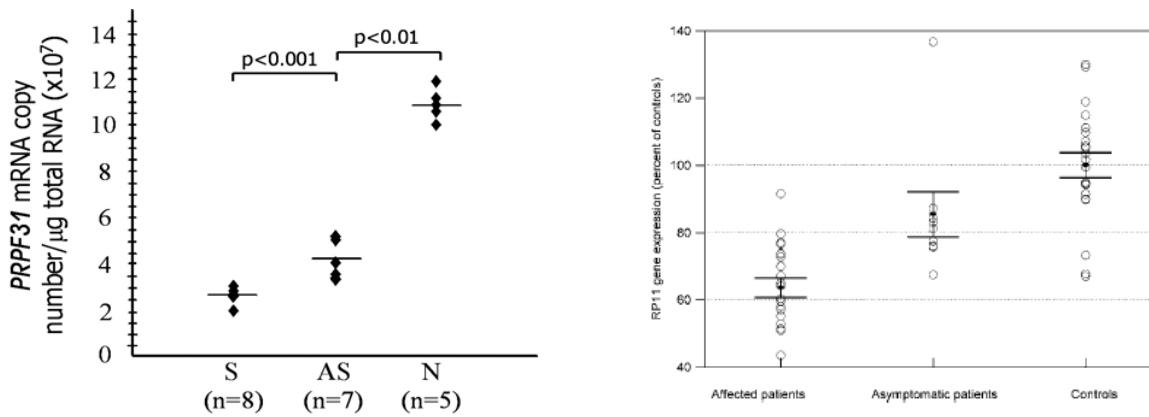
Previous linkage studies have demonstrated that the penetrance of *PRPF31* mutations would be determined by alleles, inherited from the parent who does not carry any *PRPF31* mutation, located within or close to the *PRPF31* locus itself [70, 75]. The refined chromosomal region containing these alleles corresponds to a 1.4 Mb region on chromosome 19q13.4, between polymorphic markers D19S572 and D19S926 [70]. These particular alleles, named isoalleles, do not produce any phenotype by themselves but *in trans* with respect to a mutation they determine whether or not the mutation will produce retinal degeneration [70]. The molecular basis of these isoalleles remains unknown, but evidence for such isoalleles comes from the study of 26 sib pairs from 4 different families with *PRPF31*-linked adRP [70]. In this meta-analysis, 10 sib pairs with the same phenotype (affected or asymptomatic) have inherited the same wild type *PRPF31* allele from the noncarrier parent and, on the opposite, 13 sib pairs with different phenotypes have inherited different haplotypes. However, 3 sib pairs with discordant phenotypes have been found to carry

identical wild type haplotypes. These data indicate that these isoalleles are probably the major modulators of the penetrance of *PRPF31* mutations but other modifiers could play a role as well. Another genetic element potentially capable of influencing the penetrance of *PRPF31* mutations was later mapped to chromosome 14q21-23 [89].

To investigate whether the incomplete penetrance phenotype characteristic of *PRPF31*-linked adRP was due to differentially expressed wild-type alleles in asymptomatic and affected individuals, levels of *PRPF31* wild type mRNA were measured in lymphoblastoid cell lines derived from patients from one British [90] and six American [91] adRP families, each with a distinct *PRPF31* mutation (Figure 12). Even though the methods used for evaluating mRNA levels differed between the two studies the results were similar, indicating that there is a correlation between the wild type mRNA level and the clinical status. In particular, non-carriers of *PRPF31* mutation have significantly more *PRPF31* wild type mRNA than affected patients, and asymptomatic carriers of the mutation express an intermediate level (Figure 12).

PRPF31 protein quantification confirmed the mRNA data [90], suggesting that the clinical manifestation of the disease in these families is probably due to the low expression of *PRPF31* wild-type allele in *trans* with the mutant allele.

The variable expression of *PRPF31* seems to be even present within the general population and therefore asymptomatic carriers of the mutation would be individuals that by chance are “high expressors” of the *PRPF31* wild-type allele [89].



Sources: Vithana *et al.*[90] and Rivolta *et al.* [91]

Figure 12. *PRPF31* mRNA expression levels in affected, asymptomatic patients and in controls.

On the left side scatter plot showing *PRPF31* mRNA copy numbers in symptomatic (S), asymptomatic (AS), and noncarrier (N) individuals of the AD5/RP856 pedigree [90]. On the right side *PRPF31* mRNA levels obtained integrating data from Affimetrix and CodeLink microarrays and real-time PCR experiments [91].

Studies in humans, aimed at linking mutations in this ubiquitously expressed gene and a retina-specific disease failed to prove the existence of retina-specific *PRPF31* isoforms [76]. A more convincing hypothesis seems to be the uniquely high demand for RNA processing and protein synthesis in the retina, mainly due to the continuous renewal of rod outer segments. Despite heterozygous *PRPF31* mutations have been shown to cause a generalized impairment of splicing activity, most human tissues, with the exception of the retina, are probably able to tolerate them [31, 92].

PRPF31 animal models have not provided conclusive answers to this issue. Two *PRPF31* targeted mouse models have been developed so far: one is a heterozygous knock-in mouse that carries a point mutation that was previously identified in adRP patients (*Prpf31*^{A216P/+}), while the other is an heterozygous knock-out mouse (*Prpf31*^{+/-}) [93]. After up to 18 months neither of them developed a perceptible RP phenotype [93]. Both homozygous mice are indeed embryonic lethal, indicating that no other protein or mechanism is able to compensate for *Prpf31* loss [93]. Only the ultrastructural characterization of the heterozygous *Prpf31*^{+/-} mouse model at one year of age allowed showing some degenerative changes in the RPE cells, suggesting that these may be the primary cell type affected in the splicing factor forms of RP. Two other knock-in mouse models targeting *Prpf3* and *Prpf8* presented similar results at 2 years of age [93-94]. Moreover, the late onset phenotype

observed in mice can be consistent with the adult onset phenotype observed in several patients with splicing factor forms of RP [94].

PRPF31 associated RP has been also modelled in zebrafish [95-96].

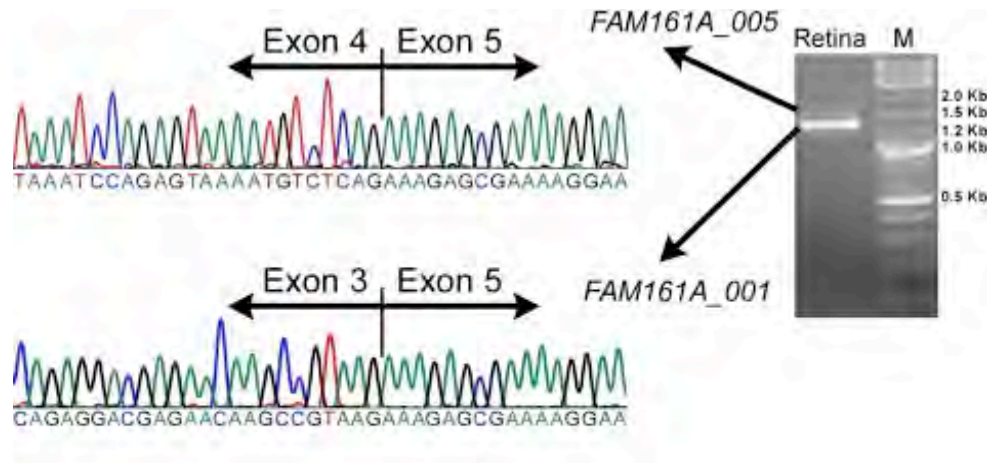
1.4.2 Autosomal recessive forms

Autosomal recessive retinitis pigmentosa (arRP) comprises a group of disorders, which includes juvenile and early-onset forms, whose symptoms may overlap with other autosomal recessive retinopathies. To date more than 30 genes and loci have been associated with arRP (RetNet database; <https://sph.uth.edu/retnet/sum-dis.htm>), and some of them are known to be responsible for LCA as well. However, the sum of the frequencies of these genes does not explain more than a third of the cases of arRP, since the majority of them contribute to less than 1% of cases and only few are responsible for more than 10% of cases (reviewed in [11, 26]). From the clinical point of view autosomal recessive forms start usually during the first decade, although there may be also milder forms [10].

The RP28 locus associated with arRP has been mapped in the past to chromosome 2p14-p15 by the analysis of a consanguineous Indian family [97].

Most of the genes contained within this locus were expressed in the eye or in the retina, but not many of them were good candidates for the disease. *MDHI* was chosen via a classical candidate gene approach, but was excluded as the possible cause of RP28-linked arRP since no mutation was found [98]. The RP28 disease-causing gene, named *FAM161A*, was finally identified thanks to two different methodological approaches, homozygosity mapping in consanguineous Israeli and Palestinian families and a combination of ultrahigh-throughput sequencing and gene expression experiments [99-100].

FAM161A is a well-conserved protein among vertebrates, and despite having multiple splicing variants, only two of them produce stable mRNA transcripts in humans (Figure 13). The main splicing isoform contains six exons and encodes for a protein of 76 kDa, while the second transcript contains a supplementary 168 bp in-frame exon between exons 3 and 5 (Figure 13). Both encode proteins that contain a single domain, called Pfam UPF0564, of unknown function.



Sources: Bandah-Rozenfeld *et al.* [99]

Figure 13. Presence of *FAM161A* alternative isoforms in human retinal cDNA. The major isoform *FAM161A_001* does not contain exon 4, while the less expressed transcript *FAM161A_005* harbours the alternative exon.

The major isoform shows expression limited only to the human retina and testis [100].

In mice, *Fam161a* is highly expressed in the developing and adult retina and its expression is driven by the transcription factor *Crx* [100]. Recently, *FAM161A* was shown to localize to the ciliary region, linking photoreceptor outer and inner segments [101-102], and to interact with other ciliary and ciliopathy-associated proteins [102], but its exact function is still unknown.

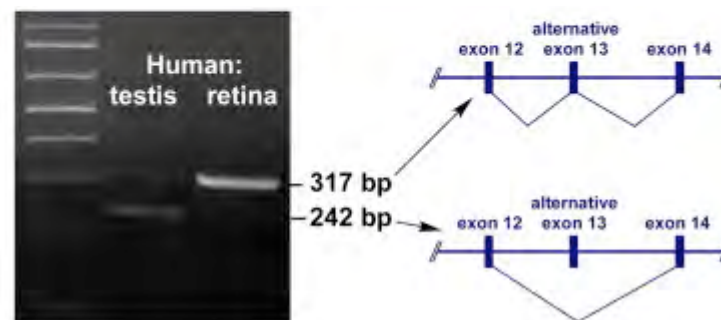
In the German cohort analyzed by *Langmann et al.* the prevalence of *FAM161A*-associated RP was in the range of 2-3%, comparable to that of other arRP genes [100]. However, in the Israeli and Palestinian populations *FAM161A* is the most frequently mutated gene in patients with arRP [99] (Dr. D.Sharon, personal communication).

From the clinical point of view, patients with *FAM161A* mutations display symptoms ranging from an atypically late-onset form of RP, detected in the German cohort, to an early-onset manifestation of the disease, observed in the Israeli and Palestinian individuals [99-100]. Unexpectedly, despite these clinical differences, all patients carry mutations that lead to loss-of-function of the encoded protein.

The male germ cell-associated kinase (MAK) is a serine/threonine protein kinase encoded in humans by the gene *MAK*, which is located on the short arm of chromosome 6. This highly

conserved protein contains a MAP kinase (mitogen-activated protein kinase) domain in its N-terminal end, and its expression is restricted only to the testis and the retina [103-104]. Both in mouse and human retina there is a longer *MAK* isoform that contains an alternative 75-bp exon between exons 11 and 12, which seems to be photoreceptor-specific [105-107] (Figure 14).

In mouse, *Mak* regulates retinal photoreceptor ciliary length and seems to be crucial for long-term survival of photoreceptors, since *Mak*^{-/-} mice develop progressive retinal degeneration [105]. Recently, mutations in *MAK* have been associated with arRP [106-107]. A homozygous insertion of a 353-bp Alu-element in exon 9 has been described in an isolated RP patient with Jewish ancestry [107]. In retinal cells derived from the patient this mutation was proven to prevent the retina-specific isoform to be expressed [107].



Sources: Ozgul *et al.* [106]

Figure 14. *The major retinal isoform of MAK includes an alternative exon.*

Prevalence of the mutation was estimated to be 1.2% in a cohort of 1798 unrelated RP patients with mixed ethnicities. Interestingly, all individuals harbouring the mutation turned to have Jewish ancestry [107]. The clinical manifestation of *MAK*-Alu element insertion resembles that of an autosomal dominant form of RP due to mutations in the *RPI* gene [108], which is intriguing considering that the two proteins co-localize in murine photoreceptors and that *Rp1* is a target of *Mak* phosphorylation [105]. Prolonged survival of the central retina island with good acuity was observed as a typical feature of patients harbouring this mutation [108]. Nonsense and missense mutations affecting critical *MAK* residues have also been associated with arRP in other cohorts; overall the patients harbouring *MAK* mutations present a less rapid and severe disease course compared with other forms of arRP [106].

1.5 Genomics technologies and disease gene identification strategies

In 2001 the first draft of the complete sequence of the human genome was published [109], and few years later the human genome assembly was already of such a high quality to cover the 99% of the euchromatic regions [110]. The remaining megabases that failed to be assembled were mostly in repetitive regions, but could eventually contain genes.

From 2007, personal genomes started to be sequenced and the 1000 genomes project was launched as an international collaboration to produce an extensive public catalog of human genetic variation by sequencing of thousands of genomes (www.1000genomes.org) [111].

What was learned from sequencing personal genomes is that the human genome is extremely variable (3.5 million single nucleotide polymorphisms and 1000 large structural rearrangements on average/individual) and that a healthy individual can be a heterozygous carrier of about 50-100 highly penetrant deleterious variants that can potentially represent a recessive carrier state for a Mendelian disease (data from the 1000 genomes project consortium 2010).

Nowadays the identification of genes that are responsible for rare Mendelian disorders is becoming increasingly important, given the possibility to develop gene-based therapies that can restore the function of the mutated gene, especially for recessive diseases.

Before the development of massively parallel sequencing, specific regions of interest of the DNA were either targeted by PCR or cloned into standard vectors and sequenced using a capillary-based, semi-automated implementation of the Sanger technique [112]. The high demand for low-cost sequencing has driven the development of high-throughput (NGS) technologies that parallelise the sequencing process, producing millions of reads (contiguous regions of DNA sequence) in one experiment [113].

NGS techniques have dramatically reduced the time and costs of conventional sequencing by simultaneously sequencing an increasing number of genes [114].

The crucial step of NGS is the production of a library of DNA fragments, which represents the template for further processing. Library preparation is accomplished by random fragmentation of the genomic DNA, followed by the ligation of special adapters. The fragmented DNA of interest is captured by targeted hybridization and then these DNA fragments are used to generate a library that is ready to be sequenced. For each variant to be analyzed the reads are reassembled using a known reference genome as a scaffold, resulting in many-fold coverage of the region of interest, or in the absence of a reference genome a *de-novo* assembly is performed.

Whole exome and whole genome sequencing (WES and WGS) are currently the preferential approaches for disease gene identification in rare Mendelian diseases [115-116]. Exome sequencing

has successfully identified the causative mutations of several highly penetrant Mendelian diseases, it is about 5 fold less expensive than WGS and exon variations are the most readily interpreted at the moment. On the other side, it interrogates only 1% of the entire genome, suggesting that it could miss mutations of interests, including those in exons that are not captured, in non-exonic regulatory regions, or structural variants such as large deletions or duplications [117-118]. Another limitation of WES could be represented by the high average coverage that is required, because of the variable efficiency of the capturing method and of “allelic imbalance” when one allele is preferentially captured over the other [119].

It is becoming increasingly evident that variations in non-coding sequences of the genome or structural rearrangements may represent an important genetic component in Mendelian diseases. Whole-genome sequencing uncovers all genetic and genomic variations, including intronic and regulatory variants as well as large structural variations and copy number variants that can otherwise cause the disease. However, both costs and capacity required to perform whole genome sequencing are still prohibitive for daily use, considering that the function of much part of the genome is still largely unknown.

By comparing results of exome sequencing of an individual with respect to genome sequencing of the same individual neither of the two techniques managed to cover all sequencing variants, suggesting that both approaches complement each other [120].

The most powerful approach to solve the genetic causes of rare Mendelian diseases has been so far the sequencing of different members of the same family or of different individuals with the same phenotype [121-125].

In addition, classical genetic approaches such as linkage analysis or homozygosity mapping, depending on the structure and inheritance pattern of the family, can help refining genomic regions of interest.

References

1. Willoughby, C.E., et al., *Anatomy and physiology of the human eye: effects of mucopolysaccharidoses disease on structure and function - a review*. Clinical and Experimental Ophthalmology, 2010. 38: p. 2-11.
2. McCaa, C.S., *The eye and visual nervous system: anatomy, physiology and toxicology*. Environ Health Perspect, 1982. 44: p. 1-8.
3. Purves D, A.G., Fitzpatrick D, et al., ed. *The Retina*. Neuroscience. 2nd edition. 2001, Sunderland (MA): Sinauer Associates.
4. Tu, D.C., et al., *Physiologic diversity and development of intrinsically photosensitive retinal ganglion cells*. Neuron, 2005. 48(6): p. 987-99.
5. Yau, K.W., *Phototransduction mechanism in retinal rods and cones. The Friedenwald Lecture*. Invest Ophthalmol Vis Sci, 1994. 35(1): p. 9-32.
6. Ebrey, T. and Y. Koutalos, *Vertebrate photoreceptors*. Prog Retin Eye Res, 2001. 20(1): p. 49-94.
7. Kolb, H., *How the retina works - Much of the construction of an image takes place in the retina itself through the use of specialized neural circuits*. American Scientist, 2003. 91(1): p. 28-35.
8. Gao, H. and J.G. Hollyfield, *Aging of the human retina. Differential loss of neurons and retinal pigment epithelial cells*. Invest Ophthalmol Vis Sci, 1992. 33(1): p. 1-17.
9. Wright, A.F., et al., *Photoreceptor degeneration: genetic and mechanistic dissection of a complex trait*. Nat Rev Genet, 2010. 11(4): p. 273-84.
10. Hamel, C., *Retinitis pigmentosa*. Orphanet J Rare Dis, 2006. 1: p. 40.
11. Hartong, D.T., E.L. Berson, and T.P. Dryja, *Retinitis pigmentosa*. Lancet, 2006. 368(9549): p. 1795-809.
12. Berson, E.L., *Retinitis pigmentosa. The Friedenwald Lecture*. Invest Ophthalmol Vis Sci, 1993. 34(5): p. 1659-76.
13. Francis, P.J., *Genetics of inherited retinal disease*. J R Soc Med, 2006. 99(4): p. 189-91.
14. Vernon, M., *Usher's syndrome--deafness and progressive blindness. Clinical cases, prevention, theory and literature survey*. J Chronic Dis, 1969. 22(3): p. 133-51.
15. Astuto, L.M., et al., *CDH23 mutation and phenotype heterogeneity: a profile of 107 diverse families with Usher syndrome and nonsyndromic deafness*. Am J Hum Genet, 2002. 71(2): p. 262-75.
16. Weil, D., et al., *The autosomal recessive isolated deafness, DFNB2, and the Usher 1B syndrome are allelic defects of the myosin-VIIA gene*. Nat Genet, 1997. 16(2): p. 191-3.
17. Rivolta, C., et al., *Retinitis pigmentosa and allied diseases: numerous diseases, genes, and inheritance patterns*. Hum Mol Genet, 2002. 11(10): p. 1219-27.
18. Perlman, I., *The Electroretinogram: ERG*, in *Webvision: The Organization of the Retina and Visual System [Internet]*, F.E. Kolb H, Nelson R., Editor. 2001: Salt Lake City (UT): University of Utah Health Sciences Center.
19. Berson, E.L., P. Gouras, and M. Hoff, *Temporal aspects of the electroretinogram*. Arch Ophthalmol, 1969. 81(2): p. 207-14.
20. Huang, D., et al., *Optical coherence tomography*. Science, 1991. 254(5035): p. 1178-81.
21. Utz, V.M., et al., *Autosomal Dominant Retinitis Pigmentosa Secondary to Pre-mRNA Splicing-Factor Gene PRPF31 (RP11): Review of Disease Mechanism and Report of a Family with a Novel 3-Base Pair Insertion*. Ophthalmic Genet, 2013.
22. Maubaret, C.G., et al., *Autosomal dominant retinitis pigmentosa with intrafamilial variability and incomplete penetrance in two families carrying mutations in PRPF8*. Invest Ophthalmol Vis Sci, 2011. 52(13): p. 9304-9.

23. Jacobson, S.G., et al., *Disease expression of RP1 mutations causing autosomal dominant retinitis pigmentosa*. Invest Ophthalmol Vis Sci, 2000. 41(7): p. 1898-908.
24. Berson, E.L., J.B. Rosen, and E.A. Simonoff, *Electroretinographic testing as an aid in detection of carriers of X-chromosome-linked retinitis pigmentosa*. Am J Ophthalmol, 1979. 87(4): p. 460-8.
25. Kajiwara, K., E.L. Berson, and T.P. Dryja, *Digenic retinitis pigmentosa due to mutations at the unlinked peripherin/RDS and ROM1 loci*. Science, 1994. 264(5165): p. 1604-8.
26. Daiger, S.P., S.J. Bowne, and L.S. Sullivan, *Perspective on genes and mutations causing retinitis pigmentosa*. Arch Ophthalmol, 2007. 125(2): p. 151-8.
27. Bessant, D.A., et al., *A mutation in NRL is associated with autosomal dominant retinitis pigmentosa*. Nat Genet, 1999. 21(4): p. 355-6.
28. Nishiguchi, K.M., et al., *Recessive NRL mutations in patients with clumped pigmentary retinal degeneration and relative preservation of blue cone function*. Proc Natl Acad Sci U S A, 2004. 101(51): p. 17819-24.
29. Dryja, T.P., et al., *Mutations within the rhodopsin gene in patients with autosomal dominant retinitis pigmentosa*. N Engl J Med, 1990. 323(19): p. 1302-7.
30. Dryja, T.P., et al., *A point mutation of the rhodopsin gene in one form of retinitis pigmentosa*. Nature, 1990. 343(6256): p. 364-6.
31. Tanackovic, G., et al., *PRPF mutations are associated with generalized defects in spliceosome formation and pre-mRNA splicing in patients with retinitis pigmentosa*. Hum Mol Genet, 2011. 20(11): p. 2116-30.
32. Berson, E.L., et al., *A randomized trial of vitamin A and vitamin E supplementation for retinitis pigmentosa*. Arch Ophthalmol, 1993. 111(6): p. 761-72.
33. Berson, E.L., et al., *Vitamin A supplementation for retinitis pigmentosa*. Arch Ophthalmol, 1993. 111(11): p. 1456-9.
34. Berson, E.L., et al., *omega-3 intake and visual acuity in patients with retinitis pigmentosa receiving vitamin A*. Arch Ophthalmol, 2012. 130(6): p. 707-11.
35. Feskanich, D., et al., *Vitamin A intake and hip fractures among postmenopausal women*. JAMA, 2002. 287(1): p. 47-54.
36. Lammer, E.J., et al., *Retinoic acid embryopathy*. N Engl J Med, 1985. 313(14): p. 837-41.
37. Sibulesky, L., et al., *Safety of <7500 RE (<25000 IU) vitamin A daily in adults with retinitis pigmentosa*. Am J Clin Nutr, 1999. 69(4): p. 656-63.
38. Berson, E.L., et al., *Clinical trial of docosahexaenoic acid in patients with retinitis pigmentosa receiving vitamin A treatment*. Arch Ophthalmol, 2004. 122(9): p. 1297-305.
39. Berson, E.L., et al., *Further evaluation of docosahexaenoic acid in patients with retinitis pigmentosa receiving vitamin A treatment: subgroup analyses*. Arch Ophthalmol, 2004. 122(9): p. 1306-14.
40. Berson, E.L., et al., *Clinical trial of lutein in patients with retinitis pigmentosa receiving vitamin A*. Arch Ophthalmol, 2010. 128(4): p. 403-11.
41. Berson, E.L., et al., *omega-3 Intake in Patients With Retinitis Pigmentosa Receiving Vitamin A-Reply*. JAMA Ophthalmol, 2013. 131(2): p. 267-8.
42. Thumann, G., *Prospectives for gene therapy of retinal degenerations*. Curr Genomics, 2012. 13(5): p. 350-62.
43. Rossmiller, B., H. Mao, and A.S. Lewin, *Gene therapy in animal models of autosomal dominant retinitis pigmentosa*. Mol Vis, 2012. 18: p. 2479-96.
44. Stieger, K., et al., *Adeno-associated virus mediated gene therapy for retinal degenerative diseases*. Methods Mol Biol, 2011. 807: p. 179-218.
45. Farrar, G.J., et al., *Gene-based therapies for dominantly inherited retinopathies*. Gene Ther, 2012. 19(2): p. 137-44.
46. Acland, G.M., et al., *Gene therapy restores vision in a canine model of childhood blindness*. Nat Genet, 2001. 28(1): p. 92-5.

47. Narfstrom, K., et al., *Functional and structural recovery of the retina after gene therapy in the RPE65 null mutation dog*. Invest Ophthalmol Vis Sci, 2003. 44(4): p. 1663-72.
48. Narfstrom, K., et al., *In vivo gene therapy in young and adult RPE65-/- dogs produces long-term visual improvement*. J Hered, 2003. 94(1): p. 31-7.
49. Acland, G.M., et al., *Long-term restoration of rod and cone vision by single dose rAAV-mediated gene transfer to the retina in a canine model of childhood blindness*. Mol Ther, 2005. 12(6): p. 1072-82.
50. Le Meur, G., et al., *Restoration of vision in RPE65-deficient Briard dogs using an AAV serotype 4 vector that specifically targets the retinal pigmented epithelium*. Gene Ther, 2007. 14(4): p. 292-303.
51. Maguire, A.M., et al., *Safety and efficacy of gene transfer for Leber's congenital amaurosis*. N Engl J Med, 2008. 358(21): p. 2240-8.
52. Bainbridge, J.W., et al., *Effect of gene therapy on visual function in Leber's congenital amaurosis*. N Engl J Med, 2008. 358(21): p. 2231-9.
53. Cideciyan, A.V., et al., *Human gene therapy for RPE65 isomerase deficiency activates the retinoid cycle of vision but with slow rod kinetics*. Proc Natl Acad Sci U S A, 2008. 105(39): p. 15112-7.
54. Sahni, J.N., et al., *Therapeutic challenges to retinitis pigmentosa: from neuroprotection to gene therapy*. Curr Genomics, 2011. 12(4): p. 276-84.
55. Musarella, M.A. and I.M. Macdonald, *Current concepts in the treatment of retinitis pigmentosa*. J Ophthalmol, 2011. 2011: p. 753547.
56. Tao, W., et al., *Encapsulated cell-based delivery of CNTF reduces photoreceptor degeneration in animal models of retinitis pigmentosa*. Invest Ophthalmol Vis Sci, 2002. 43(10): p. 3292-8.
57. Sieving, P.A., et al., *Ciliary neurotrophic factor (CNTF) for human retinal degeneration: phase I trial of CNTF delivered by encapsulated cell intraocular implants*. Proc Natl Acad Sci U S A, 2006. 103(10): p. 3896-901.
58. Emerich, D.F. and C.G. Thanos, *NT-501: an ophthalmic implant of polymer-encapsulated ciliary neurotrophic factor-producing cells*. Curr Opin Mol Ther, 2008. 10(5): p. 506-15.
59. Singh, M.S., et al., *Reversal of end-stage retinal degeneration and restoration of visual function by photoreceptor transplantation*. Proc Natl Acad Sci U S A, 2013. 110(3): p. 1101-6.
60. Barber, A.C., et al., *Repair of the degenerate retina by photoreceptor transplantation*. Proc Natl Acad Sci U S A, 2013. 110(1): p. 354-9.
61. Seiler, M.J. and R.B. Aramant, *Cell replacement and visual restoration by retinal sheet transplants*. Prog Retin Eye Res, 2012. 31(6): p. 661-87.
62. Rowland, T.J., D.E. Buchholz, and D.O. Clegg, *Pluripotent human stem cells for the treatment of retinal disease*. J Cell Physiol, 2012. 227(2): p. 457-66.
63. Ahuja, A.K. and M.R. Behrend, *The Argus II retinal prosthesis: Factors affecting patient selection for implantation*. Prog Retin Eye Res, 2013.
64. Berson, E.L., et al., *Dominant retinitis pigmentosa with reduced penetrance*. Arch Ophthalmol, 1969. 81(2): p. 226-34.
65. Berson, E.L. and E.A. Simonoff, *Dominant retinitis pigmentosa with reduced penetrance. Further studies of the electroretinogram*. Arch Ophthalmol, 1979. 97(7): p. 1286-91.
66. Moore, A.T., et al., *Autosomal-Dominant Retinitis-Pigmentosa with Apparent Incomplete Penetrance - a Clinical, Electrophysiological, Psychophysical, and Molecular-Genetic Study*. British Journal of Ophthalmology, 1993. 77(8): p. 473-479.
67. Jay, M., et al., *Nine generations of a family with autosomal dominant retinitis pigmentosa and evidence of variable expressivity from census records*. J Med Genet, 1992. 29(12): p. 906-10.

68. al-Magthteh, M., et al., *Identification of a sixth locus for autosomal dominant retinitis pigmentosa on chromosome 19*. Hum Mol Genet, 1994. 3(2): p. 351-4.
69. Xu, S.Y., et al., *Autosomal-Dominant Retinitis-Pigmentosa Locus on Chromosome 19q in a Japanese Family*. Journal of Medical Genetics, 1995. 32(11): p. 915-916.
70. McGee, T.L., et al., *Evidence that the penetrance of mutations at the RP11 locus causing dominant retinitis pigmentosa is influenced by a gene linked to the homologous RP11 allele*. Am J Hum Genet, 1997. 61(5): p. 1059-66.
71. Nakazawa, M., et al., *Variable expressivity in a Japanese family with autosomal dominant retinitis pigmentosa closely linked to chromosome 19q*. Arch Ophthalmol, 1996. 114(3): p. 318-22.
72. Al-Magthteh, M., et al., *Evidence for a major retinitis pigmentosa locus on 19q13.4 (RP11) and association with a unique bimodal expressivity phenotype*. Am J Hum Genet, 1996. 59(4): p. 864-71.
73. Evans, K., et al., *Bimodal expressivity in dominant retinitis pigmentosa genetically linked to chromosome 19q*. Br J Ophthalmol, 1995. 79(9): p. 841-6.
74. Weidenhammer, E.M., et al., *The PRP31 gene encodes a novel protein required for pre-mRNA splicing in Saccharomyces cerevisiae*. Nucleic Acids Res, 1996. 24(6): p. 1164-70.
75. Vithana, E.N., et al., *A human homolog of yeast pre-mRNA splicing gene, PRP31, underlies autosomal dominant retinitis pigmentosa on chromosome 19q13.4 (RP11)*. Mol Cell, 2001. 8(2): p. 375-81.
76. Tanackovic, G. and C. Rivolta, *PRPF31 alternative splicing and expression in human retina*. Ophthalmic Genet, 2009. 30(2): p. 76-83.
77. Kramer, A., *The structure and function of proteins involved in mammalian pre-mRNA splicing*. Annu Rev Biochem, 1996. 65: p. 367-409.
78. Liu, S., et al., *The network of protein-protein interactions within the human U4/U6.U5 tri-snRNP*. RNA, 2006. 12(7): p. 1418-30.
79. Makarova, O.V., et al., *Protein 61K, encoded by a gene (PRPF31) linked to autosomal dominant retinitis pigmentosa, is required for U4/U6*U5 tri-snRNP formation and pre-mRNA splicing*. EMBO J, 2002. 21(5): p. 1148-57.
80. Weidenhammer, E.M., M. Ruiz-Noriega, and J.L. Woolford, Jr., *Prp31p promotes the association of the U4/U6 x U5 tri-snRNP with prespliceosomes to form spliceosomes in Saccharomyces cerevisiae*. Mol Cell Biol, 1997. 17(7): p. 3580-8.
81. Schaffert, N., et al., *RNAi knockdown of hPrp31 leads to an accumulation of U4/U6 di-snRNPs in Cajal bodies*. EMBO J, 2004. 23(15): p. 3000-9.
82. Nottrott, S., H. Urlaub, and R. Luhrmann, *Hierarchical, clustered protein interactions with U4/U6 snRNA: a biochemical role for U4/U6 proteins*. EMBO J, 2002. 21(20): p. 5527-38.
83. Waseem, N.H., et al., *Mutations in the gene coding for the pre-mRNA splicing factor, PRPF31, in patients with autosomal dominant retinitis pigmentosa*. Invest Ophthalmol Vis Sci, 2007. 48(3): p. 1330-4.
84. Rio Frio, T., et al., *Premature termination codons in PRPF31 cause retinitis pigmentosa via haploinsufficiency due to nonsense-mediated mRNA decay*. J Clin Invest, 2008. 118(4): p. 1519-31.
85. Audo, I., et al., *Prevalence and novelty of PRPF31 mutations in French autosomal dominant rod-cone dystrophy patients and a review of published reports*. BMC Med Genet, 2010. 11: p. 145.
86. Sullivan, L.S., et al., *Genomic rearrangements of the PRPF31 gene account for 2.5% of autosomal dominant retinitis pigmentosa*. Invest Ophthalmol Vis Sci, 2006. 47(10): p. 4579-88.
87. Abu-Safieh, L., et al., *A large deletion in the adRP gene PRPF31: evidence that haploinsufficiency is the cause of disease*. Mol Vis, 2006. 12: p. 384-8.

88. Rose, A.M., et al., *Expression of PRPF31 and TFPT: regulation in health and retinal disease*. Hum Mol Genet, 2012. 21(18): p. 4126-37.
89. Rio Frio, T., et al., *Two trans-acting eQTLs modulate the penetrance of PRPF31 mutations*. Hum Mol Genet, 2008. 17(20): p. 3154-65.
90. Vithana, E.N., et al., *Expression of PRPF31 mRNA in patients with autosomal dominant retinitis pigmentosa: a molecular clue for incomplete penetrance?* Invest Ophthalmol Vis Sci, 2003. 44(10): p. 4204-9.
91. Rivolta, C., et al., *Variation in retinitis pigmentosa-11 (PRPF31 or RP11) gene expression between symptomatic and asymptomatic patients with dominant RP11 mutations*. Hum Mutat, 2006. 27(7): p. 644-53.
92. Cao, H., et al., *Temporal and tissue specific regulation of RP-associated splicing factor genes PRPF3, PRPF31 and PRPC8--implications in the pathogenesis of RP*. PLoS One, 2011. 6(1): p. e15860.
93. Bujakowska, K., et al., *Study of gene-targeted mouse models of splicing factor gene Prpf31 implicated in human autosomal dominant retinitis pigmentosa (RP)*. Invest Ophthalmol Vis Sci, 2009. 50(12): p. 5927-33.
94. Graziotto, J.J., et al., *Three gene-targeted mouse models of RNA splicing factor RP show late-onset RPE and retinal degeneration*. Invest Ophthalmol Vis Sci, 2011. 52(1): p. 190-8.
95. Linder, B., et al., *Systemic splicing factor deficiency causes tissue-specific defects: a zebrafish model for retinitis pigmentosa*. Hum Mol Genet, 2011. 20(2): p. 368-77.
96. Yin, J., et al., *Mutant Prpf31 causes pre-mRNA splicing defects and rod photoreceptor cell degeneration in a zebrafish model for Retinitis pigmentosa*. Mol Neurodegener, 2011. 6: p. 56.
97. Gu, S., et al., *Autosomal recessive retinitis pigmentosa locus RP28 maps between D2S1337 and D2S286 on chromosome 2p11-p15 in an Indian family*. J Med Genet, 1999. 36(9): p. 705-7.
98. Rio Frio, T., et al., *Ultra high throughput sequencing excludes MDH1 as candidate gene for RP28-linked retinitis pigmentosa*. Mol Vis, 2009. 15: p. 2627-33.
99. Bandah-Rozenfeld, D., et al., *Homozygosity mapping reveals null mutations in FAM161A as a cause of autosomal-recessive retinitis pigmentosa*. Am J Hum Genet, 2010. 87(3): p. 382-91.
100. Langmann, T., et al., *Nonsense mutations in FAM161A cause RP28-associated recessive retinitis pigmentosa*. Am J Hum Genet, 2010. 87(3): p. 376-81.
101. Zach, F., et al., *The retinitis pigmentosa 28 protein FAM161A is a novel ciliary protein involved in intermolecular protein interaction and microtubule association*. Hum Mol Genet, 2012. 21(21): p. 4573-86.
102. Di Gioia, S.A., et al., *FAM161A, associated with retinitis pigmentosa, is a component of the cilia-basal body complex and interacts with proteins involved in ciliopathies*. Hum Mol Genet, 2012. 21(23): p. 5174-84.
103. Blackshaw, S., et al., *Genomic analysis of mouse retinal development*. PLoS Biol, 2004. 2(9): p. E247.
104. Matsushime, H., et al., *A novel mammalian protein kinase gene (mak) is highly expressed in testicular germ cells at and after meiosis*. Mol Cell Biol, 1990. 10(5): p. 2261-8.
105. Omori, Y., et al., *Negative regulation of ciliary length by ciliary male germ cell-associated kinase (Mak) is required for retinal photoreceptor survival*. Proc Natl Acad Sci U S A, 2010. 107(52): p. 22671-6.
106. Ozgul, R.K., et al., *Exome sequencing and cis-regulatory mapping identify mutations in MAK, a gene encoding a regulator of ciliary length, as a cause of retinitis pigmentosa*. Am J Hum Genet, 2011. 89(2): p. 253-64.

107. Tucker, B.A., et al., *Exome sequencing and analysis of induced pluripotent stem cells identify the cilia-related gene male germ cell-associated kinase (MAK) as a cause of retinitis pigmentosa*. Proc Natl Acad Sci U S A, 2011. 108(34): p. E569-76.
108. Stone, E.M., et al., *Autosomal recessive retinitis pigmentosa caused by mutations in the MAK gene*. Invest Ophthalmol Vis Sci, 2011. 52(13): p. 9665-73.
109. Lander, E.S., et al., *Initial sequencing and analysis of the human genome*. Nature, 2001. 409(6822): p. 860-921.
110. *Finishing the euchromatic sequence of the human genome*. Nature, 2004. 431(7011): p. 931-45.
111. Levy, S., et al., *The diploid genome sequence of an individual human*. PLoS Biol, 2007. 5(10): p. e254.
112. Sanger, F., et al., *Nucleotide sequence of bacteriophage phi X174 DNA*. Nature, 1977. 265(5596): p. 687-95.
113. Church, G.M., *Genomes for all*. Sci Am, 2006. 294(1): p. 46-54.
114. Tucker, T., M. Marra, and J.M. Friedman, *Massively parallel sequencing: the next big thing in genetic medicine*. Am J Hum Genet, 2009. 85(2): p. 142-54.
115. Lyon, G.J. and K. Wang, *Identifying disease mutations in genomic medicine settings: current challenges and how to accelerate progress*. Genome Med, 2012. 4(7): p. 58.
116. Cordero, P. and E.A. Ashley, *Whole-genome sequencing in personalized therapeutics*. Clin Pharmacol Ther, 2012. 91(6): p. 1001-9.
117. Gonzaga-Jauregui, C., J.R. Lupski, and R.A. Gibbs, *Human genome sequencing in health and disease*. Annu Rev Med, 2012. 63: p. 35-61.
118. Albert, T.J., et al., *Direct selection of human genomic loci by microarray hybridization*. Nat Methods, 2007. 4(11): p. 903-5.
119. Sobreira, N.L., et al., *Whole-genome sequencing of a single proband together with linkage analysis identifies a Mendelian disease gene*. PLoS Genet, 2010. 6(6): p. e1000991.
120. Clark, M.J., et al., *Performance comparison of exome DNA sequencing technologies*. Nat Biotechnol, 2011. 29(10): p. 908-14.
121. Roach, J.C., et al., *Analysis of genetic inheritance in a family quartet by whole-genome sequencing*. Science, 2010. 328(5978): p. 636-9.
122. Bainbridge, M.N., et al., *Whole-genome sequencing for optimized patient management*. Sci Transl Med, 2011. 3(87): p. 87re3.
123. Rios, J., et al., *Identification by whole-genome resequencing of gene defect responsible for severe hypercholesterolemia*. Hum Mol Genet, 2010. 19(22): p. 4313-8.
124. Veeramah, K.R., et al., *De novo pathogenic SCN8A mutation identified by whole-genome sequencing of a family quartet affected by infantile epileptic encephalopathy and SUDEP*. Am J Hum Genet, 2012. 90(3): p. 502-10.
125. Lupski, J.R., et al., *Whole-genome sequencing in a patient with Charcot-Marie-Tooth neuropathy*. N Engl J Med, 2010. 362(13): p. 1181-91.

***CNOT3* is a modifier of *PRPF31* mutations in retinitis pigmentosa
with incomplete penetrance**

Published in *PLOS Genetics* (November 2012 | Volume 8 | Issue 11 | e1003040)

The aim of this project was to look for genetic elements that could influence the penetrance of *PRPF31*-linked autosomal dominant retinitis pigmentosa, by which some obligate carriers of the disease allele do not show pathological symptoms. At least one of these elements was mapped by linkage analysis to chromosome 19q13.4, where *PRPF31* lies as well. Isoalleles from this locus, inherited by the patients from the parent who does not carry the mutation, determine an increased level of wild-type *PRPF31*, which in turn prevents the clinical manifestation of the disease.

The project was a collaboration with the group of Prof. S.S. Bhattacharya (Institute of Ophthalmology, University College London), who provided us lymphoblastoid cell lines derived from patients belonging to a large British family (RP856/AD5), which segregates a frameshift *PRPF31* mutation.

This study has led to the identification of the major regulator of the penetrance of *PRPF31* mutations, named *CNOT3*, and to the characterization of its mechanism of action in regulating *PRPF31* expression.

In this study I performed all the experiments except the sequencing of the polymorphic alleles, and I wrote the draft for the journal.

CNOT3 Is a Modifier of *PRPF31* Mutations in Retinitis Pigmentosa with Incomplete Penetrance

Giulia Venturini¹, Anna M. Rose², Amna Z. Shah², Shomi S. Bhattacharya², Carlo Rivolta^{1*}

1 Department of Medical Genetics, University of Lausanne, Lausanne, Switzerland, **2** Department of Genetics, UCL Institute of Ophthalmology, University College London, London, United Kingdom

Abstract

Heterozygous mutations in the *PRPF31* gene cause autosomal dominant retinitis pigmentosa (adRP), a hereditary disorder leading to progressive blindness. In some cases, such mutations display incomplete penetrance, implying that certain carriers develop retinal degeneration while others have no symptoms at all. Asymptomatic carriers are protected from the disease by a higher than average expression of the *PRPF31* allele that is not mutated, mainly through the action of an unknown modifier gene mapping to chromosome 19q13.4. We investigated a large family with adRP segregating an 11-bp deletion in *PRPF31*. The analysis of cell lines derived from asymptomatic and affected individuals revealed that the expression of only one gene among a number of candidates within the 19q13.4 interval significantly correlated with that of *PRPF31*, both at the mRNA and protein levels, and according to an inverse relationship. This gene was *CNOT3*, encoding a subunit of the Ccr4-not transcription complex. In cultured cells, siRNA-mediated silencing of *CNOT3* provoked an increase in *PRPF31* expression, confirming a repressive nature of *CNOT3* on *PRPF31*. Furthermore, chromatin immunoprecipitation revealed that *CNOT3* directly binds to a specific *PRPF31* promoter sequence, while next-generation sequencing of the *CNOT3* genomic region indicated that its variable expression is associated with a common intronic SNP. In conclusion, we identify *CNOT3* as the main modifier gene determining penetrance of *PRPF31* mutations, via a mechanism of transcriptional repression. In asymptomatic carriers *CNOT3* is expressed at low levels, allowing higher amounts of wild-type *PRPF31* transcripts to be produced and preventing manifestation of retinal degeneration.

Citation: Venturini G, Rose AM, Shah AZ, Bhattacharya SS, Rivolta C (2012) *CNOT3* Is a Modifier of *PRPF31* Mutations in Retinitis Pigmentosa with Incomplete Penetrance. *PLoS Genet* 8(11): e1003040. doi:10.1371/journal.pgen.1003040

Editor: Janey L. Wiggs, Harvard University, United States of America

Received: July 6, 2012; **Accepted:** September 5, 2012; **Published:** November 8, 2012

Copyright: © 2012 Venturini et al. This is an open-access article distributed under the terms of the Creative Commons Attribution License, which permits unrestricted use, distribution, and reproduction in any medium, provided the original author and source are credited.

Funding: This work was supported by the Swiss National Science Foundation (grants 320030-121929 and 310030_138346), the Gebert R uf Foundation (Rare Diseases - New Technologies grant), the Rosetrees Trust, and Fight for Sight. The funders had no role in study design, data collection and analysis, decision to publish, or preparation of the manuscript.

Competing Interests: The authors have declared that no competing interests exist.

* E-mail: carlo.rivolta@unil.ch

Introduction

The penetrance of a disease-causing mutation corresponds to the proportion of individuals who carry such variant and develop clinical symptoms. In the majority of Mendelian disorders penetrance is 100%, but incomplete penetrance is far from being uncommon [1]. Although in medical genetics penetrance is still largely uncharacterized at the molecular level, it is usually determined by genetic or epigenetic factors, and sometimes even by environmental modifiers [2].

Retinitis pigmentosa (RP) is a group of inherited degenerative diseases of the retina that cause the progressive death of photoreceptors, the neurons of the eye that are sensitive to light. Typically, patients affected by RP first suffer from night blindness, most often during adolescence. Rod and cone photoreceptor cells start to degenerate from the mid periphery to the far periphery and the center of the retina, resulting in the so-called tunnel vision. Later in life, central vision is also lost, leading to legal or complete blindness [3]. Clinically, RP is a highly-heterogeneous disease, reflecting not only genetic heterogeneity (mutations in different genes), but also inter-individual diversity (penetrance and expressivity) [4].

The *PRPF31* gene encodes in humans a pre-mRNA processing factor. In autosomal dominant RP (adRP) due to mutations in

PRPF31 penetrance of the disease can be incomplete. Specifically, in families with *PRPF31* mutations it is not uncommon to observe the presence of asymptomatic individuals who have affected parents, affected children, or both [5–8]. Although they carry the same *PRPF31* mutation as their affected relatives, asymptomatic subjects show no visual impairment, even at older ages, and normal to slightly reduced electroretinographic recordings [7].

PRPF31 mutations causing adRP are largely null alleles, such as deletions, nonsense, or DNA changes leading to premature termination codons and to mRNA degradation [9–14]. Patients are therefore hemizygotes for *PRPF31*, suggesting that the molecular pathophysiology of the disease is due to the functional loss of one allele and to haploinsufficiency [10,12,15]. The ubiquitous expression of *PRPF31* has allowed a number of functional studies to be performed in immortalized lymphoblastoid cell lines (LCLs) from patients and asymptomatic carriers of mutations [16–18]. In particular, it has been shown that penetrance of mutations is due to the differential expression of the *PRPF31* allele that is not inactivated by mutations, in both symptomatic and asymptomatic individuals. Unlike affected persons, asymptomatic carriers naturally express high amounts of functional *PRPF31* mRNA, a phenomenon that compensates for the mutation-induced loss of one allele and prevents manifestation of symptoms [16–18].

Author Summary

Retinitis pigmentosa (RP) is an inherited disorder of the retina that is caused by mutations in more than 50 genes. Dominant mutations in one of these, *PRPF31*, can be non-penetrant. That is, some carriers of mutations suffer from the disease while others do not display any symptoms. In these particular individuals, functional *PRPF31* transcripts are expressed at higher levels compared to affected persons, thus compensating for the deleterious effects of the mutated allele. Up to now, the nature of such a stochastic and protective effect was unknown. In this work, we identify *CNOT3* as the modifier gene responsible for penetrance of *PRPF31* mutations. We show that *CNOT3* is a negative regulator of *PRPF31* expression and modulates *PRPF31* transcription by directly binding to its promoter. In asymptomatic carriers of mutations, *CNOT3* expression is lower, allowing higher amounts of *PRPF31* to be produced and therefore inhibiting the development of symptoms. Finally, we find that a polymorphism within a *CNOT3* intronic region is associated with the clinical manifestation of the disease.

This variable expression of *PRPF31* seems to be present within the general population [16] and therefore asymptomatic carriers of mutations would be individuals that by chance are “high expressors”. Furthermore, protection from *PRPF31* mutations (and therefore variable *PRPF31* expression) is itself an inheritable character [16,19]. In an elegant meta-analytic study, McGee *et al.* [19] have shown that protective alleles, named isoalleles, are inherited by carriers of *PRPF31* mutations from the parent who does not transmit the mutation (i.e. they are *in trans* with respect to the mutation). Furthermore, such isoalleles would be responsible for the majority of incomplete penetrance cases, and map to chromosome 19q13.4, in proximity to *PRPF31* itself [19]. The same study also indicated that these isoalleles were not the only modulators of *PRPF31* penetrance, since some individuals with discordant phenotypes carried an identical wild-type haplotype for the isoalleles on chromosome 19. Another genetic element potentially capable of influencing the penetrance of *PRPF31* mutation was later mapped to chromosome 14q21–23 [16].

In this study, we search for and identify the major modifier gene responsible for penetrance of *PRPF31* mutations, through the analysis of LCLs from a very large family with adRP due to a *PRPF31* microdeletion [6,20].

Results

CNOT3 expression is inversely proportional to that of *PRPF31* in asymptomatic and affected carriers of mutations

The region on chromosome 19q13.4 harboring the main modifier gene for *PRPF31* penetrance was determined by McGee *et al.* to lie between microsatellite markers D19S572 and D19S926 [19]. This interval contains 118 genes, including 50 protein-coding genes, 50 miRNAs and 18 pseudogenes.

Based on data from lymphoblast studies describing the nature and the possible mechanism of action of the penetrance modifier gene [16–18], we selected protein-coding genes that were consistently expressed in LCLs, as detected by q-PCR (18 genes). We also excluded some of the genes that in this region belong to the leukocyte receptor cluster (LRC) and are implicated exclusively in leukocyte functions. We were left with 10 sequences, namely: *NDUFA3*, *TFPT*, *CNOT3*, *LENG1*, *MBOAT7*, *TSEN34*, *RPS9*,

LILRB3, *ILT7*, and *NALP2*. We then measured by q-PCR the mRNA expression levels of these genes in LCLs from 4 asymptomatic and 6 affected individuals from the RP856/AD5 family (Table S1 and Figure S1). All genes showed consistent expression across the family members. Of these, only *CNOT3* showed a statistically significant difference in mRNA expression between the two groups of individuals ($p < 0.01$) (Figure 1 and Figure S1). Unexpectedly, *CNOT3* trend of expression was the opposite to that of *PRPF31*, as it showed lower expression in asymptomatic than in the affected carriers of *PRPF31* mutations (Figure 1B). This phenomenon was particularly clear when expression of *CNOT3* and *PRPF31* were paired by cell lines and the relevant regression lines calculated (Figure 1C).

Assessment of *CNOT3* protein by quantitative western blotting confirmed the differential expression detected by q-PCR (Figure 1D).

CNOT3 is a negative regulator of *PRPF31* expression

CNOT3 belongs to the Ccr4-Not complex, a conserved multi-protein structure involved in the regulation of gene expression [21].

To investigate if *CNOT3* could influence *PRPF31* expression, we silenced its expression in ARPE-19 cell lines, by using two different siRNA sequences. Suppression of *CNOT3* resulted in significant increase of *PRPF31* mRNA and protein ($p < 0.001$, Figure 2). This effect was very specific, as no influence was observed in negative controls and in *TFPT* expression, a neighboring gene sharing part of the promoter with *PRPF31* (Figure S2).

CNOT3-dependent modulation of *PRPF31* expression is achieved at the transcriptional level

CNOT3 can negatively regulate transcription by either directly binding to the promoter of target genes or by affecting their mRNA rate of degradation [22,23].

To understand which could be the mechanism through which *CNOT3* modulates *PRPF31* expression, we incubated LCLs from two asymptomatic-affected pairs with Actinomycin D, a drug that inhibits *de novo* transcription, and then measured the rate of decay of *PRPF31* mRNA. No statistically significant difference was observed between the asymptomatic and affected individuals (Figure S3), suggesting that the modulation of *PRPF31* expression happens most probably at the transcriptional level.

CNOT3 binds directly to the *PRPF31* promoter

To test this hypothesis, we performed a Chromatin Immunoprecipitation (ChIP) assay in LCLs from 3 healthy individuals, using an anti-*CNOT3* antibody and serum IgG as a negative control. To confirm that *CNOT3* enrichment of a target DNA region was due to a specific immunoprecipitation rather than to a random precipitation of DNA, we designed primers targeting genomic regions that were not supposed to be bound by *CNOT3*. Primers targeting *CNOT3* promoter were used as a positive control, since it has been previously shown that *CNOT3* self-regulates its expression by binding to its own promoter [23]. Both qualitative and quantitative PCR showed a statistically significant enrichment in *PRPF31* promoter sequences in DNA that was immunoprecipitated by the *CNOT3* antibody, compared to that exposed to serum IgG (Figure 3A, 3B).

CNOT3 rs4806718 alleles are associated with the clinical manifestation of the disease

In order to identify genetic markers that could be associated with variable expression of *CNOT3* and therefore with penetrance

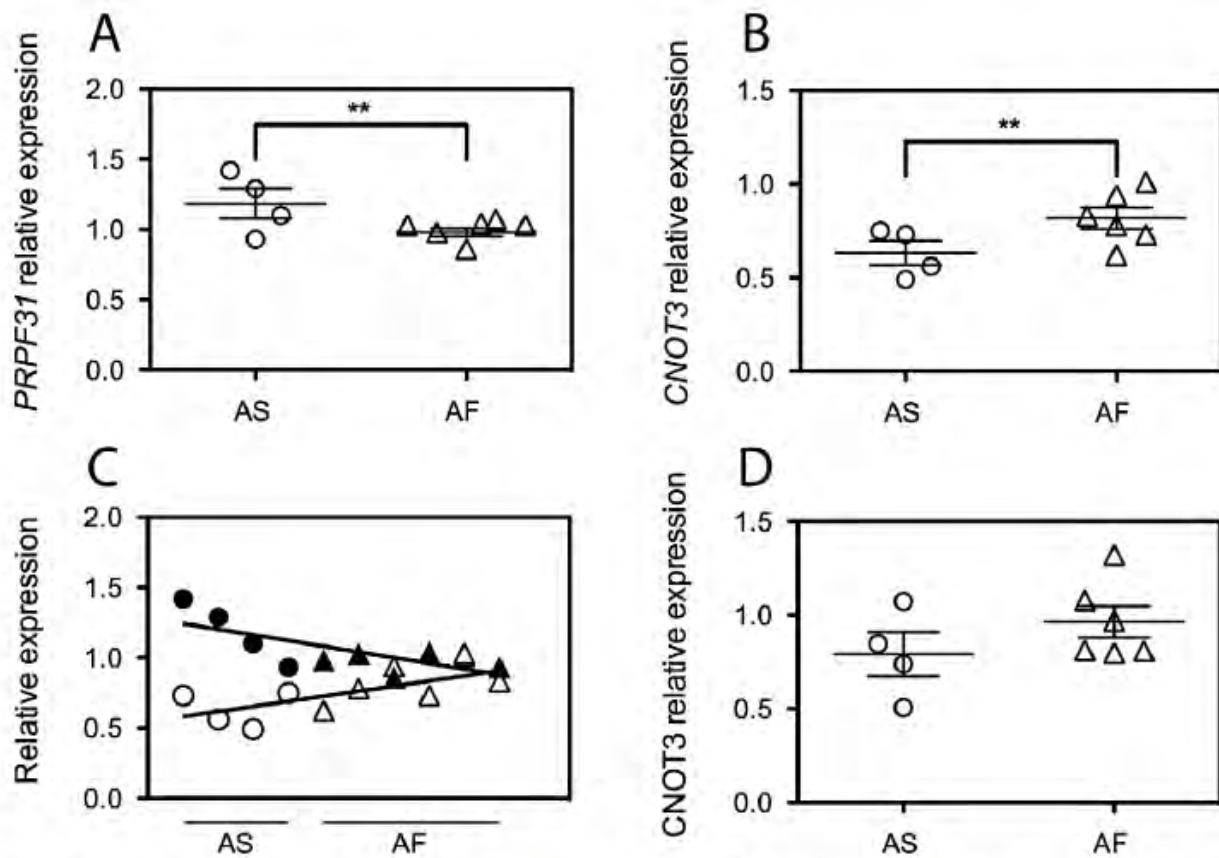


Figure 1. *CNOT3* shows an opposite trend of expression with respect to that of *PRPF31* between the asymptomatic (AS) and affected (AF) individuals of the AD5 family. (A) *PRPF31* mRNA expression normalized to the housekeeping gene *GAPDH*. Error bars refer to the standard deviation of the mean for 5 independent experiments for each group. (B) *CNOT3* mRNA expression from the same 5 experiments used to generate *PRPF31* data. **, $p < 0.01$. (C) Linear regression analysis of *PRPF31* and *CNOT3* mRNA expression, which shows an inverse trend of the two genes in each cell line. Circles, asymptomatic subjects; triangles, affected individuals; open symbols, *CNOT3* expression; filled symbols, *PRPF31* expression. Data having the same value for the x axis have been obtained from the same individual. (D) Quantification of *CNOT3* protein abundance relative to β -actin from 3 independent SDS-PAGE gels, after simultaneous detection of the two proteins by quantitative LI-COR western blot
doi:10.1371/journal.pgen.1003040.g001

of *PRPF31* mutations, we sequenced the entire *CNOT3* genomic region by next-generation sequencing (NGS) in one asymptomatic-affected sibling pair. We identified five polymorphic variants (rs36643, rs56079424, rs36661, rs4806718, rs105234) that

differed between the two subjects. These five variants were subsequently analyzed in a second asymptomatic-affected sibling pair from the same pedigree, showing that only alleles of rs4806718, lying in intron 17 of *CNOT3*, segregated with the trait.

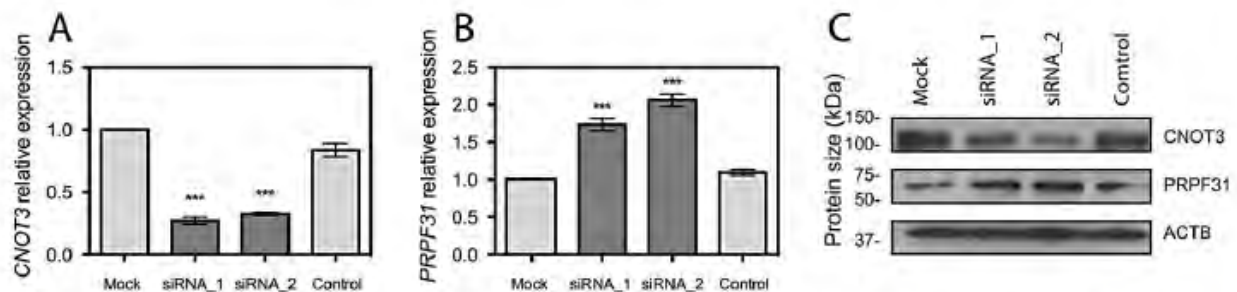


Figure 2. *CNOT3* silencing stimulates *PRPF31* expression in ARPE-19 cells. (A) *CNOT3* mRNA depletion by 2 different siRNA sequences and its effect on *PRPF31* mRNA expression (B). ***, $p < 0.001$. (C) Representative western blot of *CNOT3* silencing and effect on *PRPF31* protein expression. siRNA_1 and siRNA_2, different *CNOT3*-specific siRNA sequences; Control, treatment with transfection reagent with no siRNA; Mock, treatment with transfection reagent and scrambled siRNA.
doi:10.1371/journal.pgen.1003040.g002

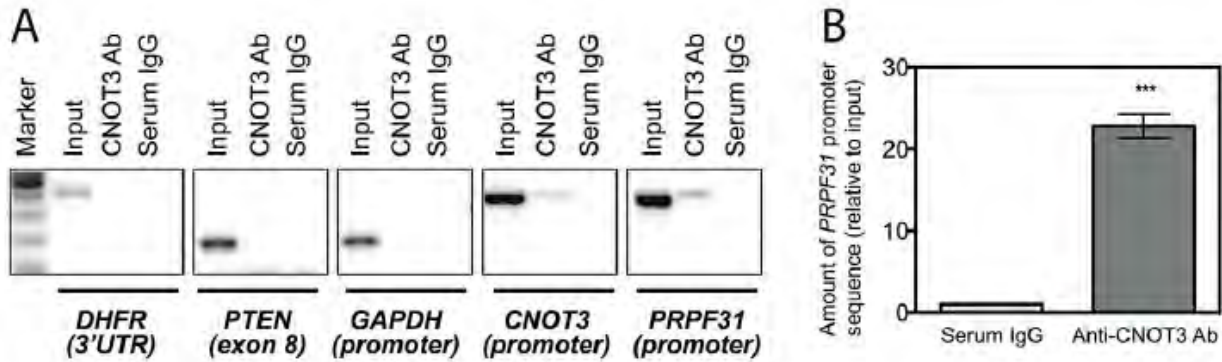


Figure 3. CNOT3 binds to the *PRPF31* promoter in cells. (A) CNOT3 ChIP-PCRs on different target sequences. Enrichment is visible only for *PRPF31* promoter and *CNOT3* promoter (positive control); *DHFR* 3'UTR, *PTEN* exon8, and *GAPDH* promoter sequences are all negative controls. (B) CNOT3 ChIP-qPCR on *PRPF31* promoter sequence. Error bars indicate the standard deviation of the mean for three independent ChIP-qPCR experiments. Serum IgG is used as IP negative control. ***, $p < 0.001$. doi:10.1371/journal.pgen.1003040.g003

This SNP was then sequenced in a total of 38 asymptomatic and affected individuals from the RP856/AD5 family, as well as from an unrelated family for which the modifier gene for *PRPF31* penetrance was also found to be linked to chromosome 19q13.4 [24] (Figure 4). Association between the C allele of rs4806718 with the affected status and the T allele with the asymptomatic status was moderately significant ($p = 0.04$, by Fisher exact test).

Discussion

Despite penetrance being an old concept in genetics, little is known about its molecular causes, especially in inherited human diseases. Notable positive examples include dominant erythropoietic protoporphyria, caused by mutations in the *FECH* gene, and

dominant elliptocytosis, due to mutations in *SPTA1*. In these disorders, an imbalance of expression between the wild-type and the mutated alleles causes the manifestation of the symptoms [25–27].

Similar mechanisms determine penetrance of *PRPF31* mutations, since asymptomatic carriers are individuals who display increased levels of wild-type mRNA alleles, which in turn compensate for the deficiency caused by the mutation [16–18]. However, unlike erythropoietic protoporphyria and elliptocytosis, in *PRPF31*-linked adRP the molecular causes of such beneficial hyper-expression have remained, up to now, unexplained. Previous mapping studies have shown that the penetrance and expression of *PRPF31* is influenced by at least two loci: one, likely having a major effect, lies within the same chromosomal region as

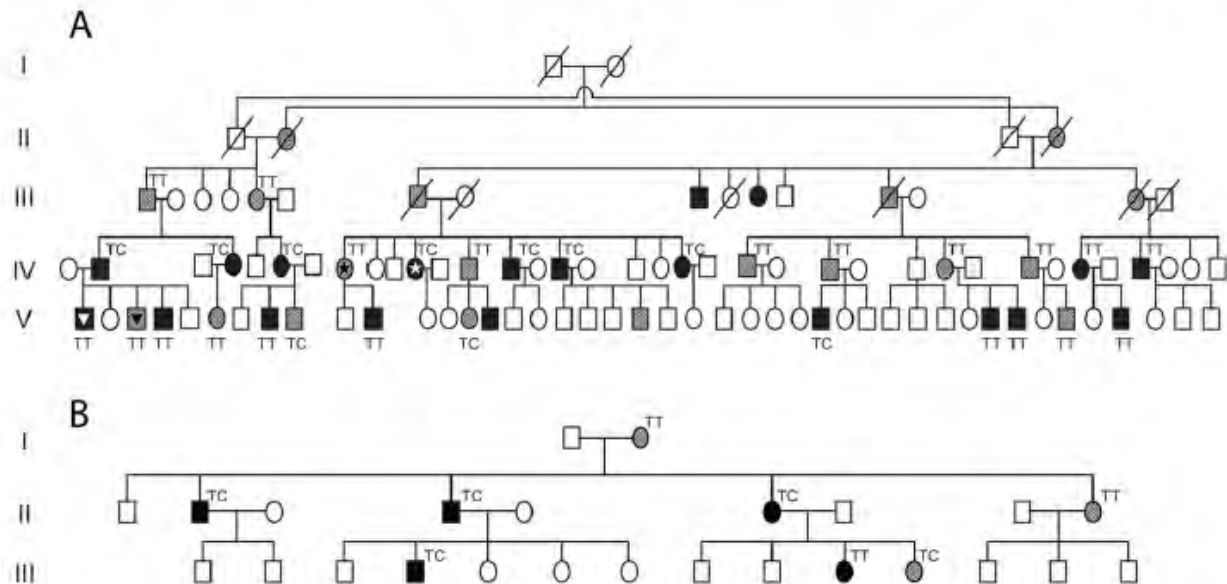


Figure 4. Analysis of rs4806718 alleles in two unrelated pedigrees. (A) Family RP856/AD5. The individuals initially tested with NGS are marked with a star. The individuals marked with a triangle belong to a sibship pair, which was previously shown by McGee et al. to have the same isoallele haplotype but different phenotypes. (B) Family ADB1, a Bulgarian gypsy family carrying a heterozygous splice site mutation in *PRPF31* (NM_015629.3:c.527+1G>T, or IVS6+1G>T). In both pedigrees carriers of mutations are either in black (affected individuals) or in grey (asymptomatic individuals). doi:10.1371/journal.pgen.1003040.g004

PRPF31 (proximal modifier), the other is on chromosome 14 (distant modifier) [16,19]. Our previous work has also demonstrated that both modifiers would act through diffusible elements (e.g. transcription factors) since their effects on *PRPF31* mRNA expression concerns equally both copies of the gene [16]. This observation probably explains the failure of previous attempts to identify the proximal modifier as a polymorphic variant of the *PRPF31* sequence itself, according to the *FECH* or *SPTA1* models.

Based on this previous knowledge, we reasoned that the expression of the proximal modifier of *PRPF31* mutations should correlate with that of *PRPF31*. Therefore we started assessing mRNA levels of genes that reside within the mapped 19q13.4 interval, by using the same cellular model successfully used in previous studies of PRPF molecular genetics, and in particular of *PRPF31* penetrance [10,15–18,28,29]. Specifically, we studied cells derived from members of one of the largest pedigrees known to segregate a *PRPF31* mutation, family RP856/AD5 [6,20], for which incomplete penetrance could also be, at least in part, determined by the proximal modifier [19]. Following a filtering process based on both *in silico* analyses and on mRNA expression, we were left with only 10 candidates. Of these, only one, *CNOT3*, showed a pattern of expression that significantly correlated to that of *PRPF31*. Interestingly, its trend of expression was inverse to that of *PRPF31*, raising the possibility that *CNOT3* may be a negative regulator of *PRPF31* expression.

CNOT3 encodes a protein that is part of the Ccr4-Not multi-subunit complex, an evolutionary conserved multimeric structure involved in modulation of gene expression [21,30–34]. Evidences that *CNOT3* could be a negative regulator of transcription have been provided in yeast [31], and then confirmed in human cell lines, by the identification of a conserved motif at its C-terminus, called the Not-Box. This motif was originally identified in another subunit of the complex, *CNOT2*, where it was shown to repress reporter gene activity upon promoter targeting [35]. We confirmed the role of *CNOT3* as a negative regulator of *PRPF31* expression by siRNA-mediated silencing experiments in ARPE-19 cells. Specifically, we observed that 70% depletion of *CNOT3* induced approximately a 2-fold increase in *PRPF31* expression, but had no effects on *TFPT*, a gene that is contiguous to *PRPF31* and shares with it part of the promoter [36].

CNOT3 can modulate transcription of its targets by the direct binding to their promoters [23] or by promoting the recruitment of deadenylases at the 3' end of their transcripts [22]. Our data provide evidence showing that regulation of *PRPF31* expression should be mainly at the transcriptional level. First, we observed that decay of *PRPF31* mRNA was roughly the same in cells from individuals expressing different levels of *CNOT3*, disfavoring gene modulation through post-transcriptional mechanisms. Second, we showed by ChIP that *CNOT3* could bind directly to the *bona fide* *PRPF31* promoter.

In their work, McGee *et al.* identified the chromosomal interval containing the proximal modifier through linkage analysis, a technique that searches for relationships between phenotypes and physical elements on the DNA sequence [19]. This implies that variable expression of *CNOT3* must be determined by a DNA variant that is present in this same region, possibly within *CNOT3* itself. Given their supposedly high frequency within the general population, these isoalleles would very likely be polymorphic elements. Our search for *CNOT3* DNA changes that would be present in asymptomatic but not in affected carriers of mutations (or vice versa) resulted in the identification of particular alleles of rs4806718.

Are these the isoalleles originally mapped by McGee *et al.*? Although statistically significant, the association between

rs4806718's C allele and disease (and the T allele with an unaffected status) was not perfect. This phenomenon can be explained by the presence of additional factors capable of determining *PRPF31* penetrance, such as the one mapped on chromosome 14 [16]. These modifiers could interfere with or even mask the effects of rs4806718 alleles, ultimately allowing the "wrong" rs4806718 variant to be associated with either phenotype. Such a hypothesis is in perfect agreement with the original data on *PRPF31* isoalleles, as a few discordant phenotype-genotype associations concerning the mapped locus for the proximal modifier were also clearly recognized. Amongst other examples, 2 siblings from the last generation of RP856/AD5 had discordant phenotypes but concordant haplotypes [19,37]. These same individuals, genotyped by us at the rs4806718 locus, were found indeed to share the same parental allele. Furthermore, if the modifier allele is truly inherited from the parent who does not transmit the mutation, then the chance that this does not forcibly correspond to an rs4806718 allele is relatively high in RP856/AD5, given the number of spouses external to the family who are present in this pedigree.

Another important element to consider is whether rs4806718 alleles have a direct effect on *CNOT3* expression, or whether the two factors are simply in linkage disequilibrium with other elements (e.g. transcription enhancers) lying somewhere else in the region. According to *in silico* prediction tools, the rs4806718 C variant, which has a frequency of 0.38 in the European population, could affect *CNOT3* splicing by decreasing the binding energy for one acceptor splice site. Therefore, at least potentially, rs4806718 alleles could represent the true *PRPF31* isoalleles.

Taken together, all our observations suggest that *CNOT3* is the modifier gene on chromosome 19q13.4 that is responsible for penetrance of *PRPF31* mutations. Through direct repression of *PRPF31* transcription and in virtue of its own variable expression, *CNOT3* would differentially reduce the amount of available *PRPF31* mRNA, thus determining incomplete penetrance. Although further studies on the physiological role of *CNOT3* in human cells and tissues are definitely needed, our data open the way for a possible treatment of *PRPF31*-linked RP through the inhibition of this transcriptional regulator.

Materials and Methods

Patients and cell lines

This study involved 10 individuals from the British family RP856/AD5, segregating an 11-bp deletion in exon 11 of *PRPF31* (c.1115_1125del) [6,20]. Our research has been conducted in accordance with the tenets of the Declaration of Helsinki and has been approved by the IRBs of our Institutions. Lymphoblastoid cell lines derived from peripheral blood leukocytes of each individual were either obtained from the Coriell Cell Repositories or through the immortalization of peripheral blood leukocytes. Cells were grown and maintained as previously described [18].

The human retinal pigment epithelial cell line ARPE-19 (kindly provided by Dr. Yvan Arsenijevic) was grown and maintained at 37°C with 5% CO₂ in N1 medium (DMEM/F12 complemented with 2.5 mM L-glutamine, 56 mM NaHCO₃, and 10% fetal bovine serum).

RNA extraction and cDNA synthesis

Lymphoblasts were harvested during their exponential growth phase (500,000–1,000,000 cells/ml) and RNA was isolated from 10⁷ cells using the QIAGEN RNeasy Mini Kit, following the manufacturer's instructions. The only modification to the protocol concerned the DNase treatment, since we used double the amount

of enzyme compared to the suggested quantity. RNA concentration was measured with the DropSense 96 spectrophotometer (Trinean). cDNA synthesis was carried out as previously described [10].

q-PCR primer design and optimization

Most of the primer sequences used in this study were annotated in the qPrimerDepot database (<http://primerdepot.nci.nih.gov/>). These sequences are specifically designed to span exon-exon junctions, thus avoiding genomic DNA to be amplified during q-PCR. To design other primer sequences, which were not present in the qPrimerDepot database, we used the Primer Blast tool from NCBI (<http://www.ncbi.nlm.nih.gov/tools/primer-blast/>). To validate each primer pair for q-PCR we first optimized the primer amounts (50–200 nM), and then loaded 10 μ l of the q-PCR product obtained on a 1% agarose gel, in order to check the specificity of the amplification product. Finally, a standard curve using a control cDNA template was used to test each primer pair's efficiency. We considered as acceptable ranges of efficiency between 90 and 110%, corresponding to standard curve slopes between -3.6 and -3.1 . All primer pairs used for this study are listed in Table S2. For *GAPDH* and *PRPF31* amplification we used primers and probes previously described [16].

Real-time quantitative PCR

All genes but *PRPF31* and *GAPDH* were amplified with the Sybr Green PCR Master Mix (Applied Biosystems). Q-PCR reactions were performed as published [16]. After having assessed that PCR efficiencies for all genes were comparable, mRNA expression of each of them was normalized with respect to *GAPDH*, using the $\Delta\Delta C_t$ method.

Protein extraction

Total protein was extracted from lymphoblastoid cell lines in RIPA buffer as reported before [10]. ARPE-19 whole cell lysate was obtained by scraping the cells into 150 μ l of lysis buffer (20 mM Tris HCl, pH 8.0, 150 mM NaCl, 10% glycerol, 2 mM EDTA, 1% TritonX-100) complemented with protease and phosphatase inhibitors, and incubated on ice for 15 minutes followed by a centrifugation at 14,000 rpm for 30 minutes at 4°C. Proteins concentration was measured with the BCA protein assay kit (Pierce), using BSA to generate a standard curve.

Western blot

Anti-PRPF31 antibody was raised in rabbit as previously described [10]. Rabbit anti-CNOT3 antibody was purchased by Bethyl Laboratories. This targets residues 525 to 575 of the human CNOT3 protein (NP_055331.1), allowing detection of a 117-kDa protein. Mouse anti- β -actin antibody (Sigma) was used as a loading control.

Equal amounts of proteins were loaded and run on an 8% SDS-PAGE gel. Proteins were transferred to a nitrocellulose membrane and blocked in 5% milk overnight at 4°C or alternatively for 1 hour at room temperature. The incubation of all primary antibodies was performed for 1 hour at room temperature using the following dilutions: anti-PRPF31 (1:500), anti-CNOT3 (1:2,000), and anti- β -ACTIN (1:2,500). The membrane was washed 3 times with 0.05% Tween-20 in TBS. Rabbit and mouse HRP-conjugated secondary antibodies were diluted 1:1,000 in 2% milk and incubated for 1 hour at room temperature. Bands were detected using enhanced chemiluminescence (Pierce).

Signal detection via the Odyssey infrared imaging system (LI-COR) was performed by using fluorescently-labeled secondary antibodies provided by LI-COR, diluted 1:5,000 in 0.5% milk and

incubated in the dark, for 1 hour at room temperature. The membrane was then washed twice with 0.05% Tween-20 in TBS and once in PBS to remove residual Tween-20 prior to the laser scanning.

In vitro silencing experiments

We used two different siRNA sequences targeting *CNOT3* (QIAGEN, FlexiTube siRNA, Hs_CNOT3_5 and Hs_CNOT3_8, 1 nmol) and a negative control siRNA for human genes (Santa Cruz Biotechnology). One day before transfection ARPE-19 cells were seeded at a concentration of 2×10^5 cells/well in a 6 well-plate, and transfection was achieved by using 5 μ l Lipofectamine (Invitrogen) and 50 pmol siRNA. RNA was extracted 48 hrs after transfection.

Actinomycin D treatment of cells

Lymphoblasts grown at a concentration of ~ 8 million cells in a T75 flask were treated with Actinomycin D (5 μ g/ml in DMSO) (Sigma) by adding it directly to the medium. Cell pellets were collected at seven different time points (0–24 hrs) and total RNA was extracted and analyzed by q-PCR.

Chromatin immunoprecipitation (ChIP)

Three control lymphoblastoid cells from the Centre d'Etude du Polymorphisme Humain (CEPH) were grown to have 10^7 cells per ChIP experiment. DNA and proteins were cross-linked by adding 1% formaldehyde directly to the medium and by incubating the cells on a rotating hybridization oven at 37°C for 10 minutes. To quench cross-linking, we then added 125 mM glycine and incubated the cells at 37°C for 5 minutes. Cells were pelleted by centrifugation (800 g for 5 minutes at 4°C) and washed twice with cold PBS, supplemented with protease inhibitors. Optimization of the chromatin shearing was performed by using a Covaris sonicator, to obtain on average cross-linked DNA fragments of 150–400 bp. ChIP was performed using buffers provided with the Ep-iT Chromatin Immunoprecipitation kit (Bio-AAB). Immunoprecipitation was performed using three different antibodies: anti-CNOT3, anti-pol2 (Bio-AAB) as a positive control for IP, and serum IgG (Santa Cruz Biotechnology) as a negative control for IP. Antibody-protein-DNA complexes were collected on protein A agarose beads (2 hrs, 4°C), then washed with the low salt buffer, high salt buffer, LiCl buffer, and TE buffer (pH 8.0) provided in the kit to remove non-specific binding. Complexes were eluted from the beads by using the elution buffer (0.1 mM NaHCO₃ and 1% SDS) in an orbital shaker. Cross-links were removed by an overnight incubation at 65°C. Ribonuclease and proteinase K digestion were added to remove specific contaminants, before the eluted DNA was extracted once in 25:24:1 phenol-chloroform-isoamyl alcohol and once in 24:1 chloroform-isoamyl alcohol. DNA was ethanol precipitated, washed in 70% ethanol, and finally eluted in TE.

ChIP-PCR was performed using the GoTaq DNA Polymerase (Promega) and 0.5 μ l of the ChIP DNA, by using standard cycling conditions and primers described in Table S3. *GAPDH* primer sequences are the ones provided by Millipore for the EZ-ChIP kit, while primers for *DHFR* have been previously described [38].

Two microliters of ChIP DNA were also amplified by q-PCR using Sybr Green PCR Master Mix (Applied Biosystems) and the *PRPF31* promoter primer pair (Table S3).

Ultra-high-throughput sequencing

CNOT3 genomic region was amplified by 3 overlapping long-range PCRs (Table S4), for a total length of 34 Kb. PCR was

performed in 20 μ l using TaKaRa LA Taq and GC buffer I (Takara Bio Inc.). Final primers concentration was 1 μ M, and 200 ng of genomic DNA were used as template. PCR amplification conditions were: an initial step at 94°C for 1 minute, 30 cycles of denaturation at 98°C for 5 seconds and annealing/extension at 68°C for 15 minutes, and a final extension step at 72°C for 10 minutes. Long-range PCR products were sequenced with an Illumina HiSeq 2000 machine, to obtain coverage values in the range of thousands of reads. Mapping of the reads and variant detection was performed by using the CLCbio Genomics Workbench software.

Statistical analysis

Differences of gene expression between asymptomatic and affected individuals were tested by t-test, and likelihood computed by 100 Monte Carlo label-swapping simulations per each gene.

One-way ANOVA followed by Bonferroni's multiple comparison tests was used to analyze the effect of CNOT3 silencing on the expression of the target genes. The enrichment of PRPF31 promoter sequence after CNOT3 immunoprecipitation compared to the serum IgG was evaluated by using the Mann Whitney non-parametric statistical hypothesis test.

In figures, $p < 0.05$ is indicated by one star, $p < 0.01$ by 2 stars, and $p < 0.001$ by 3 stars.

Supporting Information

Figure S1 Gene expression analysis of candidate genes in LCLs derived from asymptomatic (AS) and affected (AF) carriers of mutations. mRNA expression of each gene is normalized to the housekeeping gene *GAPDH*. Error bars refer to the standard deviation of the mean for each group. (PDF)

Figure S2 Effect of CNOT3 silencing on the mRNA expression of two housekeeping genes and *TFPT*, in ARPE-19 cells. The data presented here are from the same experiments shown in Figure 2. Depletion of CNOT3 has no effects on the mRNA expression of

these control genes. Mock, scrambled siRNA sequence; siRNA_1 and siRNA_2, sequences specific for CNOT3; Control, cells treated with no siRNA. Error bars refer to the standard deviation of the mean for three independent experiments. (PDF)

Figure S3 PRPF31 mRNA decay in LCLs from asymptomatic and affected carriers of mutations, following treatment with actinomycin D. mRNA half-life is similar in both groups. Error bars refer to the standard deviation of the mean at different time points for at least three independent experiments. (PDF)

Table S1 Lymphoblastoid cell lines from the RP856/AD5 family used in this work. (PDF)

Table S2 Primers for q-PCR amplification. Annealing temperature for all primers is 60°C. (PDF)

Table S3 Primers for ChIP-PCR. (PDF)

Table S4 Primers for CNOT3 long-range PCR amplification. (PDF)

Acknowledgments

We would like to thank A. Ransijn for technical assistance, P. Zavad'akova for q-PCR optimization protocols, and P. Benaglio for help with NGS data analysis. NGS sequencing was performed at the Lausanne Genomic Technologies Facility. We are also grateful to G. Tanackovic and L. Carliato for helpful discussions.

Author Contributions

Conceived and designed the experiments: GV SSB CR. Performed the experiments: GV AMR AZS CR. Analyzed the data: GV CR. Contributed reagents/materials/analysis tools: AMR AZS SSB. Wrote the paper: GV CR.

References

- Ahluwalia JK, Hariharan M, Bargaje R, Pillai B, Brahmachari V (2009) Incomplete penetrance and variable expressivity: is there a microRNA connection? *Bioessays* 31: 981–992.
- Zlotogora J (2003) Penetrance and expressivity in the molecular age. *Genet Med* 5: 347–352.
- Berson EL (1993) Retinitis pigmentosa. The Friedenwald Lecture. *Invest Ophthalmol Vis Sci* 34: 1659–1676.
- Hantong DT, Berson EL, Dryja TP (2006) Retinitis pigmentosa. *Lancet* 368: 1795–1809.
- Evans K, al-Maghitheh M, Fitzke FW, Moore AT, Jay M, et al. (1995) Binodal expressivity in dominant retinitis pigmentosa genetically linked to chromosome 19q. *Br J Ophthalmol* 79: 841–846.
- Moore AT, Fitzke F, Jay M, Arden GB, Inglehearn CF, et al. (1993) Autosomal dominant retinitis pigmentosa with apparent incomplete penetrance: a clinical, electrophysiological, psychophysical, and molecular genetic study. *Br J Ophthalmol* 77: 473–479.
- Berson EL, Simonoff EA (1979) Dominant retinitis pigmentosa with reduced penetrance. Further studies of the electroretinogram. *Arch Ophthalmol* 97: 1286–1291.
- Berson EL, Gouras P, Gunkel RD, Myrianthopoulos NC (1969) Dominant retinitis pigmentosa with reduced penetrance. *Arch Ophthalmol* 81: 226–234.
- Rose AM, Mukhopadhyay R, Webster AR, Bhattacharya SS, Waseem NH (2011) A 112 kb deletion in chromosome 19q13.42 leads to retinitis pigmentosa. *Invest Ophthalmol Vis Sci* 52: 6597–6603.
- Rio Frio T, Wade NM, Ransijn A, Berson EL, Beckmann JS, et al. (2008) Premature termination codons in PRPF31 cause retinitis pigmentosa via haploinsufficiency due to nonsense-mediated mRNA decay. *J Clin Invest* 118: 1519–1531.
- Waseem NH, Vavilavik V, Welster A, Jenkins SA, Bird AC, et al. (2007) Mutations in the gene coding for the pre-mRNA splicing factor, PRPF31, in patients with autosomal dominant retinitis pigmentosa. *Invest Ophthalmol Vis Sci* 48: 1330–1334.
- Abu-Safieh L, Vithana EN, Mantel I, Holder GE, Pelosini I, et al. (2006) A large deletion in the adRP gene PRPF31: evidence that haploinsufficiency is the cause of disease. *Mol Vis* 12: 384–388.
- Sullivan LS, Bowne SJ, Seaman CR, Blanton SH, Lewis RA, et al. (2006) Genomic rearrangements of the PRPF31 gene account for 2.5% of autosomal dominant retinitis pigmentosa. *Invest Ophthalmol Vis Sci* 47: 4579–4588.
- Vithana EN, Abu-Safieh L, Allen MJ, Carey A, Papaioannou M, et al. (2001) A human homolog of yeast pre-mRNA splicing gene, PRP31, underlies autosomal dominant retinitis pigmentosa on chromosome 19q13.4 (RP11). *Mol Cell* 8: 375–381.
- Tanackovic G, Ransijn A, Thibault P, Abou Elela S, Klinck R, et al. (2011) PRPF mutations are associated with generalized defects in spliceosome formation and pre-mRNA splicing in patients with retinitis pigmentosa. *Hum Mol Genet* 20: 2116–2130.
- Rio Frio T, Civic N, Ransijn A, Beckmann JS, Rivolta C (2008) Two transacting eQTLs modulate the penetrance of PRPF31 mutations. *Hum Mol Genet* 17: 3154–3165.
- Rivolta C, McGee TL, Rio Frio T, Jensen RV, Berson EL, et al. (2006) Variation in retinitis pigmentosa-11 (PRPF31 or RP11) gene expression between symptomatic and asymptomatic patients with dominant RP11 mutations. *Hum Mutat* 27: 644–653.
- Vithana EN, Abu-Safieh L, Pelosini I, Winchester E, Horman D, et al. (2003) Expression of PRPF31 mRNA in patients with autosomal dominant retinitis pigmentosa: a molecular clue for incomplete penetrance? *Invest Ophthalmol Vis Sci* 44: 4204–4209.
- McGee TL, Devoto M, Ott J, Berson EL, Dryja TP (1997) Evidence that the penetrance of mutations at the RP11 locus causing dominant retinitis pigmentosa is influenced by a gene linked to the homologous RP11 allele. *Am J Hum Genet* 61: 1059–1066.
- al-Maghitheh M, Inglehearn CF, Keen TJ, Evans K, Moore AT, et al. (1994) Identification of a sixth locus for autosomal dominant retinitis pigmentosa on chromosome 19. *Hum Mol Genet* 3: 351–354.

21. Collart MA, Panasenko OO (2012) The Ccr4-not complex. *Gene* 492: 42–53.
22. Morita M, Oike Y, Nagashima T, Kadamatsu T, Tahara M, et al. (2011) Obesity resistance and increased hepatic expression of catabolism-related mRNAs in *Ccr4-not3*^{-/-} mice. *EMBO J* 30: 4678–4691.
23. Hu G, Kim J, Xu Q, Leng Y, Orkin SH, et al. (2009) A genome-wide RNAi screen identifies a new transcriptional module required for self-renewal. *Genes Dev* 23: 837–848.
24. Chakarova CF, Cherninkova S, Tournev I, Waseem N, Kaneva R, et al. (2006) Molecular genetics of retinitis pigmentosa in two Romani (Gypsy) families. *Mol Vis* 12: 909–914.
25. Gratzner W (1994) Human genetics. Silence speaks in spectrin. *Nature* 372: 620–621.
26. Gouya L, Puy H, Robreau AM, Bourgeois M, Lamoril J, et al. (2002) The penetrance of dominant erythropoietic protoporphyria is modulated by expression of wildtype FECH. *Nat Genet* 30: 27–28.
27. Gouya L, Puy H, Robreau AM, Lyoumi S, Lamoril J, et al. (2004) Modulation of penetrance by the wild-type allele in dominantly inherited erythropoietic protoporphyria and acute hepatic porphyrias. *Hum Genet* 114: 256–262.
28. Ivings L, Tows KV, Matin MA, Taylor C, Ponchel F, et al. (2008) Evaluation of splicing efficiency in lymphoblastoid cell lines from patients with splicing-factor retinitis pigmentosa. *Mol Vis* 14: 2357–2366.
29. Rio Frio T, McGee TL, Wade NM, Iseli C, Beckmann JS, et al. (2009) A single-base substitution within an intronic repetitive element causes dominant retinitis pigmentosa with reduced penetrance. *Hum Mutat* 30: 1340–1347.
30. Winkler GS, Mulder KW, Bardwell VJ, Kalkhoven E, Timmers HT (2006) Human Ccr4-Not complex is a ligand-dependent repressor of nuclear receptor-mediated transcription. *EMBO J* 25: 3089–3099.
31. Collart MA, Strahl K (1994) NOT1(CDC39), NOT2(CDC36), NOT3, and NOT4 encode a global-negative regulator of transcription that differentially affects TATA-element utilization. *Genes Dev* 8: 525–537.
32. Lau NC, Kolkman A, van Schaik FM, Mulder KW, Fijnappel WW, et al. (2009) Human Ccr4-Not complexes contain variable deadenylase subunits. *Biochem J* 422: 443–453.
33. Albert TK, Lemaire M, van Berkum NI, Gentz R, Collart MA, et al. (2000) Isolation and characterization of human orthologs of yeast CCR4-NOT complex subunits. *Nucleic Acids Res* 28: 809–817.
34. Kerr SC, Azzouz N, Fuchs SM, Collart MA, Strahl BD, et al. (2011) The Ccr4-Not complex interacts with the mRNA export machinery. *PLoS ONE* 6: e18302. doi:10.1371/journal.pone.0018302
35. Zwartjes CG, Jayne S, van den Berg DJ, Timmers HT (2004) Repression of promoter activity by CNOT2, a subunit of the transcription regulatory Ccr4-not complex. *J Biol Chem* 279: 10848–10854.
36. Rose AM, Shah AZ, Waseem NH, Chakarova CF, Alfano G, et al. (2012) Expression of *PRPF31* and *TFPT*: regulation in health and retinal disease. *Hum Mol Genet*. In press.
37. Al-Magtheth M, Vithana E, Tattelin E, Jay M, Evans K, et al. (1996) Evidence for a major retinitis pigmentosa locus on 19q13.4 (RP11) and association with a unique bimodal expressivity phenotype. *Am J Hum Genet* 59: 864–871.
38. Oberley MJ, Inman DR, Farnham PJ (2003) E2F6 negatively regulates BRCA1 in human cancer cells without methylation of histone H3 on lysine 9. *J Biol Chem* 278: 42466–42476.

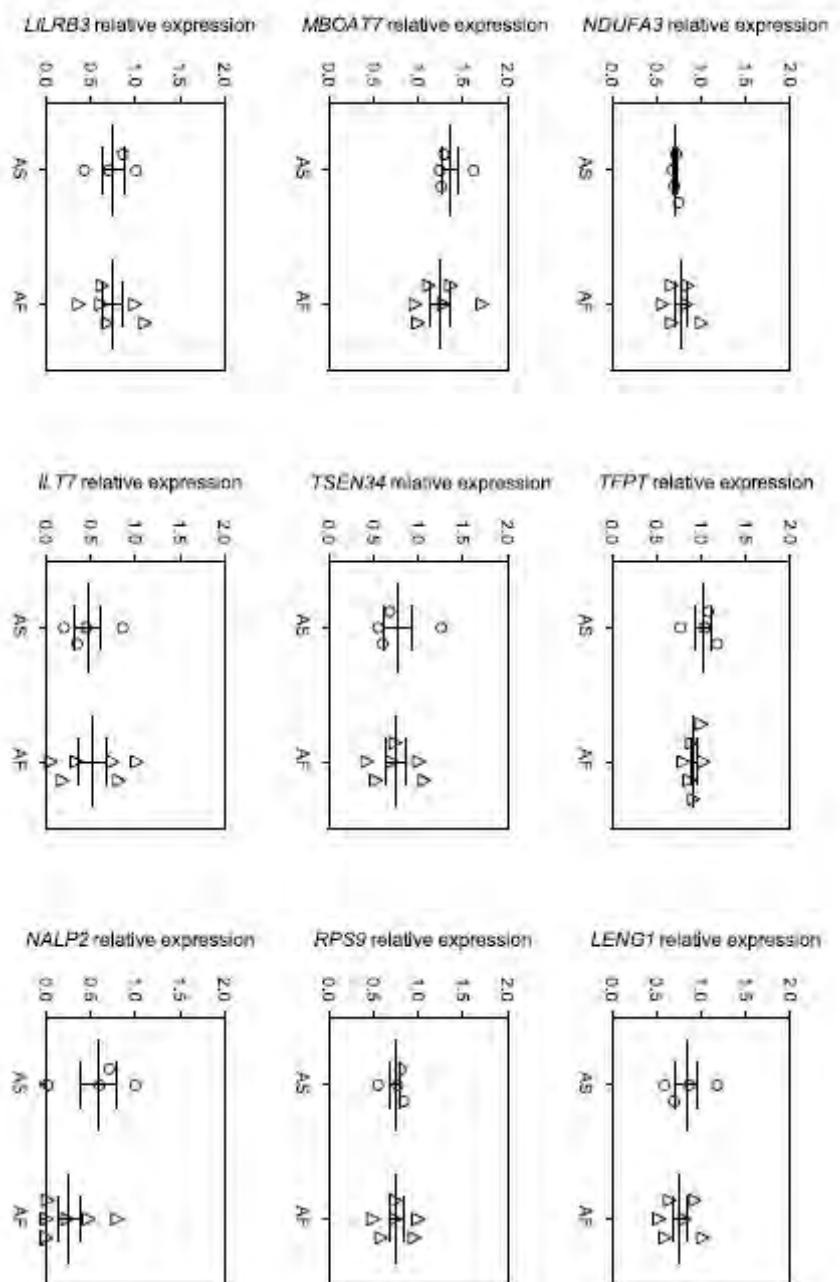


Figure S1. Gene expression analysis of candidate genes in LCLs derived from asymptomatic (AS) and affected (AF) carriers of mutations. mRNA expression of each gene is normalized to the housekeeping gene GAPDH. Error bars refer to the standard deviation of the mean for each group.

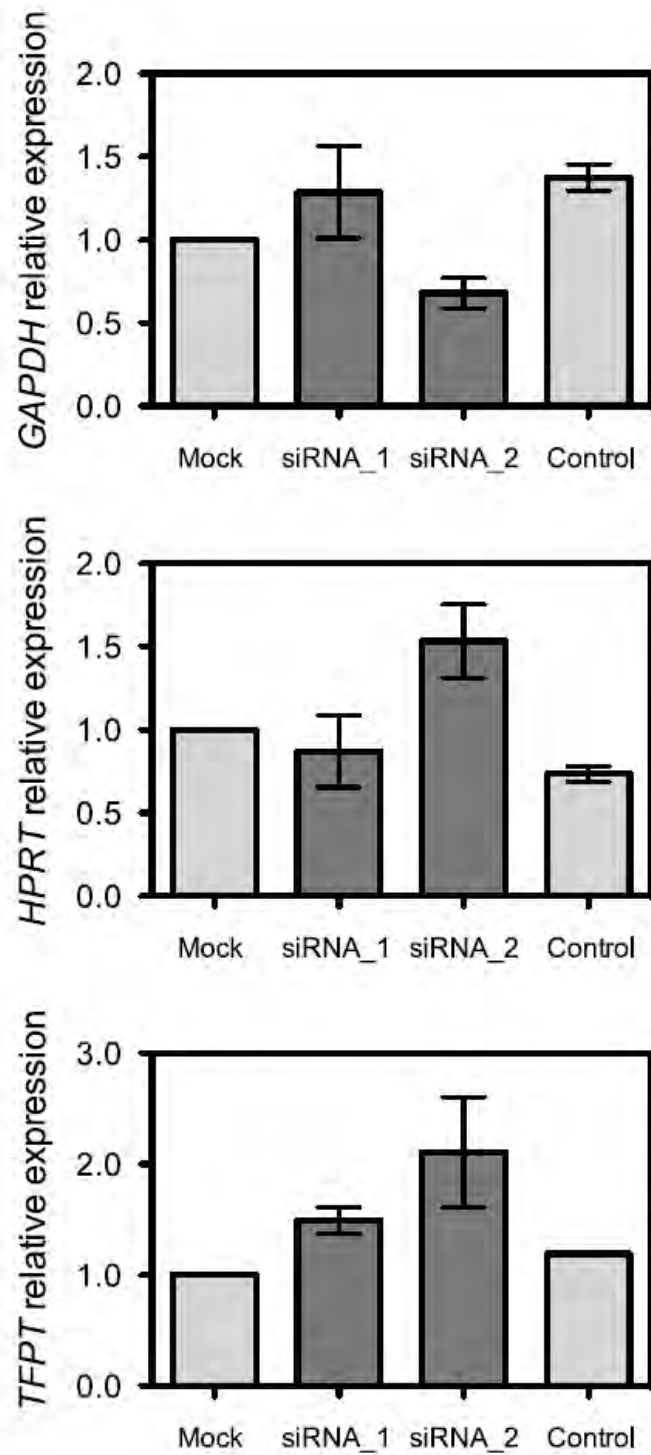


Figure S2. Effect of *CNOT3* silencing on the mRNA expression of two housekeeping genes and *TFPT*, in ARPE-19 cells. The data presented here are from the same experiments shown in Figure 2. Depletion of *CNOT3* has no effects on the mRNA expression of these control genes. Mock, scrambled siRNA sequence; siRNA_1 and siRNA_2, sequences specific for *CNOT3*; Control, cells treated with no siRNA. Error bars refer to the standard deviation of the mean for three independent experiments.

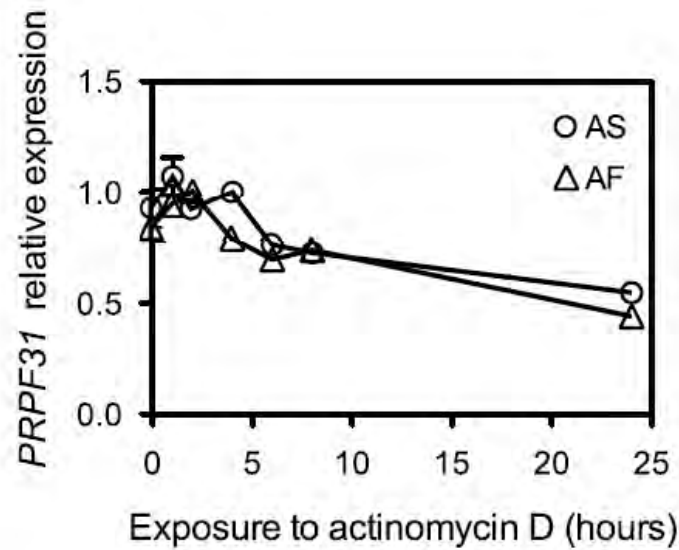


Figure S3. *PRPF31* mRNA decay in LCLs from asymptomatic and affected carriers of mutations, following treatment with actinomycin D. mRNA half-life is similar in both groups. Error bars refer to the standard deviation of the mean at different time points for at least three independent experiments.

Table S1. Lymphoblastoid cell lines from the RP856/AD5 family used in this work.

Cell line	Individual	Clinical status*
AG 307	IV-2	affected
AG 316	IV-8	asymptomatic carrier
AG 319	IV-11	affected
AG 320	IV-14	affected
AG 305	V-1	affected
AG 311	V-6	asymptomatic carrier
AG 353	V-9	asymptomatic carrier
AG 293	V-11	affected
AG 271	V-28	affected
AG 340	V-38	asymptomatic carrier

*As described before in: Vithana et al. (18), Al-Magthteh et al. (37), and Moore et al. (6).

Table S2. Primers for q-PCR amplification. Annealing temperature for all primers is 60°C.

Gene name	Forward primer (5'-3')	Reverse primer (5'-3')	Primer concentration (nM)	Amplification product (bp)
<i>DPRX</i>	GGACCTGAACCCAGGCGCAC	TGCATCTGGCTCTTGCCITTACGA	200/200	78
<i>NALP12</i>	GCACCTTTGAGCGGATAAAC	AAGGCATGTTGACTGGTTCC	200/200	116
<i>MYADM</i>	CCACCAGATCTTTCTCCGTG	AAGATGACGTCGTGGTGGTT	200/200	96
<i>PRKCG</i>	GCCACGAATTTGTGACCTTC	TAGCTATGCAGGCGGAACTT	200/200	94
<i>CACNG7</i>	TACTATCGGGCCTCTCCTTG	GACCACCCGTAGCGATAATG	200/200	118
<i>CACNG8</i>	GAGGATCTGCTGCCTGGA	TAAGGATGGGGAAGATGCTG	200/200	140
<i>CACNG6</i>	AGTTGGAGCCGTCTGCTTT	TACTCGTAGGTGAGGCGTGG	200/200	135
<i>VSTM1</i>	TGGCAGAAGGGACGCTATGA	GCTTGGGCGGTTTCTCATTTC	200/200	101
<i>OLT-2</i>	CGGTGGTCCCTGCCAACAGC	GAAATTCGGCCGCGCCCTCT	200/200	138
<i>OSCAR</i>	TGATCTCCAGCTGCTGAC	CCATGGCTTAGGGTGGTATG	200/200	101
<i>NDUFA3</i>	ACAAAGATGGCTGCGAGAGT	CTCAATGGGGGCAGAATTAC	200/200	113
<i>TFPT</i>	TCGCAGAAAGTACCAGGCACT	CTGCAGCTCCGAGTTATCC	200/100	109
<i>PRPF31</i>	CAGCAAGCAAGCCAAAGCT	CCGGATGAACTTATGGATGATG	200/200	133
<i>LOC100288135</i>	CTGCCGACTTGCCAGGTG	CTGGTGGAGGGGGTGCCCTCG	200/200	142
<i>CNOT3</i>	CGCAAATGGAACGGTTCAAAG	GTATTCTGAGCCACTGGCCA	200/200	136
<i>LENG1</i>	CTCAGCAAGAGGCCCTTACA	AGCAGCTCCCGAAACAGGTC	200/200	127
<i>TMC4</i>	CTCATCTGCCTCTGCTCA	GCTGTAGCTGGTCAGAGCCT	200/200	90
<i>LENG4</i>	AACATGACGGTGCAGTGGT	GATGGTCAGGAAGCTCAGGT	200/100	147
<i>LENG5</i>	ATGAGGTGACTCGCTGGTTC	CACCTCCACCACCAGCAT	200/200	106
<i>RPS9</i>	CTGCTGACGCTTGATGAGAA	CAGCTTCATCTTGCCCTCAT	200/100	105
<i>LILRB3</i>	TGCTATGGTGACACACACCT	ACAGGGAGACGGTGCATAGA	200/200	97
<i>LILRB6</i>	TCACGGTCTGATCTGTCTC	CCAGCTGATCACAGAGCCT	100/200	110
<i>LILRB5</i>	CCGCTGCACAGCTGAGTCC	GGTTTGGGGAGGGTGCCCTGC	200/50	122
<i>LILRB2</i>	GCAGCTGATGCCCCACTCCG	GGGCTGCAGGTGTGGAGATG	200/200	236
<i>LILRA3</i>	CACCTAGCTCCAACCCTAC	GACTTGTTTTGTGGTGGGCT	200/200	100
<i>LIR9</i>	TGATCTGAGICTGCCTGTGG	CAGCTGTGCAGATGGATGAG	200/200	105
<i>ILT7</i>	AACCCCTACCTGCTGTCTCA	GGCAGTCTTGGAACTGAC	200/100	106
<i>LAIR1</i>	AGCCCCCTAAATGGTCTGAG	AGGTGCATGCTATTGTGAC	200/200	98
<i>TTYH1</i>	CACCAGTTGGTGGCACTG	GAGTAGCAGGAAGAGCAGGC	200/200	108
<i>LENG8</i>	CAACTACCACCCTTTTTTCC	AGGGCGGAAGGTTTTGAT	200/200	124
<i>LENG9</i>	ACAGCCACACAGGAAAGAC	ACTGAGCACCATTGGAAAGC	100/200	94
<i>LOC100288231</i>	GCAGCGTGTGCCGGAAGTC	GCGCTGACCCTCCCGTGCC	200/200	130
<i>CDC42EP5</i>	GGCTAGAGCTGGAGTCTGTA	ATCAGGCCCTTCTTGG	200/200	105
<i>LAIR2</i>	TGTCCTCACACCTCACTGCT	GAGATGGAGGGTCTGGGAA	200/200	94
<i>LILRA2</i>	CACCTAGCTCCAACCCTAC	CTGTGTAATCTGGGGGTGT	200/100	147
<i>LILRA1</i>	CACCTAGCTCCAACCCTAC	GACTTGTTTTGTGGTGGGCT	200/200	100
<i>LILRB1</i>	GTCTCAGGACCGICTGGGGGC	TCTGGGGATCCGACCCGGTG	200/200	106
<i>LILRB4</i>	CTGCCGTGAAGAACACACAG	CACCTTGGCATACTGACTG	100/200	98
<i>KIR3DL3</i>	ACAGATGCTTCGGCTCTTTC	ACGTGCAGGTGTCTGGAGTT	200/200	100
<i>KIR2DL3</i>	AACTCGAGTGACCCACTGCT	AACATGCAGGTGTATGGGGT	200/200	108
<i>KIR2DL1</i>	CCCCTGCTTGTCTTCTGTCA	CCAATCAGAATGTGCAGGTG	200/200	105
<i>KIR2DL4</i>	ACCCACTGCCTGTTTCTGTC	ATCACAGCATGCAGGTGTCT	200/200	103
<i>KIR3DL1</i>	ATGTTGCTCATGGTCTGTCAG	AGACAGGAAGGGCTTGTCC	200/200	96
<i>KIR2DS4</i>	AAATAGTTGGCCTTCAACCA	GGAGGATGGTGAAGGGATT	200/200	107
<i>KIR3DL2</i>	AGGTCCCAATCAGAACATGC	AGGTCCCAATCAGAACATGC	200/200	95
<i>FCAR</i>	AAACAGACCACCCTCCTGTG	ATCACAGGACTCGATTTGGC	200/200	107
<i>NCR1</i>	CCACAGCCCACCGAGGGACA	GTGCTGCAGGAAAGGTGGGGTC	200/200	148
<i>NALP7</i>	GGAAGCAAGACCTGACCTGA	CTCGTTACGCTGTCCAGA	200/200	121
<i>NALP2</i>	ATGACCCGAATGGATCTGTC	CGTTCTTCCGTGTTATCCC	200/200	110
<i>GP6</i>	AGCTTGTGGTCACAGGAACC	ATGAGACGGTCAGTTCAGCG	200/200	105

Table S3. Primers for ChIP-PCR.

Gene name	Forward primer (5'-3')	Reverse primer (5'-3')	Annealing temperature (°C)	Amplification product (bp)
<i>DHFR</i>	CTGATGTCCAGGAGGAGAAAGG	AGCCCGACAATGTCAAGGACTG	60	349
<i>PTEN</i>	GTCATTTCATTTCCTTTTCTTTTCT	CTGCACGCTCTATACTGCAAATG	60	169
<i>GAPDH</i>	TACTAGCGGTTTTACGGGCG	TCGAACAGGAGGAGCAGAGAGCGA	65	166
<i>CNOT3</i>	CCCAATCCGCGAAAGGGGGC	ATAGCGGC GCGAAGCGGAAG	69	302
<i>PRPF31</i>	GTCGTCCGGCCACAGCGATT	TCTCCAGACCCAGGAGCCCA	69	306

Table S4. Primers for *CNOT3* long-range PCR amplification.

PCR	Forward primer (5'-3')	Reverse primer (5'-3')	Amplification product (kbp)
#1	GGGCTACGAACTGAAGGATGAGATCGAG	ACCTCAAATCCAGAAAAGCAGCCATACCAATA	11.8
#2	CCTCCCTTCACCCCTGCCTGAGTATGAG	CCCACCGTCTATCCTGCTACACCCACTATCT	11.2
#3	CTGGGTCTCTTTTCTTTCTCTTGGTTGCACT	TGTTTCAGAGCCCTTTTCTCCGTGCT	11.2

2.1 Additional experiments (unpublished results)

Results, Part 1 and 2) After the publication of the paper we had access to two other families with *PRPF31*-linked adRP showing incomplete penetrance, thanks to which we were able to extend our analysis on *CNOT3* expression and on the association of *CNOT3* polymorphic alleles with the clinical manifestation of the disease.

Results, Part 3) Together with the gene expression analysis in lymphoblastoid cells derived from patients belonging to the RP856/AD5 family (data published in *PLOS Genetics*) we performed also a microRNA analysis to see if there was an altered expression of microRNAs, which are known to be involved in the regulation of gene expression.

Results, Part 4) We checked if the asymptomatic individuals of *PRPF31*-linked adRP families presented a higher expression not only of *PRPF31* but also of other splicing factors.

Results, Part 5 and 6) We tested *in vitro* if *CNOT3* could affect the transcription of other splicing factors.

Results, Part 7) As another subunit of the Ccr4-Not complex, called *CNOT2*, shares the same functional domain with *CNOT3*, we investigated if it could also modulate *PRPF31* expression and whether its expression was altered in *PRPF31*-linked adRP families.

2.1.1 CNOT3 mRNA expression in two other families with PRPF31-linked autosomal dominant retinitis pigmentosa showing incomplete penetrance

We measured *CNOT3* expression levels in two North American adRP families that showed an incomplete penetrance phenotype linked to *PRPF31*-mutations.

Family #1562 was originally described by *Berson et al.* [1] and later included in the large meta-analysis that led to the identification of the major modifier of *PRPF31* penetrance on chromosome 19q13.4 [2]. The *PRPF31* mutation, which causes the disease in the family, is deeply intronic (c.1374+654C>G) and represents the first *PRPF31* pathological variant for which it has been proven that some residual wild-type transcript is derived from the mutated allele [3-4].

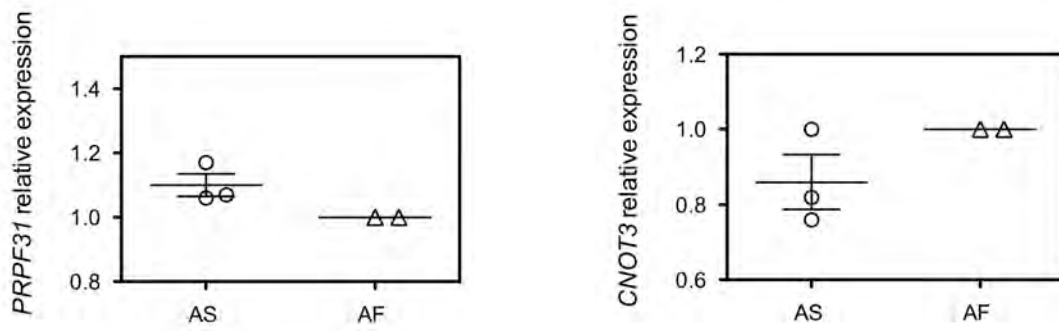
Family #2474 harbors a 34 base pairs deletion in exon 9 of *PRPF31*, which leads to a premature stop at the amino acidic position 320 and to degradation of the transcript by nonsense-mediated mRNA decay [5].

We had access to lymphoblastoid cell lines derived from two asymptomatic and one affected individual belonging to family #1562 and from one asymptomatic and one affected individual of family #2474.

The inverse trend of expression between *PRPF31* and *CNOT3*, which was observed in the RP856/AD5 family (*PLOS Genetics* paper, figure 1A and 1B), was confirmed in the two new families (Figure 1A).

Cumulative expression of *PRPF31* and *CNOT3* in all families with different *PRPF31* mutations is represented in Figure 1B.

A



B

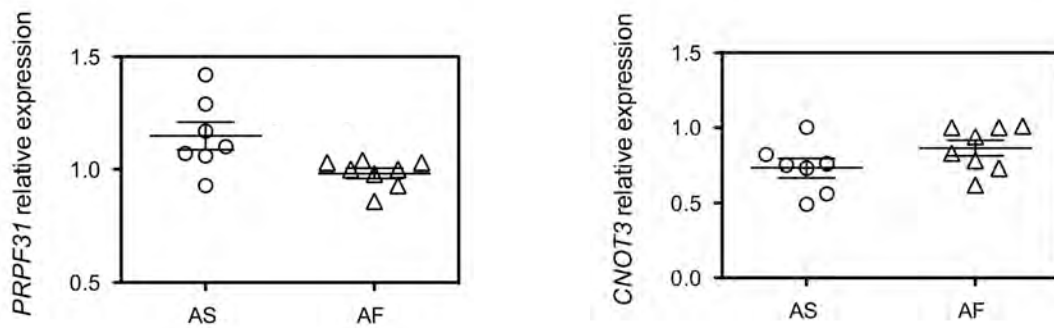


Figure 1. *CNOT3* expression with respect to that of *PRPF31*. A) Asymptomatic (AS) and affected (AF) individuals of families #1562 and #2474. *PRPF31* and *CNOT3* mRNA expression was normalized to the housekeeping gene *GAPDH*. Error bars refer to the standard deviation of the mean for 3 independent experiments for each group. B) Individuals of families RP856/AD5, #1562 and #2474 (in total 7 asymptomatic and 8 affected individuals).

2.1.2 *CNOT3* polymorphic alleles in an additional pedigree of *PRPF31*-linked autosomal dominant retinitis pigmentosa showing incomplete penetrance

CNOT3 rs4806718 alleles have been associated with the clinical manifestation of the disease in two unrelated pedigrees of *PRPF31*-linked adRP with incomplete penetrance (*PLOS Genetics* paper, figure 4). Association between the minor C allele with the affected status and the ancestral T allele with the asymptomatic status was moderately significant in the two families ($p=0.04$, *PLOS Genetics* paper, figure 4).

Lately we had access to the DNA from 8 asymptomatic and 8 affected individuals belonging to family #1562.

In 13 out of 16 individuals of the latter family there is a genotype-phenotype correlation for the rs4806718 alleles (Figure 2).

Adding the data of this family to those of the other two families analyzed in the paper we obtain a highly significant association between the *CNOT3* rs4806718 alleles and the clinical manifestation of the disease ($p=0.002$, by Fisher exact test).

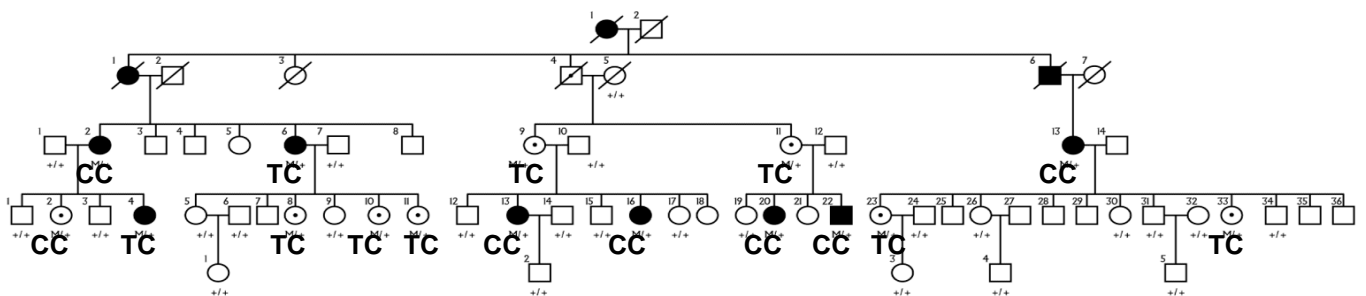


Figure 2. Analysis of *CNOT3* rs4806718 alleles in the family #1562. Affected individuals are in black, while asymptomatic individuals are represented with a dot. M indicates the carriers of the *PRPF31* mutation.

2.1.3 microRNA expression analysis in the asymptomatic and affected individuals of the RP856/AD5 family

microRNAs (miRNAs) are small noncoding RNA molecules (≈ 22 nucleotides) that are broadly involved in the regulation of gene expression. By pairing with complementary mRNA sequences, they lead to translational repression or degradation of the target transcript, which finally results in gene silencing.

Within the region on chromosome 19q13.4 that harbors the major modifier for *PRPF31* penetrance there is the largest miRNA cluster of the human genome, known as the C19MC cluster, which contains 46 pre-miRNA genes.

While we were testing the expression levels of all the genes that are present in the region on chromosome 19q13.4 in lymphoblastoid cells derived from patients belonging to the RP856/AD5 family, we also performed miRNA expression analysis by using the nCounter human miRNA expression assay kit (Nanostring Technologies, Seattle, USA), which allows the contemporary digital detection of 654 human miRNAs in a single reaction without amplification.

Only a minority of microRNAs that are detected by the kit (about 12%) are expressed in lymphoblastoid cells from the patients. Among these, we selected five miRNAs that show a statistically significant difference in expression between the asymptomatic and affected individuals of the R856/AD5 family (Figure 3).

miR-518f belongs to the C19MC miRNA cluster on chromosome 19q13.4, but, according to three different prediction tools (miRanda, RNAhybrid, and TargetScan) is supposed to target neither *PRPF31* nor *CNOT3*. However, we looked for a polymorphism within its sequence that could explain the different haplotypes observed on chromosome 19 by *McGee et al.* [2], but we could not find any polymorphism among the individuals of the R856/AD5 family.

miR-193b is predicted to target both *PRPF31* and *CNOT3* by two different prediction tools (miRanda and RNAhybrid). Interestingly, in the miRNAMap database (<http://mirnamap.mbc.nctu.edu.tw/>), which reports experimentally verified miRNAs with their target genes, miR-193b expression positively correlates with that of *CNOT3* and negatively correlates with that of *PRPF31*, which fits with the output of our experiment (Figure 3).

The other three miRNAs that we selected (miR-191, miR-342-3p, and miR-425) are all predicted to target *CNOT3* by the same prediction algorithm, which is interesting since in our experiment they show an opposite trend of expression with respect to that of *CNOT3* (Figure 3).

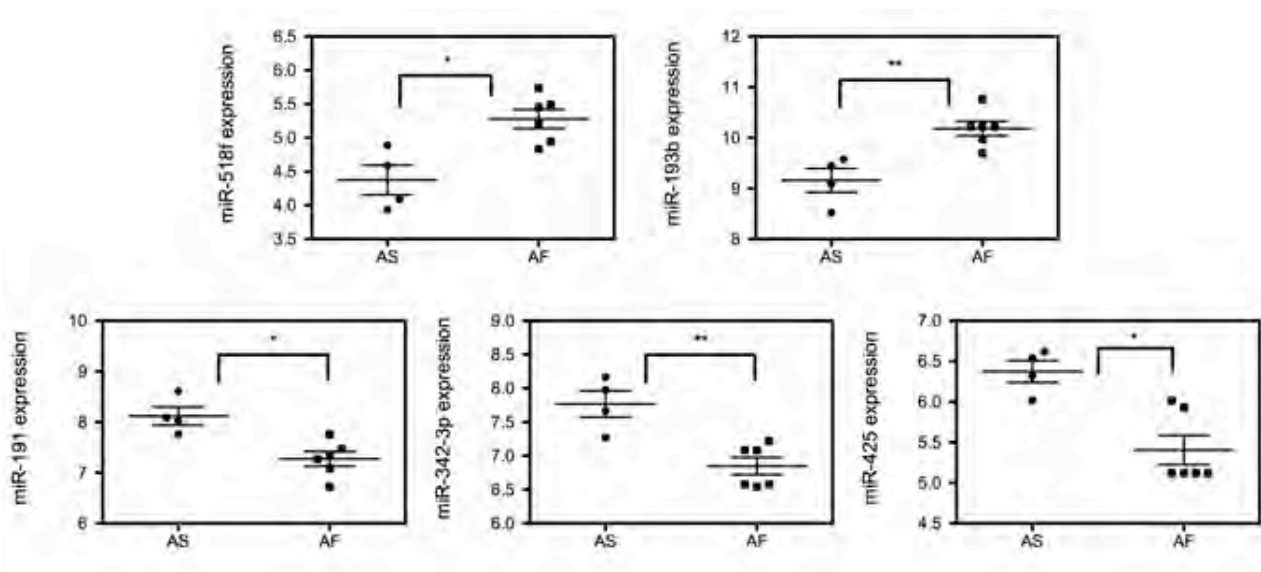


Figure 3. Expression profiles of five miRNAs that show a statistically significant difference in expression between the asymptomatic (AS) and affected (AF) individuals of the RP856/AD5 family. Mann Whitney non-parametric statistical hypothesis test was used to compare the expression level of each miRNA between the two groups of individuals. One star indicates $p < 0.05$, two stars indicate $p < 0.01$.

The data presented here are still preliminary and need to be validated with other techniques, such as Real-time PCR. Then, to confirm the possible effect of the five miRNAs on *PRPF31* and *CNOT3* expression functional *in vitro* experiments should be performed.

2.1.4 Expression of other splicing factors in families with *PRPF31*-linked autosomal dominant retinitis pigmentosa showing incomplete penetrance

Expression of *PRPF3*, *PRPF8*, *BRR2*, and *PRPF6* was assessed in 7 asymptomatic and 8 affected individuals of families RP856/AD5, #1562, and #2474.

Results show a tendency for all other components of the spliceosome we tested to be more highly expressed in the asymptomatic compared to the affected individuals (Figure 4). The result could be explained by a stoichiometric mechanism of the other spliceosome subunits to counteract the increased expression of *PRPF31* in the asymptomatic individuals, although they are carriers of the mutation.

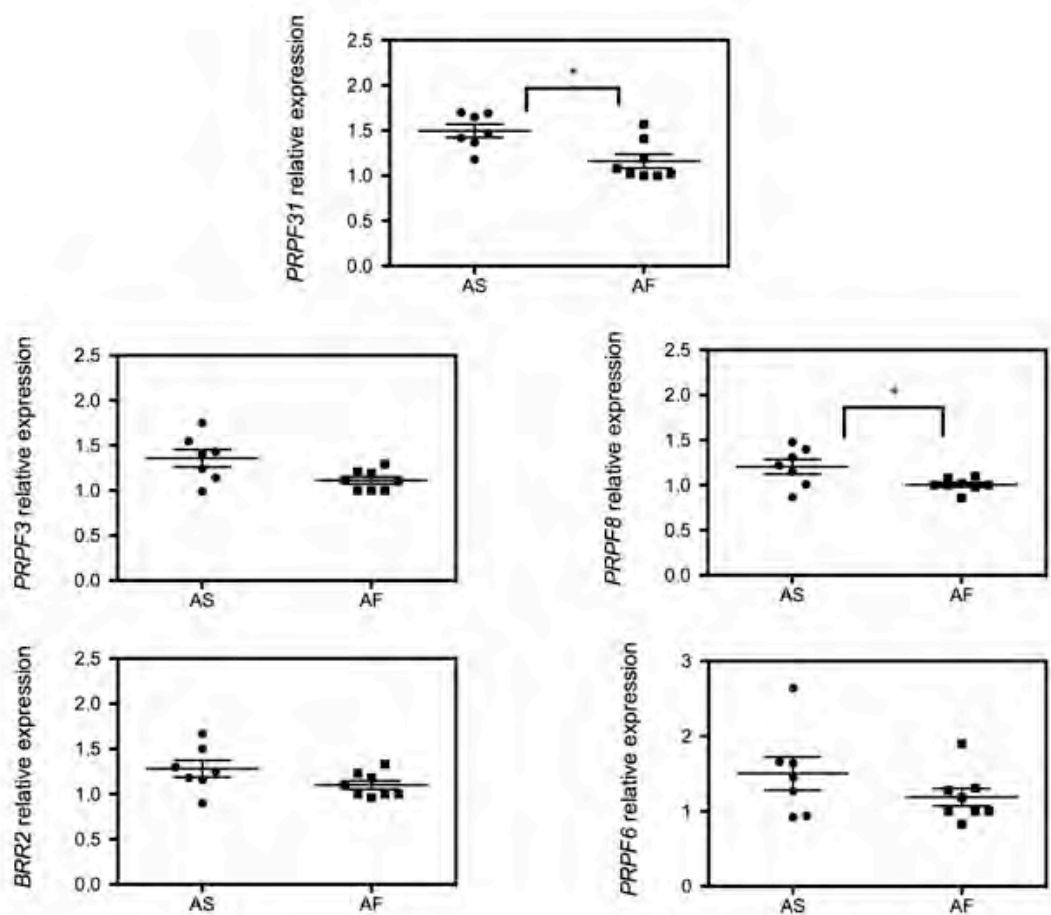


Figure 4. Expression of other splicing factors between the asymptomatic (AS) and affected (AF) individuals of families RP856/AD5, #1562 and #2474. Mann Whitney non-parametric statistical hypothesis test was used to compare the expression of each gene among the two groups of individuals. $p < 0.05$ is indicated by one star.

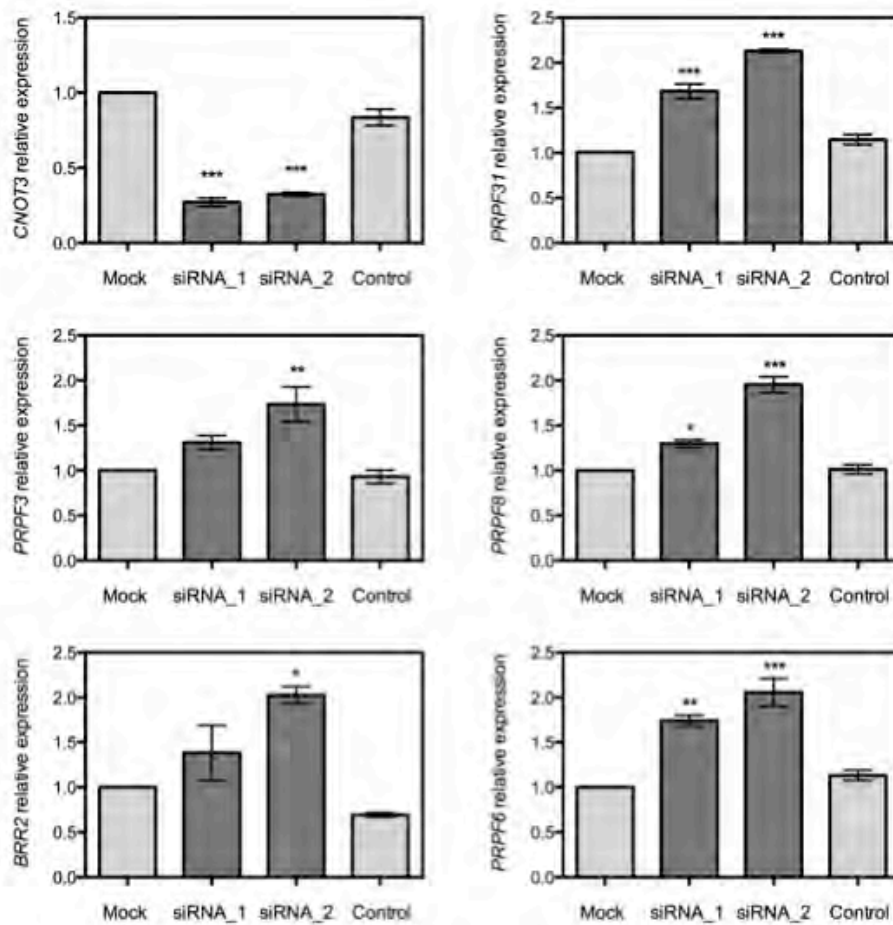
2.1.5 Effect of CNOT3 on the transcription of other splicing factors

We wanted to investigate if CNOT3 could influence the transcription not only of *PRPF31*, but also of other proteins that make up the spliceosome, and in particular of those that have been associated with autosomal dominant forms of retinitis pigmentosa (*PRPF3*, *PRPF8*, *BRR2*, *PRPF6*).

CNOT3 expression was inhibited in ARPE-19 cell lines, by using two different *CNOT3*-specific siRNA sequences. We observed a statistically significant effect with both *CNOT3*-specific siRNAs on the expression of *PRPF31*, *PRPF6*, and *PRPF8* (Figure 5A), which was even confirmed at the protein level (Figure 5B). The effect on the expression of *PRPF3* and *BRR2* was less evident, since it was observed only by using one out of two *CNOT3*-specific siRNA sequences.

This experiment is however not conclusive to establish if CNOT3 could directly affect the expression of the other spliceosome components; it may in fact be simply that the tendency of the other splicing factors to increase after *CNOT3* suppression is only due to a stoichiometric mechanism in response to the increased expression level of *PRPF31*.

A



B

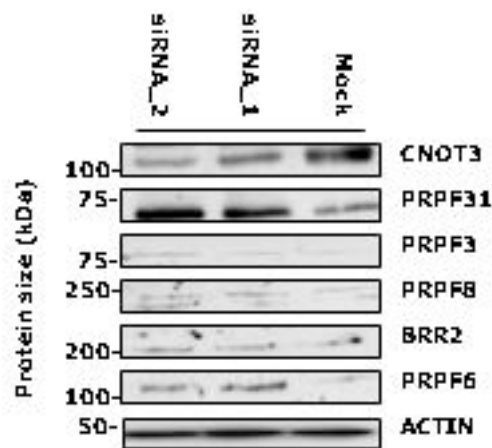


Figure 5. Effect of *CNOT3* silencing on *PRPF31*, *PRPF3*, *PRPF8*, *BRR2*, and *PRPF6* expression. A) mRNA expression. siRNA_1 and siRNA_2, different *CNOT3*-specific siRNA sequences; Control, treatment with transfection reagent with no siRNA; Mock, treatment with transfection reagent and scrambled siRNA. mRNA expression normalized to the housekeeping gene *GAPDH*. Error bars refer to the standard deviation of the mean for 3 independent experiments for each group. One-way ANOVA followed by Bonferroni's multiple comparison tests was used to analyze the effect of *CNOT3* silencing on the expression of the target genes. $p < 0.05$ is indicated by one star, $p < 0.01$ by 2 stars, and $p < 0.001$ by 3 stars. B) Representative western blot of the effect of *CNOT3* silencing on *PRPF31*, *PRPF3*, *PRPF8*, *BRR2*, and *PRPF6* protein expression.

2.1.6 CNOT3 binding to the promoter of the other splicing factors

In order to check if CNOT3 could directly affect the transcription of the other spliceosome components by binding to their predicted promoter sequences we performed chromatin immunoprecipitation (ChIP) in lymphoblastoid cells from three healthy individuals using an anti-CNOT3 antibody and serum IgG as a negative control.

Previously, a statistically significant enrichment of *PRPF31* experimentally validated promoter sequences was found in the fraction that was immunoprecipitated with anti-CNOT3 antibody, compared to that immunoprecipitated with serum IgG (*PLOS Genetics* paper, Figure 3A and 3B).

Predicted promoter sequences of the other splicing factors were retrieved from the Transcriptional Regulatory Element Database (<http://rulai.cshl.edu/cgi-bin/TRED/tred.cgi?process=home>).

Our data show that CNOT3 seems to be able to bind weakly to the promoter sequences of other splicing factors (Figure 6), even if we only performed a qualitative estimation and not a quantification of the enrichment of the different promoter sequences in the fraction immunoprecipitated with the CNOT3 antibody compared to that immunoprecipitated with the serum IgG.

Before jumping to conclusions we would still need to test many more negative control sequences, to make sure that the results we got are not due to a technical artifact.

Moreover, promoter sequences of *PRPF3*, *PRPF8*, *BRR2*, *PRPF6* should be tested with luciferase assay to determine if they are functionally active.

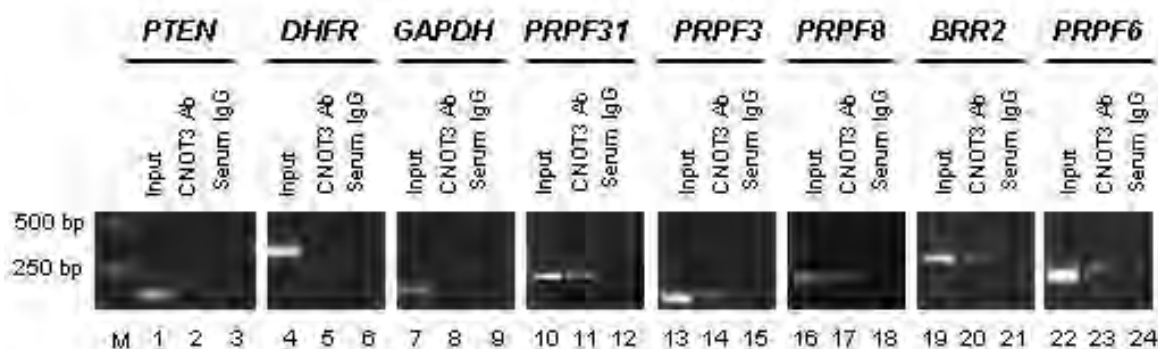
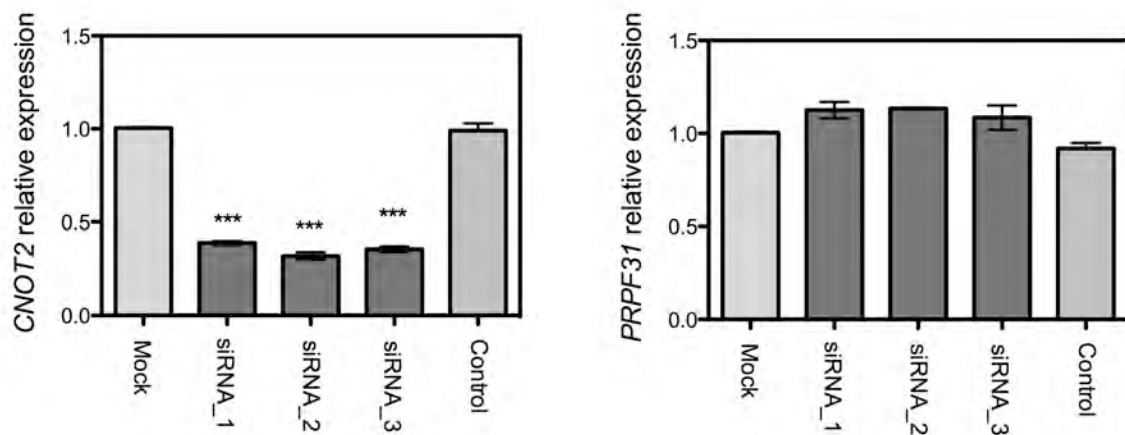


Figure 6. CNOT3 binds to the promoter of *PRPF31*, *PRPF3*, *PRPF8*, *BRR2*, *PRPF6* in lymphoblastoid cell lines. CNOT3 ChIP-PCRs on different target sequences. *PTEN* exon 8, *DHFR* 3'UTR, and *GAPDH* promoter sequences were used as negative controls.

2.1.7 *CNOT2* expression in the RP856/AD5 family and effect of *CNOT2* on *PRPF31* transcription

The Ccr4-Not complex consists of nine different subunits that control mRNA metabolism at different levels. Two of these subunits, *CNOT3* and *CNOT2*, share a conserved protein motif, called the Not-Box domain, which has been shown to repress reporter gene activity upon promoter targeting [6]. We thought to test whether *CNOT2* could also be a negative regulator of *PRPF31* expression and if it was differentially expressed between the asymptomatic and affected individuals of the RP856/AD5 family. Silencing of *CNOT2* by three different *CNOT2*-specific siRNA sequences in HeLa cells shows no effect on *PRPF31* mRNA expression (Figure 7A) and no alteration of *CNOT2* expression levels was observed between the asymptomatic and affected individuals of the RP856/AD5 family (Figure 7B).

A



B

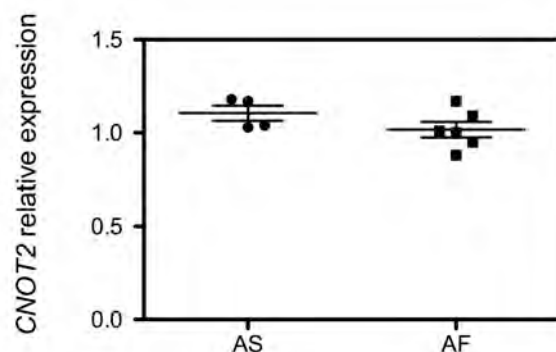


Figure 7. A) Effect of *CNOT2* silencing on *PRPF31* mRNA expression. siRNA_1, siRNA_2, and siRNA_3, different *CNOT2*-specific siRNA sequences; Control, treatment with transfection reagent with no siRNA; Mock, treatment with transfection reagent and scrambled siRNA. mRNA expression normalized to the housekeeping gene *GAPDH*. Error bars refer to the standard deviation of the mean for 3 independent experiments for each group. $p < 0.001$ is indicated by three stars. B) *CNOT2* mRNA expression between the asymptomatic (AS) and affected (AF) individuals of the RP856/AD5 family.

References

1. Berson, E.L., et al., *Dominant retinitis pigmentosa with reduced penetrance*. Arch Ophthalmol, 1969. 81(2): p. 226-34.
2. McGee, T.L., et al., *Evidence that the penetrance of mutations at the RP11 locus causing dominant retinitis pigmentosa is influenced by a gene linked to the homologous RP11 allele*. Am J Hum Genet, 1997. 61(5): p. 1059-66.
3. Rio Frio, T., et al., *A single-base substitution within an intronic repetitive element causes dominant retinitis pigmentosa with reduced penetrance*. Hum Mutat, 2009. 30(9): p. 1340-7.
4. Rivolta, C., et al., *Variation in retinitis pigmentosa-11 (PRPF31 or RP11) gene expression between symptomatic and asymptomatic patients with dominant RP11 mutations*. Hum Mutat, 2006. 27(7): p. 644-53.
5. Rio Frio, T., et al., *Premature termination codons in PRPF31 cause retinitis pigmentosa via haploinsufficiency due to nonsense-mediated mRNA decay*. J Clin Invest, 2008. 118(4): p. 1519-31.
6. Zwartjes, C.G., et al., *Repression of promoter activity by CNOT2, a subunit of the transcription regulatory Ccr4-not complex*. J Biol Chem, 2004. 279(12): p. 10848-54.

***FAM161A* mutations in patients with early-onset retinitis pigmentosa
in North America**

The paper is ready to be submitted for publication.

The aim of this project was to screen the recently identified *FAM161A* gene in a large cohort of North American individuals with autosomal recessive retinitis pigmentosa in order to identify novel mutations and better understand genotype-phenotype relationships.

The project was a collaboration with Dr. Eliot L. Berson (The Berman-Gund Laboratory for the Study of Retinal Degenerations, Harvard Medical School, Massachusetts Eye and Ear, Boston, MA), who performed the clinical examination of patients.

This project has led to the assessment of the prevalence of *FAM161A* mutations in North America, the ascertainment of genotype-phenotype correlations, and the identification of two alternative *FAM161A* transcripts in the human retina.

In this study I performed all experiments except clinical examination of the patients and treatment of lymphoblastoid cell lines with cycloheximide, and I wrote the draft for the journal.

***FAM161A* mutations in patients with early-onset retinitis pigmentosa
in North America**

Giulia Venturini, MSc; Silvio A. Di Gioia, MSc; Shyana Harper, MSc; Carol Weigel-DiFranco, MA; Carlo Rivolta, PhD; Eliot L. Berson, MD.

Author Affiliations: Department of Medical Genetics, University of Lausanne, Lausanne, Switzerland (Venturini, Di Gioia, and Rivolta), and Berman-Gund Laboratory for the Study of Retinal Degenerations, Harvard Medical School, Massachusetts Eye and Ear (Harper, Weigel-DiFranco, and Berson).

Correspondence: Eliot L. Berson, MD, Berman-Gund Laboratory, Massachusetts Eye and Ear, 243 Charles St, Boston, MA02114 (marilyn_sullivan@meei.harvard.edu).

Objective: To assess *FAM161A* genotype-phenotype correlations in a cohort of North American patients.

Methods: DNA from peripheral blood leukocytes was extracted from 273 unrelated patients with autosomal recessive retinitis pigmentosa (arRP) and 270 control individuals with no history of retinal degeneration. Mutational screening of coding regions and flanking intron boundaries was carried out by Sanger sequencing. Patients were clinically evaluated by ophthalmologic examination, including Goldmann visual field testing and computerized electroretinography (ERGs). Follow-up data were collected over 10 to 20 years.

Results: Four patients carried the null-mutation p.T452Sfx3, which was previously reported as a founder DNA variant in the Israeli and Palestinian populations. ERG recordings displayed a 30 Hz flicker response in the range of 0.10 to 1.75 microvolts in all patients at first visit (age 12 to 23) and of 0.06 to 0.80 microvolts at their most recent examination (age 27-43). Visual fields areas to the V-4e white light were all in the range of 80 deg².

Conclusions: Our data indicate that mutations in *FAM161A* are responsible for a small fraction of cases of arRP in North America (1.5%), similar to the prevalence detected in Germany and unlike the data from Israel and the Palestinian territories. All patients had ERG recordings compatible with early-onset arRP.

Clinical Relevance: Patients with arRP so far studied with *FAM161A* mutations have early-onset retinal degeneration as monitored by full-field electroretinograms (ERGs).

Introduction

Retinitis pigmentosa (RP) is a group of hereditary degenerative diseases of the retina associated with significant phenotypic and genotypic diversity. RP causes progressive loss of rod and cone photoreceptors function. Patients typically report loss of night vision in adolescence, loss of mid and far peripheral field in young adulthood, and loss of central vision in later life. Patients have elevated final dark adaptation thresholds and reduced and delayed full-field ERGs [1]. Studies of autopsy eyes have shown that the loss of visual function is due to degeneration of the photoreceptor cells [1].

At present, according to the RetNet database, over 60 genes have been associated with nonsyndromic RP, which account for 50-60% of patients with this condition [2-3]. Mutations in *FAM161A* have been found to represent the cause of *RP28*-associated autosomal recessive RP in the initial Indian family in which the *RP28* locus was mapped, as well as in a cohort of German patients [4]. Frequent nonsense mutations in *FAM161A* were also identified in patients from Israel and the Palestinian territories [5].

FAM161A is well-conserved among vertebrates and, despite having multiple splicing variants, only two of them produce stable mRNA transcripts. The main splicing variant contains six exons and encodes for a protein of 76 kDa, while the second variant contains a supplementary 168 bp in-frame exon between exons 3 and 4. The protein is mainly expressed in the retina and in the testis and localizes in photoreceptor cells during mouse retinal development [4-5].

Patients with *FAM161A* mutations have been reported to have symptoms ranging from an atypically late-onset form of RP, detected in a German cohort, to an early-onset manifestation of the disease, as observed in Israeli and Palestinian individuals. Unexpectedly, despite these clinical differences, patients so far reported carry the same class of mutations, leading to the loss-of-function of the encoded protein.

Here we report results of our mutational screening of *FAM161A* in a cohort of patients with autosomal recessive RP from North America, with the aim of assessing the mutation spectrum in this population and to increase our knowledge of the relationship between genotype and phenotype.

Methods

Patients and controls

This research was carried out in accordance with the tenets of the Declaration of Helsinki and was approved by the Institutional Review Boards of the University of Lausanne and of Harvard Medical School and the Massachusetts Eye and Ear, where the blood was collected and the patients were followed. Written informed consent was obtained from patients who participated in this study before they donated 10-30 ml of their blood for research.

DNA from peripheral blood leukocytes was extracted from 273 unrelated patients with arRP. Controls included 95 individuals with no history of retinal degeneration, and 80 subjects with normal ERGs. In addition, DNA samples from 95 ethnically-matched healthy individuals were purchased from the Coriell Institute Repository. For some individuals the quantity of DNA was insufficient to perform direct mutation screening and therefore a whole-genome amplification kit (REPLI-g Mini Kit, Qiagen) was used.

Mutation screening

Primer pairs for individual exons and relevant intron boundaries were designed using the CLC bio genomics workbench (see **Table 1 Appendix**). Amplifications by PCR were performed in 25 μ l reactions containing 20 ng genomic DNA, 1x GoTaq buffer, 1.2 mM MgCl₂, 0.1 mM dNTPs, 0.4 μ M of each primer, and 0.01 U/ μ l of GoTaq polymerase (Promega). Amplification conditions were: an initial step at 95°C for 2 minutes, 35 cycles of denaturation at 94°C for 30 seconds, annealing according to primers' melting temperature for 30 seconds, and extension at 72°C for 1 minute. Before the end of the reaction, a final extension step at 72°C for 5 minutes was performed.

Sequencing reactions were carried out by Sanger sequencing, after purification of PCR products (ExoSAP-IT, USB), by using 1 µl of 3.3 µM sequencing primer (see **Table 2 Appendix**) and 0.5 µl of BigDye Terminator v1.1 (Applied Biosystems). The products of these sequencing reactions were run on an ABI-3130XLS sequencer (Applied Biosystems).

Cell culture and drug treatment

The Epstein-Barr virus immortalized lymphoblastoid cell lines used in this study were derived from two affected patients (003-161 and her sibling 012-001), and were cultured as previously described [6]. Normal control cell lines were purchased from the Coriell Cell Repository. Treatment of cells with cycloheximide was performed as previously reported [7].

FAM161A primers for cDNA amplification were 5'-ggaagaaacgaaaagaatgg-3' and 5'-ttctcgttggtattctctcatcc-3', yielding a 1,115 bp product. 18S ribosomal RNA was used as a housekeeping gene for this analysis, and primers for its cDNA amplification were 5'-cggctaccacatccaaggaa-3' and 5'-gctggaattaccgcggt-3' (resulting in a 187 bp product).

RLM- RACE

To perform RLM-RACE we used the FirstChoice RLM-RACE kit (Invitrogen), following the manufacturer's instruction. One microgram of total RNA from human retina (Clontech) was used to perform 3'UTR RLM-RACE, and ten micrograms of total RNA from human retina (Clontech) and from retinoblastoma cell line Y79 were used for 5'UTR RLM-RACE.

Results

We screened *FAM161A* in 273 unrelated patients with arRP from North America, and in 270 ethnically matched healthy individuals. In three of these patients we identified the null mutation p.Thr452SerfsX3 (**Table 1**), which was previously reported as a founder mutation in an Israeli

Jewish population [5]. The same mutation was subsequently identified in one of the index patient's relatives (012-001, sister of 003-161). All four patients carrying p.Thr452SerfsX3 were homozygotes for this mutation.

Mutation p.Thr452SerfsX3 is predicted to produce a transcript that could be a target for nonsense mediated mRNA decay (NMD) and therefore result in no protein product. In order to test this hypothesis, we treated lymphoblastoid cell lines derived from the two siblings carrying this change (003-161 and 012-001) with the chemical NMD inhibitor cycloheximide. Upon supplementation of this inhibitor, mRNA degradation was blocked in both cell lines, confirming that p.Thr452SerfsX3 is a null allele (**Figure 1**).

In our cohort we also found a few other rare variants, likely having no pathological relevance (**Table 2**). Variant p.Q385E (rs139266382, MAF<0.01) was previously identified as heterozygous change in arRP patients and in healthy controls with a frequency of 2/400 alleles [4]. In our screening, we identified it in one patient and in 2 individuals from our control cohort. Variant p.H464R (rs201315315, MAF<0.01) was found in homozygous state in two arRP patients and in no healthy controls. The remaining variants were neither annotated in the dbSNP database nor were found in the control cohort. However, they all involved amino acid residues that are not evolutionary conserved and were predicted to result in benign changes by *in silico* analyses.

Variant p.L378R was previously identified in the German cohort of patients who were screened for *FAM161A* mutations and was not present in 400 control alleles, thus was classified as a rare variant with uncertain pathogenicity. It involves a highly conserved residue and is predicted to be deleterious by 3 out of 4 prediction programs (Polyphen, SIFT, MutPred, and PMut). Recently, it has been annotated in the dbSNP database (build 135/137, rs187695569), with a minor allele frequency (MAF) of 0.4%. We identified it in a heterozygous state in 5 out of 273 arRP patients and in 2 healthy individuals from the Coriell control cohort.

To test the hypothesis that heterozygous changes detected in our cohort of patients could in fact represent unrecognized mutations, we ascertain whether there were other non-annotated *FAM161A*

exons in retina. We therefore performed 5' and 3' RLM-RACE PCR using pooled retinal RNA from different donors, and identified two additional transcripts with an alternative 5'UTR in intron 1, whose sequence corresponds to the annotated exon 2 of *FAM161A-003* isoform. In these transcripts the translation-initiation codon lies on the canonical exon 2 (**Figure 2**). These transcripts were expressed in the retina at lower levels compared to the major isoforms. Interestingly, one of them completely skipped the highly-conserved exon 3, where most *FAM161A* mutations have been so far reported. We therefore screened this alternative 5'UTR sequence in the patients, but we did not find any possible-pathological variant.

Discussion

FAM161A mutations were recently identified in patients with recessive retinitis pigmentosa [4-5]. All reported mutations lead to loss-of-function of the encoded protein, but clinical manifestations of the disease may vary widely depending on the mutation. Prevalence of *FAM161A*-linked recessive RP is also different in individuals from different ethnicities, being in the German population comparable to the prevalence of most arRP genes [4], while, in the Israeli and Palestinian populations, *FAM161A* is the most frequently mutated gene in patients with arRP [5].

We found 4 patients with arRP and *FAM161A* mutations out of the 273 whom were screened, indicating that this is a relatively rare cause of RP in North America. Interestingly, one variant that had previously been reported as a founder mutation in the Israeli and Palestinian population (p.T452Sfx3) [5] is the most frequent mutation in patients from our cohort, and all but one of them reported Jewish ancestry.

Furthermore, from our study it emerged that there are many rare variants in *FAM161A*, which are reported in dbSNP with a minor allele frequency of less than 1%, that are frequently found in patients but not in controls, whose functional meaning is uncertain.

Patients with *FAM161A* mutations clinically showed early onset RP with relatively good acuity and very reduced ERGs (**Table 3**). Follow up examinations 10-20 years after the initial visit showed that all retained good acuity in at least one eye, 3 of 4 showed further loss of visual field, and 1 showed further decline in the ERG (**Table 3**). A floor effect may have occurred in those with less than or equal to 0.34 μ V at their initial visit that could simulate stabilization. Visual field areas to the V-4e white test light were all in the range of 80deg². The long-term course of arRP associated with *FAM161A* mutations remains to be defined.

References

1. Berson, E.L., *Retinitis pigmentosa. The Friedenwald Lecture*. Invest Ophthalmol Vis Sci, 1993. **34**(5): p. 1659-76.
2. Hartong, D.T., E.L. Berson, and T.P. Dryja, *Retinitis pigmentosa*. Lancet, 2006. **368**(9549): p. 1795-809.
3. Daiger, S.P., S.J. Bowne, and L.S. Sullivan, *Perspective on genes and mutations causing retinitis pigmentosa*. Arch Ophthalmol, 2007. **125**(2): p. 151-8.
4. Langmann, T., et al., *Nonsense mutations in FAM161A cause RP28-associated recessive retinitis pigmentosa*. Am J Hum Genet, 2010. **87**(3): p. 376-81.
5. Bandah-Rozenfeld, D., et al., *Homozygosity mapping reveals null mutations in FAM161A as a cause of autosomal-recessive retinitis pigmentosa*. Am J Hum Genet, 2010. **87**(3): p. 382-91.
6. Rivolta, C., et al., *Variation in retinitis pigmentosa-11 (PRPF31 or RP11) gene expression between symptomatic and asymptomatic patients with dominant RP11 mutations*. Hum Mutat, 2006. **27**(7): p. 644-53.
7. Rio Frio, T., et al., *Premature termination codons in PRPF31 cause retinitis pigmentosa via haploinsufficiency due to nonsense-mediated mRNA decay*. J Clin Invest, 2008. **118**(4): p. 1519-31.

Table 1 Appendix. Primers for polymerase chain reaction amplification of *FAM161A* exons

Targeted Exon	Sense primer	Antisense primer	Annealing temperature (°C)	Amplification product (bp)
Exon 1	AGTGGATTTTGCCTGACTTTTG	AATAACGAAACACACCTGACAGAAC	59	728
Exon 2	CTCCCTCTCGTTCTTAAAATATCAC	TGGGTGGGTCAGAAAGAAAAGAC	59	668
Exon 3 (I)	GTAAAATGAAGGAGTCAAAGTGGA	CACCTAACCTTGTGTTTACACTTC	58	1359
Exon 3 (II)	GATTTAAAGCCAGACCCATTCT	CCCAGCCAGGTAAACTAGAAATC	56	768
Exon 3a	ATTCTGATTGGCTTAAAGTGG	TGGCTTTGAGGGAGATAGTTTC	62	807
Exon 4	GAGAATTAACCGGTATAGAAGAGGA	ATGATGAAGCCAACACAAACAACA	56	437
Exon 5	GGAGTGAATTGTTGGTCATAGGGT	AAACGCTATAAAAGTGCCCATG	53.5	969
Exon 6	ATACTTGCAGAGGGTTTGTTC	AACCACCAAAGACCAATACTTCTC	59	591

bp: base pair

Table 2 Appendix. Primers for Sanger sequencing of *FAM161A* exons

Targeted Exon	Sequencing primer
Exon 1	GTAGGGACTATGTGCACAGG
Exon 2	AAGCAGCATTTTGGATCAGTG
Exon 3 (I)	TACAAGGCAGAGGAGATGA
Exon 3 (II)	CAACATAAACTCCACAGAGC
Exon 3a	ATTCTGATTGGCTTAAAGTGG
Exon 4	CTTTGTACAAGTTGATAAGT
Exon 5	CTCGTCTAAAAAGGTTTGTC
Exon 6	TAAACACAAATGCGGCTGCT

Table 1. Pathogenic variants detected

Patient ID	Ethnic origin	Gene exon	Nucleotide change	Predicted effect	Polyphen	SIFT	MutPred	PMut	Controls frequency (alleles)	Reference of the variation
003-161	Jewish (European)	3	c.1355_6delCA	p.Thr452SerfsX3/ p.Thr452SerfsX3	-	-	-	-	0/540	Bandah-Rozenfeld et al.
003-257	Jewish (Moroccan)	3	c.1355_6delCA	p.Thr452SerfsX3/ p.Thr452SerfsX3	-	-	-	-	0/540	Bandah-Rozenfeld et al.
121-385	Caucasian	3	c.1355_6delCA	p.Thr452SerfsX3/ p.Thr452SerfsX3	-	-	-	-	0/540	Bandah-Rozenfeld et al.
012-001	Jewish (European)	3	c.1355_6delCA	p.Thr452SerfsX3/ p.Thr452SerfsX3	-	-	-	-	0/540	Bandah-Rozenfeld et al.

Table 2. Possible non-pathogenic variants identified in this study

Gene exon	Nucleotide change	Predicted effect	Polyphen	SIFT	MutPred	PMut	NNSPLICE 0.9	Controls frequency (alleles)	Reference of the variation
3	c.1133 T>G	p.Leu378Arg/+	probably damaging	tolerated	disrupted	pathological		2/540	Langmann et al.
3	c.1113 C>G	p.Asp371Glu/+	benign	tolerated	benign	neutral		0/540	This study
3	c.1153 C>G	p.Gln385Glu/+	probably damaging	tolerated	benign	neutral		2/540	Langmann et al.
3	c.1391 A>G	p.His464Arg/ p.His464Arg	benign	tolerated	benign	pathological		0/540	This study
intronic	c.362+89 C>T	-	-	-	-	-	acceptor site score increased	NA	This study

Table 3. Clinical summary of patients with *FAM161A* mutations associated with retinitis pigmentosa

First Visit

#	BGLid	Age	Sex	VA OD	VA OS	ERG OD	ERG OS	Visual Field OD	Visual Field OS	DA	Lens OD	Lens OS	Macula OD	Macula OS	Periphery OD	Periphery OS
1	003-161	12	F	20/40	20/30	0.10	0.10	1174	2016	3.0	-	-	-	-	+	+
2	003-257	21	F	20/50	20/40	0.10	0.10	108	76	3.0	-	+	-	-	+	+
3	121-385	23	M	20/20	20/20	0.24	0.6	2060	1795	3.0	+	+	-	-	+	+
4	012-001	12	F	20/40	20/40	0.10	0.10	78	78	3.0	+	+	-	-	+	+

Last Visit

#	BGLid	Age	Sex	VA OD	VA OS	ERG OD	ERG OS	Visual Field OD	Visual Field OS	DA	Lens OD	Lens OS	Macula OD	Macula OS	Periphery OD	Periphery OS
1	003-161	27	F	20/30	20/25	0.17	0.24	123	118	NA	-	-	-	-	+	+
2	003-257	38	F	HM	20/60	0.06	0.10	NA	NA	4.0	+	+	AS	+	+	+
3	121-385	43	M	20/20	20/30	0.22	0.32	69	65	4.0	PP	PP	+	+	+	+
4	012-001	30	F	20/30	20/30	NA	NA	43	73	NA	+	+	-	-	+	+

Visual Acuity: best corrected Snellen visual acuity

Visual Field: Goldmann total field area to V-4e white test light (lower norm = 11,399 degrees squared)

DA (dark adaptation): final threshold in log units above normal after 45 minutes of dark adaptation.

ERG: full field ERG amplitude in microvolts to white light 30HZ white light (lower norm =50 microvolts)

Lens: clear lens -; central posterior subcapsular cataract +; PP: pseudophakia

Macula: within normal limits -;granular +; AS: atrophic scar

Periphery: bone spicule or clumped pigment in one or more quadrants: +present, -absent

NA denotes data not available

A 353-bp Alu insertion in *MAK* is a prevalent cause of recessive retinitis pigmentosa in North American Jewish patients

For coherence with the rest of the thesis the following results are presented in the form of a scientific article even if additional experiments are necessary before submission to a journal.

The project aimed at: (1) assessing the prevalence of a recently-reported 353-bp Alu insertion in exon nine of the *male germ cell-associated kinase* gene (*MAK*) in a cohort of North American autosomal recessive retinitis pigmentosa (arRP) patients with Jewish ancestry, compared with a cohort of arRP patients with mixed ethnicity; (2) ascertaining whether the insertion could be a founder mutation in the Jewish population; (3) identifying an Ashkenazi Jewish haplogroup in all patients harbouring the mutation.

The project is a collaboration with Dr. Eliot L. Berson (The Berman-Gund Laboratory for the Study of Retinal Degenerations, Harvard Medical School, Massachusetts Eye and Ear, Boston, MA), who performed the clinical examination of patients.

So far the project has led to the ascertainment of the prevalence of the mutation in North American arRP patients with Jewish family history and with mixed ethnicity and to the identification of five homozygous SNPs around the mutation, which define a founder RP-associated haplotype in the Jewish population.

In this study I performed all experiments except the clinical examination of patients.

Hanna Koskiniemi, a postdoctoral fellow in the laboratory, has largely contributed to the haplotype analysis.

**A 353-bp Alu insertion in *MAK* is a prevalent cause of
recessive retinitis pigmentosa in North American Jewish patients**

Giulia Venturini, MSc; Hanna Koskiniemi, PhD; Shyana Harper, MSc; Eliot L. Berson, MD; Carlo Rivolta, PhD.

Author Affiliations: Department of Medical Genetics, University of Lausanne, Lausanne, Switzerland (Venturini, Koskiniemi, and Rivolta), and Berman-Gund Laboratory for the Study of Retinal Degenerations, Harvard Medical School, Massachusetts Eye and Ear (Harper, and Berson).

Objective: 1) To ascertain the prevalence of a previously reported 353-bp Alu insertion in exon nine of *male germ cell-associated kinase (MAK)* in a cohort of North American autosomal recessive retinitis pigmentosa (arRP) patients with Jewish ancestry, compared with a cohort of arRP patients with mixed ethnicity, and 2) to assess that the insertion could be a founder mutation in the Jewish population.

Methods: Thirty-five unrelated North American individuals were included in the cohort of arRP patients with Jewish ancestry and 241 North American arRP patients with mixed ethnicity were selected for the cohort of mostly Caucasian individuals. Patients were clinically evaluated by ophthalmologic examination, including Goldmann visual field testing and computerized electroretinography (ERGs). Mutational screening was performed by agarose gel analysis of PCR amplicons, followed by Sanger sequencing. Haplotype analysis was accomplished by sequencing eight polymorphic markers around the mutation.

Results: The Alu insertion in exon nine of *MAK* was identified in 9 out of 35 (26%) arRP patients with Jewish ancestry and in 5 out of 241 (2.1%) arRP patients with mixed ethnicity. The latter positive individuals reported all East European origin, which could be compatible with Ashkenazi Jewish ancestry. A founder haplotype was identified in all patients carrying the mutation.

Conclusions: A 353-bp Alu insertion in *MAK* is a prevalent cause of arRP in North American Jewish patients and represents a founder mutation among Jews.

Introduction

The male germ cell-associated kinase (MAK) is a serine/threonine protein kinase encoded in humans by the gene *MAK*, which maps on the short arm of chromosome 6.

It is a highly-conserved enzyme, the expression of which is limited to testis [1] and retina [2].

Four alternative *MAK* isoforms are present in humans; the longer isoform, containing an alternative 75-bp exon between exons 11 and 12, has a photoreceptor-specific expression both in mice and in humans [3-5].

In mice, Mak regulates photoreceptor ciliary length and is crucial for photoreceptor long-term survival, since *Mak*^{-/-} mice develop progressive retinal degeneration [3].

Recently, mutations in *MAK* have been identified as a cause of autosomal recessive retinitis pigmentosa (arRP) [4-5]. A homozygous 353-bp Alu insertion in exon 9 of *MAK* has been reported in an isolate arRP patient with Jewish ancestry [5]. The mutation results in the insertion of 31 incorrect amino acids followed by a premature termination codon; in retinal cells derived from patient's fibroblasts the mutation prevents the expression of the photoreceptor-specific isoform [5]. Screening of the Alu insertion in a cohort of 1798 unrelated arRP patients with mixed ethnicity identified 20 probands homozygous for the mutation (1.2%); interestingly, all carriers of the mutation reported Jewish ancestry [5].

Clinical manifestation in individuals harbouring the Alu insertion resembles the autosomal dominant form of RP linked to *RPI* mutations [6]. This is an intriguing finding considering that in murine photoreceptors Mak and RP1 have been shown to co-localize and RP1 is a target of Mak phosphorylation [3]. Prolonged survival of the central retina island and good visual acuity are typical features in patients with the Alu insertion in *MAK* [6].

Nonsense and missense mutations affecting critical residues of the protein have been reported among Caucasians; patients with *MAK* mutations show an overall less rapid and severe disease course compared with other recessive forms of RP [4].

Retinitis pigmentosa is a heterogeneous Mendelian disease whose recessive way of inheritance is caused by mutations in more than 30 genes and loci (according to RetNet database, <https://sph.uth.edu/retnet/>), most of which account for a small percentage of cases.

Based on the estimated carrier frequency in the Jewish population [6] the Alu insertion in *MAK* is expected to be responsible of about one third of all RP cases among Jews.

In our study we ascertained the prevalence of the Alu insertion in *MAK* in a cohort of North American patients with arRP and of Jewish ancestry, compared with a cohort of patients of mixed ethnicity. Furthermore, we proved that the insertion is a founder mutation in the Jewish population.

Methods

Patients

This research was carried out in accordance with the tenets of the Declaration of Helsinki and was approved by the Institutional Review Boards of the University of Lausanne and of Harvard Medical School and the Massachusetts Eye and Ear Infirmary, where the blood was collected and the patients were followed. Written informed consent was obtained from patients who participated in the study before they donated 10-30 ml of their blood for research.

DNA from peripheral blood leukocytes was extracted from 35 unrelated North American arRP patients with Jewish ancestry, and from 241 North American arRP patients with mixed ethnicity.

Patients were clinically evaluated with an ophtalmologic examination, including Goldmann visual field testing and computerized electroretinography (ERGs).

Genetic analyses

Mutational screening was performed by agarose gel analysis of PCR amplicons, followed by Sanger sequencing. Primer sequences to amplify the Alu insertion in exon nine of *MAK* were designed

using Primer3 software. Forward primer: 5'-TACCGCCCATTTTGTTCAT-3' (intron 8/9); Reverse primer: 5'-ACTGAGAACTGTTACTGTGAG-3' (intron 9/10).

PCR amplification was performed in a 25 µl reaction containing 20 ng genomic DNA, 1x GoTaq buffer, 1.2 mM MgCl₂, 0.1 mM dNTPs, 0.4 µM of each primer, and 0.01 U/µl of GoTaq polymerase (Promega). Amplification conditions were: an initial step at 95°C for 2 minutes, followed by 35 cycles of denaturation at 94°C for 30 seconds, annealing at 56°C for 30 seconds, and extension at 72°C for 1 minute. Before the end of the reaction, a final extension step at 72°C for 5 minutes was performed. After purification of the PCR product (ExoSAP-IT, USB), the sequencing reaction was carried out by Sanger sequencing using 3.2 µM of sequencing primer (5'-CACTGAGTCATAAAAGTGGT-3') and 0.5 µl of BigDye Terminator v1.1 (Applied Biosystems). The sequencing product was then run on an ABI-3130 XLS sequencer (Applied Biosystems).

Haplotype analysis was accomplished by sequencing eight polymorphic markers around the mutation, using PCR conditions reported above and primer pairs listed in **Table S1**.

Results

We identified 14 individuals harbouring the Alu insertion in exon nine of *MAK* in a homozygous state (**Figure 1**). Of these, 9 belonged to the cohort of arRP patients with Jewish ancestry, which corresponds to a prevalence of 26% in the Jewish population, and 5 to the cohort of arRP patients with mixed ethnicity (prevalence of 2.1%). However, the latter positive individuals reported all East European origin, which could be compatible with Ashkenazi Jewish ancestry.

The mean age of onset of the disease in patients with the mutation is 45 years (n=14; 29-64 years at first visit), indicative of a late-onset form of arRP. In agreement with what was previously observed by *Stone et al.* [6], patients carrying the Alu insertion in *MAK* have rather good visual acuity, which suggests a prolonged survival of the central retina (**Table 1**).

Interestingly, three individuals from our cohort present ocular manifestations that differ from the average of all other patients, being more severe in patient 121-847, who shows an important reduction of the visual field and almost unrecordable cone responses, but milder in patients 003-213 and 003-033, who have a more preserved photoreceptor function (**Table 1**). An assumption could be that these patients harbour additional variants that, added to the effect of the mutation, are able to modulate the phenotype.

By sequencing eight polymorphic markers in a region of about 230 kb around the mutation we identified, in all 14 patients, five homozygous SNPs, which define a founder RP-associated haplotype in the Jewish population (**Table 2**). The same haplotype was not found in 9 arRP patients with Jewish ancestry not carrying the mutation.

Discussion

In the United States there is the largest Jewish community outside of Israel in the world. The majority of Jews who live in the US are Ashkenazi Jews (AJ), a population that, around the 4th century, migrated from the Middle East to Europe. At the end of the 19th century and beginning of the 20th century they mostly moved from Central and Eastern Europe to the United States and to Israel.

Although consanguineous marriages are not common in Ashkenazis compared to other Jewish populations, there is still a high rate of intra-community marriages, therefore disease-causing mutations in recessive disorders affecting AJ are expected to be found in a homozygous state [7].

There is a growing list of genes that have been shown to be responsible for a high percentage of cases of recessive retinal degenerations in the AJ population (i.e. *CLRN1* [8], *PCDH15* [9], and *DHDDS* [10-11]).

The 353-bp Alu insertion in exon 9 of *MAK* has been predicted to be a prevalent cause of recessive retinitis pigmentosa in the AJ population, based on its high carrier frequency among individuals

with AJ ancestry [6]. In our cohort of North American arRP patients with Jewish family history we found a prevalence of the mutation of 26%, slightly below the estimation of 1:3 in Ashkenazi Jews [6].

RP caused by the Alu insertion in *MAK*, compared to other forms of arRP, shows a later onset and less severe symptoms, such as better visual acuity and prolonged survival of the central retina.

Haplotype analysis showed a shared homozygous region of five polymorphic markers among all individuals carrying the mutation, suggesting that the Alu insertion is a founder mutation in the Jewish population and that all individuals with mixed ethnicity who were found to harbour the mutation may probably have Jewish ancestry as well.

We still need to demonstrate that patients carrying the Alu insertion in *MAK* are indeed Ashkenazi Jews; one approach could be to sequence the entire mitochondrial genome, which contains polymorphic markers that define the four major Ashkenazi Jewish haplogroups.

In conclusion, because of its high prevalence in the Jewish population, *MAK* should definitely be included in Jewish carrier screening panels with the aim of reducing the incidence of arRP in this population.

References

1. Matsushime, H., et al., *A novel mammalian protein kinase gene (mak) is highly expressed in testicular germ cells at and after meiosis*. Mol Cell Biol, 1990. **10**(5): p. 2261-8.
2. Blackshaw, S., et al., *Genomic analysis of mouse retinal development*. PLoS Biol, 2004. **2**(9): p. E247.
3. Omori, Y., et al., *Negative regulation of ciliary length by ciliary male germ cell-associated kinase (Mak) is required for retinal photoreceptor survival*. Proc Natl Acad Sci U S A, 2010. **107**(52): p. 22671-6.
4. Ozgul, R.K., et al., *Exome sequencing and cis-regulatory mapping identify mutations in MAK, a gene encoding a regulator of ciliary length, as a cause of retinitis pigmentosa*. Am J Hum Genet, 2011. **89**(2): p. 253-64.
5. Tucker, B.A., et al., *Exome sequencing and analysis of induced pluripotent stem cells identify the cilia-related gene male germ cell-associated kinase (MAK) as a cause of retinitis pigmentosa*. Proc Natl Acad Sci U S A, 2011. **108**(34): p. E569-76.
6. Stone, E.M., et al., *Autosomal recessive retinitis pigmentosa caused by mutations in the MAK gene*. Invest Ophthalmol Vis Sci, 2011. **52**(13): p. 9665-73.
7. Zlotogora, J., G. Bach, and A. Munnich, *Molecular basis of mendelian disorders among Jews*. Mol Genet Metab, 2000. **69**(3): p. 169-80.
8. Herrera, W., et al., *Retinal disease in Usher syndrome III caused by mutations in the clarin-1 gene*. Invest Ophthalmol Vis Sci, 2008. **49**(6): p. 2651-60.
9. Ben-Yosef, T., et al., *A mutation of PCDH15 among Ashkenazi Jews with the type 1 Usher syndrome*. N Engl J Med, 2003. **348**(17): p. 1664-70.
10. Zelinger, L., et al., *A missense mutation in DHDSD, encoding dehydrodolichyl diphosphate synthase, is associated with autosomal-recessive retinitis pigmentosa in Ashkenazi Jews*. Am J Hum Genet, 2011. **88**(2): p. 207-15.
11. Zuchner, S., et al., *Whole-exome sequencing links a variant in DHDSD to retinitis pigmentosa*. Am J Hum Genet, 2011. **88**(2): p. 201-6.



Figure 1. A representative agarose gel of PCR amplicons, on which two homozygous carriers of the mutation (circled in red).

SNP ID	Chromosomal Position	003-321	121-216	121-410	003-370	121-122	003-213	003-033	121-184	121-147	121-265	121-470	121-283	121-847	003-287
rs111468923	6:10687602	CT	TT	TT	TT	TT	TT	TT	TT	CT	TT	TT	TT	TT	TT
rs1045911	6:10723449	AC	CC	CC	CC	CC	CC	CC	CC	AC	CC	CC	CC	CC	CC
rs545019	6:10745066	AA	AA	AA	AA	AA	AA	AA	AA	AA	AA	AA	AA	AA	AA
rs116734564	6:10753038	CC	CC	CC	CC	CC	CC	CC	CC	CC	CC	CC	CC	CC	CC
rs518954	6:10791859	GG	GG	GG	GG	GG	GG	GG	GG	GG	GG	GG	GG	GG	GG
rs7766477	6:10792427	CC	CC	CC	CC	CC	CC	CC	CC	CC	CC	CC	CC	CC	CC
rs9357021	6:10906154	GG	GG	GG	GG	GG	GG	GG	GG	GG	GG	GG	GG	GG	GG
rs12215477	6:10919736	GG	AA	GG	AG	GG	GG	GG	GG	GG	GG	GG	AG	GG	GG

Table 2. Polymorphic markers used for haplotype analysis. In red the SNP closest to the mutation. The shared haplotype highlighted in blue.

SNP ID	Variant	MAF	Forward primer	Reverse primer
rs111468923	C>T	0.02	TTGCCTAGCAGGAATTGCCA	GCAGAGGGGAGACTACAGGA
rs1045911	A>C	0.16	CACCGTCCCCATTCTCTGAC	TAAGCCTTTGCCTCAGGAGC
rs545019	G>A	0.34	CCTGACCTCAGGTGATCCAT	CTCTGGTTCTTCCTGCCTTG
rs116734564	G>C	0.01	CTCCCGAAGTGCTGGGATTA	GAATGTGCTAGATCTTGTCTG
rs518954 (*)	T>G	0.25	TACCGCCCATTTTTGTTTCAT	ACTGAGAACTGTTACTGTGAG
rs7766477	A>C	0.26	ATCTCCCTGCACCCAACA	CCCCATTCTCAAGGAGCGTT
rs9357021	A>G	0.21	ACAGAACCTCAGAGTGTATATAGTAGT	TCATAAAACCCCCAGTGTCCAAT
rs12215477	A>G	0.21	TCCCTCTTTTCCTATGGTTGTGG	CCTGGTAACTGAAGACTAAGGGA

Table S1. Primers used for haplotype analysis. (*) SNP closest to the mutation; to sequence it we used an additional sequencing primer (5'-ACAGGTGCACACCACACAC-3'). MAF, minor allele frequency.

MGID	Ancestry	Age (y)	Sex	Visual Acuity OD	Visual Acuity OS	Visual Field OD	Visual Field OS	DA	0.5HZ ERG OD	0.5HZ ERG OS	30HZ ERG OD	30HZ ERG OS	Lens OD	Lens OS	Macula OD	Macula OS	Periphery OD	Periphery OS
003-321	Hungarian/ Austrian/ Black Russian	29	F	20/30	20/25	5401	5877	2.0	5.80	2.10	0.53	0.76	+	+	-	-	+	+
121-216	Jewish	31	M	20/30	20/30	2497	6684	NA	1.50	3.70	0.41	0.94	+	+	+	+	+	+
121-410	Russian/ Polish/ English	31	F	20/20	20/20	5898	6102	1.0	7.00	6.00	0.98	0.87	-	-	-	-	+	+
003-370	Polish/ Israeli	35	M	20/80	20/70	2593	1920	3.5	NA	NA	0.40	0.47	+	+	+	+	+	+
121-122	Jewish	42	M	20/25	20/30	9381	9140	NA	1.40	1.00	2.11	0.88	+	+	+	+	+	+
003-213	Hungarian/ Russian	42	F	20/20	20/25	11835	10735	2.5	22.00	19.00	7.31	8.43	-	-	-	-	+	+
003-033	Jewish	43	M	20/20	20/20	6566	7412	NA	28.00	25.50	13.99	12.76	+	+	-	-	+	+
121-184	Jewish	44	M	20/30	20/20	679	1447	NA	2.30	3.20	0.41	0.51	+	+	-	-	+	+
121-147	Jewish	46	M	20/30	20/40	2163	3354	NA	NA	NA	0.20	0.13	+	+	+	+	+	+
121-265	Jewish	47	M	20/25	20/25	7694	3290	NA	0.70	1.60	0.37	0.51	+	-	+	+	+	+
121-470	Jewish	54	M	20/40	20/30	5934	4811	3.0	4.20	NA	1.75	0.63	+	+	-	-	+	+
121-283	Jewish	55	M	20/80	20/80	1665	1415	4.5	NA	NA	0.20	0.36	+	+	+	+	+	+
121-847	Jewish	63	M	20/60	20/40	264	253	3.0	NA	NA	0.09	0.08	Aphakia	Aphakia	+	+	+	+
003-287	Russian/ Romanian	64	F	20/30	20/40	277	255	4.0	NA	NA	0.19	0.19	+	+	+	+	+	+

Table 1. Clinical summary of first visit with all tests of 14 patients with the Alu insertion in *MAK*. Visual Acuity: best corrected Snellen visual acuity; Visual Field: Goldmann total field area to V-4e white test light (lower norm = 11,399 degrees squared); DA (dark adaptation): final threshold in log units above normal after 45 minutes of dark adaptation; ERG: full field ERG amplitude in microvolts to white light single 0.5HZ flash (lower norm =350), 30HZ white light (lower norm =50); Lens: clear lens -; central posterior subcapsular cataract +; Macula: within normal limits -; granular +; Periphery: bone spicule or clumped pigment in one or more quadrants: +present, -absent; NA denotes data not available.

Genome-wide sequencing to identify disease-causing mutations in patients with recessive retinitis pigmentosa

For coherence with the rest of the thesis this part will be presented in the form of a scientific paper even if additional experiments are needed to conclude the project.

The purpose of this study was to apply whole genome sequencing to identify disease-causing mutations in unrelated patients with recessive retinitis pigmentosa.

The project is in collaboration with Dr. Eliot L. Berson (The Berman-Gund Laboratory for the Study of Retinal Degenerations, Harvard Medical School, Massachusetts Eye and Ear, Boston, MA) and Dr. Koji M. Nishiguchi (Department of Ophthalmology, Nagoya University School of Medicine, Nagoya, Japan), who provided us DNA of the patients and performed the clinical examinations.

From the beginning this project was a close collaboration with Hanna Koskiniemi, a postdoctoral fellow in the laboratory, with whom we equally contributed to the results presented here.

**Genome-wide sequencing to identify disease-causing mutations
in patients with recessive retinitis pigmentosa**

Giulia Venturini, MSc[#]; Hanna Koskiniemi, PhD[#]; Koji M. Nishiguchi, MD; Shyana Harper; Eliot L. Berson, MD; Carlo Rivolta, PhD.

[#] equally contributing authors

Author Affiliations: Department of Medical Genetics, University of Lausanne, Lausanne, Switzerland (Venturini, Koskiniemi, and Rivolta), Department of Ophthalmology, Nagoya University School of Medicine, Nagoya, Japan (Nishiguchi) and Berman-Gund Laboratory for the Study of Retinal Degenerations, Harvard Medical School, Massachusetts Eye and Ear, Boston, MA (Harper, and Berson).

Objective: To identify disease-causing mutations in unrelated individuals with recessive retinitis pigmentosa for diagnostic purposes.

Methods: DNA from twelve Japanese and four North American unrelated individuals with recessive retinitis pigmentosa were subjected to whole genome sequencing, which was performed at Complete Genomics Inc. (Mountain View, CA, USA). We focused on the analysis of variants in 157 genes, which have been reported to be associated with inherited retinal degenerations.

Results: We identified causative mutations in 5 Japanese and in 2 North American individuals, accounting for about 44% of our cohort.

Conclusions: Whole genome sequencing allowed the identification of disease-causing mutations in unrelated individuals with a genetically heterogeneous Mendelian disorder, supporting the notion that such strategy can be successfully used in molecular diagnostic of RP.

Introduction

Autosomal recessive retinitis pigmentosa (arRP) starts early, usually during the first decade of life, and is caused by null mutations that lead to the loss of the normal copy of the mutated gene.

In this context, gene therapy represents a promising therapeutic approach, thanks to which the gene that is affected by the mutation can be replaced.

To date more than 30 genes and loci have been associated with arRP (RetNet database; <https://sph.uth.edu/retnet/sum-dis.htm>), but the sum of their frequencies does not explain more than a third of the arRP cases, since the majority of them contribute to less than 1% of cases and only few are responsible for more than 10% of cases [1]. However, most of these data have been obtained from European and North American countries, and studies in different populations have shown that the genetic component of the disease could not be the same [2].

Recent advances in sequencing techniques and lower costs allow nowadays analyzing many genes simultaneously. Exome sequencing has proved effective in identifying the genetic cause of several rare Mendelian disorders, including RP, by interrogating only the coding fraction of the genome, which is roughly 1% of the entire genome.

However, it is becoming increasingly evident that some of the missing causative mutations may reside in non-coding regions of the genome, such as intronic regions [3-6] or can be structural rearrangements, such as large deletions or insertions [7-8], which are very challenging to be identified by conventional screening methods and even by exome sequencing.

Whole genome sequencing (WGS) overcomes this obstacle, covering all the coding and non-coding areas of the genome and having the ability to detect large structural rearrangements.

In this study we used whole genome sequencing to identify disease-causing mutations in 16 unrelated individuals with different ethnicities, who were all diagnosed with recessive retinitis pigmentosa.

Methods

Patients and controls

Our research protocol was designed in compliance with the Declaration of Helsinki and approved by the Institutional Review Boards of the University of Lausanne, the Massachusetts Eye and Ear and Harvard Medical School, and of the Nagoya University School of Medicine. Written informed consent for providing medical information and blood samples was obtained from each participant.

Leukocyte DNA was obtained from 4 patients from the Berman-Gund Laboratory, Massachusetts Eye and Ear. These patients had a family history indicative of recessive form of inheritance and they were previously screened for a variety of known RP genes.

Leukocyte DNA was also prepared from 12 patients of Japanese ancestry from the Nagoya University Hospital. They had RP with no family history (isolate RP) or a family history indicative of arRP and were unscreened for known RP gene.

All patients were subjected to comprehensive clinical examinations including ERG, visual field testing, and fundus examination and were judged to have a non-syndromic form of the disease based on the lack of significant non-ocular medical history and symptoms.

Genomes from 69 healthy individuals, sequenced with the same methodology at Complete Genomics Inc. and publicly available (<http://www.completegenomics.com/>), together with DNA of 95 healthy Caucasians purchased by the Coriell DNA Repository (<http://www.coriell.org/>) and of 95 healthy Japanese provided by the Nagoya University Hospital, were used as controls.

Whole genome sequencing

Five to seven microgram of high quality DNA was sent to Complete Genomics Inc. (Mountain View, CA, USA), where they performed whole genome sequencing based on the technique they have been developed [9]. Variant annotation was performed by using dbSNP build 132 and the human genome version hg19 (<http://hgdownload.cse.ucsc.edu/downloads.html>).

Analysis of the mapping results

Complete Genomics provided ready annotated text files for SNPs and small indels, for junctions (larger structural rearrangements), for copy number variations, and for mobile-element insertion events.

Perl scripts were developed *in-house* and used in combination with the “CGA tools” provided by Complete Genomics (<http://www.completegenomics.com/sequence-data/cgatools/>) to help analyzing the huge amount of data.

A total of 157 genes reported to be associated with inherited retinal degenerations either in humans or in animal models, or that were shown to be essential for the functioning of the retina, were selected for the analysis of variants in known disease-associated genes (**Supplementary Table S1**).

Homozygosity mapping

To determine the presence of homozygous genomic regions, likely indicative of being identical by descent (IBD), we used about 600,000 high quality SNPs included in the Illumina 660W chip (Illumina Inc., San Diego, CA, USA) and run the autozygosity analysis with the HomozygosityMapper web-based tool (<http://www.homozygositymapper.org/>).

Results

General considerations about whole genome sequencing

In the 16 unrelated individuals we observed an average coverage for the sequencing of the whole genome of 97% and for the sequencing of the whole exome of 98%. The average sequencing depth was 50X, with 98% of the reads being sequenced with depth >10X.

We obtained an average of three to four million SNPs per genome, of which 4% were novel variants, and this data did not differ much between Japanese and North American individuals.

Specificity and sensitivity of the technique were tested by sequencing with Sanger method the calls that were flagged with an indicator of good quality; about 70% of the high-quality calls were indeed true variants.

Homozygosity mapping

Analysis of autozygosity was performed for each genome in order to check for parental consanguinity. Using genotypes of known polymorphic variants listed in the 660W Illumina chip we looked for intervals with high level of homozygosity (at least 500 consecutive SNP markers).

Only two Japanese and one North American individual from our cohort presented IBD regions, which were however not overlapping.

Sequence analysis of known RP genes

As a first analytical step, we looked for changes that could severely impair protein function, present either in a homozygous or compound heterozygous state, since we were assuming a recessive mode of inheritance. Variants annotated in dbSNP with a frequency $\geq 2\%$ were excluded from the list of likely pathogenic variants. If two strong variants were not present in the same gene, we analyzed the information deriving from discordant mate pair sequences, indicative of large structural rearrangements. These data are usually reporting changes in the range of few hundred bases that

could affect coding regions of the genome. This type of analysis was found to be highly sensitive to the quality of the DNA, in particular if the DNA was collected a long time before the sequencing.

Missense changes were prioritized by running prediction algorithms for pathogenicity (PolyPhen-2, <http://genetics.bwh.harvard.edu/pph2/>, and SIFT, <http://sift.jcvi.org/>) and by looking at the amino acidic conservation (HomoloGene, <http://www.ncbi.nlm.nih.gov/homologene>).

With the list of candidate variations we performed a literature search to check whether the variants had been already associated with arRP or other allied diseases, and to exclude variants that had been reported as non-pathogenic. The final list with the disease-causing variations we found is reported in **Table 1**. All variants have been confirmed by Sanger sequencing.

We found 2 clearly pathogenic changes in 7 out of 16 individuals (2 North Americans and 5 Japanese), in 6 different genes.

Patient 003-146 is a compound heterozygous for a frameshift mutation (p.Q465fsX505) and a large deletion in the gene *SPATA7*. The same frameshift has been previously reported in a French Canadian individual with juvenile retinitis pigmentosa [10]. Through the analysis of discordant mate pair sequences we identified a 1'313 bp deletion between intron 7 and exon 8 of *SPATA7*, which is expected to affect splicing. This structural rearrangement is novel and was not found neither in the control genomes nor in a cohort of 95 healthy Caucasians.

121-847 is a North American patient with Jewish ancestry, which was found to have an IBD region on chromosome 6. This patient indeed harbours a homozygous 353-bp Alu-element insertion in exon 9 of *male germ cell-associated kinase (MAK)*, which has been associated with recessive retinitis pigmentosa in individuals with Jewish ancestry [11].

Another IBD region was identified on chromosome 6 in patient R6, who was found to have a homozygous missense mutation (p.R515W) in *RPE65*, which was previously reported in a Japanese patient with recessive RP [12].

In two Japanese patients (R25 and R41) we identified compound heterozygous variants in *EYS*. Both individuals share the same frameshift mutation (p.S1653KfsX2) that is thought to be one of

the major causes of arRP in the Japanese population [13]. Together with the frameshift mutation, patient R25 carries a nonsense variant (p.Y2935*) that was reported as a founder mutation in the Japanese population [13]. In patient R41 we identified as a second variant in *EYS* a novel frameshift (p.NS3062fs), which affects the same amino acidic residue that was found to be mutated in a Spanish patient with arRP [14].

Patient R51 harbours a known frameshift mutation (p.EG801GEfs) in *RPGR* [15], which is causative of X-linked RP. In this case then the mode of inheritance of the disease is not recessive but X-linked.

In patient R26 we found a heterozygous novel frameshift variant (p.Q411fs) in the gene *PRPF31*, which is linked to an autosomal dominant form of the disease. The change was not present neither in the control genomes nor in a cohort of 95 healthy Japanese individuals. Cosegregation analysis in the family showed a complete concordance between the genotype and the phenotype for the mutation (**Figure 1**). The mode of inheritance in this family seems to be autosomal dominant with incomplete penetrance, although this can not be proven because the father of the proband, who was diagnosed as healthy, died and thus we could not test if he is a carrier of the mutation (**Figure 1**).

One of the North American patients (003-102) carries two variants, a frameshift (p.M1731fs) and a missense (p.G546V), in the gene *USH2A*. Both variants are novel, but the missense variant targets an amino acidic residue where a polymorphism, which causes a different amino acidic change, has been reported (rs142282413). The *in silico* prediction for the pathogenicity of the missense variant suggests that it is probably pathogenic. The patient reported hearing impairment, but there is no DNA of other family members available, therefore without the cosegregation analysis is impossible to determine with certainty whether this two variants in *USH2A* could be the cause of the disease.

Finally, one of the Japanese patients (R10) had a heterozygous missense variant (p.S343N) in the *RHO* gene. The variant is novel and was not found neither in the control genomes nor in 95 healthy Japanese individuals. Cosegregation analysis in the family, however, revealed the presence of this variant also in the unaffected relatives, suggesting that it is a polymorphism in the Japanese

population (**Figure 2**). However, what emerged from the revision of the pedigree is that the way of inheritance of the disease is dominant and not recessive (**Figure 2**).

Discussion

Massively parallel sequencing proved to be an effective approach to identify the aetiology of many Mendelian disorders, including retinitis pigmentosa.

The most commonly used strategies for the identification of disease-causing genes in Mendelian diseases have been either sequencing many individuals with the same phenotype, or sequencing several members of the same family.

Our approach was different, since we sequenced unrelated individuals with different ethnicities but the same phenotype, in order to evaluate if whole genome sequencing could be an effective strategy to reveal the causes of such a genetically heterogeneous disease.

The most obvious benefit of such an approach compared to the conventional screening methods and to whole exome sequencing seemed to be the identification of large structural rearrangements, whose junctions are located deeply in intronic regions.

In our study we identified a large deletion (> 1 kb) encompassing intron 7 and exon 8 of *SPATA7*. One of the junctions was found to be very distant from the coding sequence of the gene, so it would have been very difficult to detect it without using whole genome sequencing.

Looking only at variants in genes that have been previously associated with inherited retinal degenerations we identified the cause of disease in about 45% of the individuals in our cohort.

In the majority of individuals where we were able to identify the disease-causing gene at least one of the two variants (in case of compound heterozygosity) had a strong impact at the protein level. Aetiology of retinitis pigmentosa in the Japanese population has not been much investigated, but what emerged so far is that causative RP genes in the European and North American populations can explain only a small percentage of RP cases in Japan. An exception is *EYS* that has been reported as a major cause of arRP in the Japanese population [13]. Among the Japanese individuals

in our cohort we found two that harbour mutations in *EYS*; interestingly, both of them have one of the founder mutations that have been identified in the Japanese population (p.S1653KfsX2) [13].

Despite all patients had been diagnosed with autosomal recessive retinitis pigmentosa, two Japanese individuals resulted to have a dominant way of inheritance instead. In at least one of them it was possible, even starting from nearly 4 million variants, to identify the heterozygous change that is responsible for the disease.

Whole genome sequencing proved also to be effective in identifying a few hundred bp Alu-element insertion in *MAK*, which was previously reported in a patient with recessive RP [11]. In the “mobile element insertion events” file information on whether the rearrangements occur in coding or non-coding genomic regions are provided. This is a fast and easy way to go through this class of variations that would not be otherwise taken into account by standard screening methods.

We can hypothesize that part of the unsolved cases in our cohort may be explained by mutations in genes that have not yet been associated with the disease. Other explanations may also be that the disease-causing variants are structural rearrangements that we failed to detect due to mapping or sequencing limitations or less obvious pathogenic changes that may otherwise alter splicing or transcription. Oligogenic inheritance should also be considered as a further hypothesis to explain the pathogenesis of the disease, since it has been already proven in inherited retinal disorders, like digenic inheritance in RP or triallelic inheritance in Bardet-Biedl syndrome [16-17].

Limitations of whole genome sequencing are represented mainly by the high cost, although it is rapidly decreasing, and by the large quantity and high quality of DNA that is required for analysis.

In addition, a technical limitation is the lack of a pipeline to detect structural variants ranging from 50 to a few hundred base pairs, which should be implemented in the coming years in order not to fail to detect causative variants.

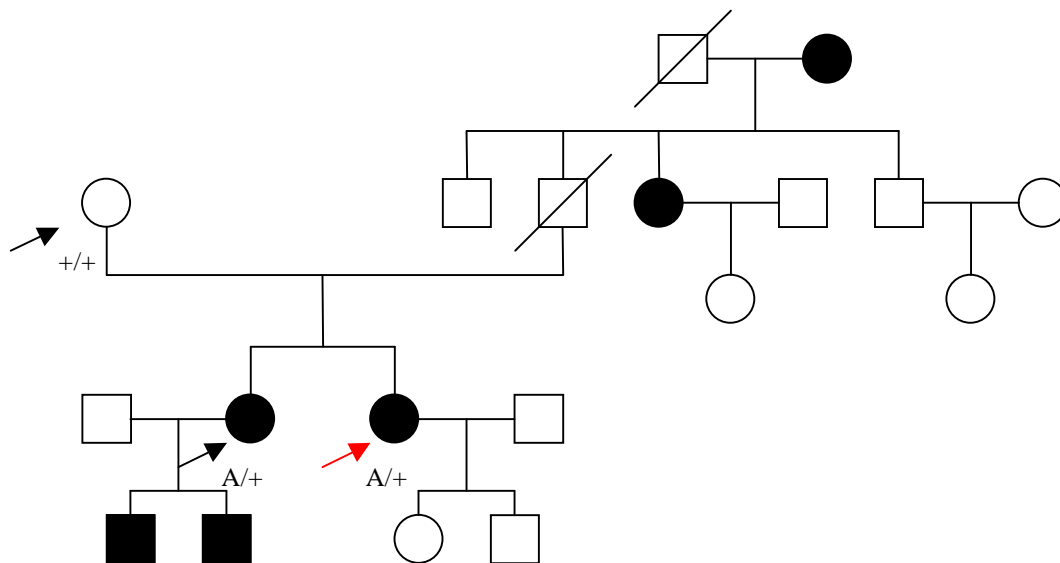
In conclusion, this approach, starting from a huge amount of genomic variants, has allowed us to identify the disease-causing mutation in unrelated individuals with a genetically heterogeneous Mendelian disease.

References

1. Hartong, D.T., E.L. Berson, and T.P. Dryja, *Retinitis pigmentosa*. *Lancet*, 2006. **368**(9549): p. 1795-809.
2. Jin, Z.B., et al., *Identifying pathogenic genetic background of simplex or multiplex retinitis pigmentosa patients: a large scale mutation screening study*. *J Med Genet*, 2008. **45**(7): p. 465-72.
3. Rio Frio, T., et al., *A single-base substitution within an intronic repetitive element causes dominant retinitis pigmentosa with reduced penetrance*. *Hum Mutat*, 2009. **30**(9): p. 1340-7.
4. den Hollander, A.I., et al., *Mutations in the CEP290 (NPHP6) gene are a frequent cause of Leber congenital amaurosis*. *Am J Hum Genet*, 2006. **79**(3): p. 556-61.
5. Webb, T.R., et al., *Deep intronic mutation in OFD1, identified by targeted genomic next-generation sequencing, causes a severe form of X-linked retinitis pigmentosa (RP23)*. *Hum Mol Genet*, 2012. **21**(16): p. 3647-54.
6. Pomares, E., et al., *Identification of an intronic single-point mutation in RP2 as the cause of semidominant X-linked retinitis pigmentosa*. *Invest Ophthalmol Vis Sci*, 2009. **50**(11): p. 5107-14.
7. Rose, A.M., et al., *A 112 kb deletion in chromosome 19q13.42 leads to retinitis pigmentosa*. *Invest Ophthalmol Vis Sci*, 2011. **52**(9): p. 6597-603.
8. Restagno, G., et al., *A large deletion at the 3' end of the rhodopsin gene in an Italian family with a diffuse form of autosomal dominant retinitis pigmentosa*. *Hum Mol Genet*, 1993. **2**(2): p. 207-8.
9. Drmanac, R., et al., *Human genome sequencing using unchained base reads on self-assembling DNA nanoarrays*. *Science*, 2010. **327**(5961): p. 78-81.
10. Wang, H., et al., *Mutations in SPATA7 cause Leber congenital amaurosis and juvenile retinitis pigmentosa*. *Am J Hum Genet*, 2009. **84**(3): p. 380-7.
11. Tucker, B.A., et al., *Exome sequencing and analysis of induced pluripotent stem cells identify the cilia-related gene male germ cell-associated kinase (MAK) as a cause of retinitis pigmentosa*. *Proc Natl Acad Sci U S A*, 2011. **108**(34): p. E569-76.
12. Kondo, H., et al., *A homozygosity-based search for mutations in patients with autosomal recessive retinitis pigmentosa, using microsatellite markers*. *Invest Ophthalmol Vis Sci*, 2004. **45**(12): p. 4433-9.
13. Hosono, K., et al., *Two novel mutations in the EYS gene are possible major causes of autosomal recessive retinitis pigmentosa in the Japanese population*. *PLoS One*, 2012. **7**(2): p. e31036.
14. Barragan, I., et al., *Mutation spectrum of EYS in Spanish patients with autosomal recessive retinitis pigmentosa*. *Hum Mutat*, 2010. **31**(11): p. E1772-800.
15. Vervoort, R., et al., *Mutational hot spot within a new RPGR exon in X-linked retinitis pigmentosa*. *Nat Genet*, 2000. **25**(4): p. 462-6.
16. Katsanis, N., et al., *Triallelic inheritance in Bardet-Biedl syndrome, a Mendelian recessive disorder*. *Science*, 2001. **293**(5538): p. 2256-9.
17. Kajiwara, K., E.L. Berson, and T.P. Dryja, *Digenic retinitis pigmentosa due to mutations at the unlinked peripherin/RDS and ROM1 loci*. *Science*, 1994. **264**(5165): p. 1604-8.

Patient ID	Gene	Protein change	State	Reference	Interpretation
003-102	<i>USH2A</i>	M1731fs	Het	Novel	Possibly pathogenic
		G546V	Het	Novel	
003-146	<i>SPATA7</i>	Q465fsX505	Het	Wang <i>et al.</i> 2009	Pathogenic
		1'313 bp deletion	Het	Novel	
003-154					No candidates
121-847	<i>MAK</i>	K433	Hom	Tucker <i>et al.</i> 2011	Pathogenic
R5					No candidates
R6	<i>RPE65</i>	R515W	Hom	Kondo <i>et al.</i> 2004	Pathogenic
R7					No candidates
R10	<i>RHO</i>	S343N	Het	Novel	Non-pathogenic
R25	<i>EYS</i>	S1653KfsX2	Het	Hosono <i>et al.</i> 2012	Pathogenic
		Y2935*	Het	Iwanami <i>et al.</i> 2012	
R26	<i>PRPF31</i>	Q411fs	Het	Novel	Pathogenic
R28					No candidates
R31					No candidates
R35					No candidates
R38					No candidates
R41	<i>EYS</i>	S1653KfsX2	Het	Hosono <i>et al.</i> 2012	Pathogenic
		NS3062fs	Het	Same amino acidic position of another variant reported by Barragan <i>et al.</i> 2010	
R51	<i>RPGR</i>	EG801GEfs	Hemi	Vervoort <i>et al.</i> 2000	Pathogenic

Table 1. Summary of non-polymorphic variants found in known arRP genes. North American patients are highlighted in yellow; Japanese patients are highlighted in blue. Abbreviations: Het, heterozygous; Hom, homozygous; Hemi, hemizygous.



A --- *PRPF31* p.Q411fs

Figure 1. Cosegregation analysis in the family of proband R26. Arrows indicate the individuals for which it was possible to perform the analysis. The red arrow indicates the proband.

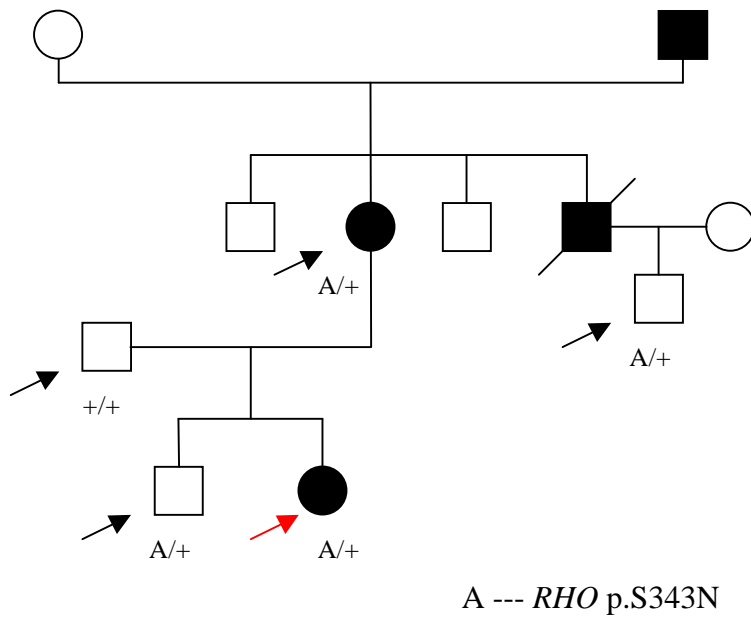


Figure 2. Cosegregation analysis in the family of proband R10.

ABCA4	ERCC8	PEX7
ABHD12	EYS	PHYH
ADAM9	FAM57B	PLA2G5
AGTPBP1	FAM161A	PRCD
AHI1	FAM169A	PROM1
AIPL1	FLVCR1	PRPF3
ALDH3A2	GNAT1	PRPF31
ALMS1	GNPTG	PRPF6
ARL3	GPR98	PRPF8
ARL6	GPR179	PRPH2
ATP6	GRK1	PXMP3
ATXN2	GUCA1A	RBP3
BBS1	GUCA1B	RBP4
BBS10	GUCY2D	RD3
BBS12	HARS	RDH12
BBS2	HMX1	RGR
BBS4	IDH3B	RHO
BBS5	IMPDH1	RIMS1
BBS7	IMPG2	RLBP1
BBS9	INPP5E	ROM1
C10ORF2	INVS	RP1
C2orf71	IQCB1	RP2 RP9
C8orf37	KCNV2	RPE65
CA4	KIF11	RPGR
CABP4	KLHL7	RPGRIP1
CACNA1F	LCA5	RPGRIP1L
CC2D2A	LRAT	SAG
CCDC66	LZTFL1	SDCCA68
CCL2	MAK	SEMA4A
CDH23	MERTK	SLC4A3
CEP290	MFN2	SNRNP200
CERKL	MFRP	SPATA7
CHM	MKKS	TMEM216
CLN3	MPDZ	TMEM237
CLN5	MTTP	TOPORS
CLN6	MYO7A	TPP1
CLN8	NPHP1	TRIM32
CLRN1	NPHP3	TRIM37
CNGA1	NR2E3	TRNH
CNGB1	NRL	TRNL1
CNNM4	NYX	TRNP
CRB1	OAT	TRNS2
CRX	OFD1	TRPM1
CTNS	PCDH15	TTC8
CUL3	PCDH21	TTPA
CX3CL1	PDE6A	TULP1
CYP4V2	PDE6B	UNC119
DFNB31	PDE6G	USH1C
DHDDS	PEX1	USH1G
ELOVL4	PEX12	USH2A
ERCC2	PEX26	WDR19
ERCC6	PEX5	ZNF513

Supplementary Table S1. List of 157 genes that we used for our analysis.

**Clinicopathologic and molecular analysis of a choroidal pigmented schwannoma
in the context of a *PTEN* hamartoma tumor syndrome**

Published in *Ophthalmology* 119(4):857-64, 2012

The aim of this project was to characterize the clinical and molecular nature of a rare ocular tumor, described for the first time in the choroid of a patient diagnosed with *PTEN* hamartoma tumor syndrome.

The project was a collaboration with Dr. Alexandre P. Moulin (Ophthalmology, Jules Gonin Eye Hospital, Lausanne, Switzerland).

This project led to the clinical description of a rare tumor and to the discovery that at the molecular level the tumor presented a unique combination of reduction of *PTEN* and absence of *NF2* expression, two ubiquitously expressed tumor-suppressor genes that had never been proven to contribute together to tumorigenesis.

In this study I performed the molecular genetic analyses and I participated in the article writing.

Clinicopathologic and Molecular Analysis of a Choroidal Pigmented Schwannoma in the Context of a *PTEN* Hamartoma Tumor Syndrome

Giulia Venturini, MSc,^{1,*} Alexandre P. Moulin, MD,^{2,3,*} Manuel Deprez, MD, PhD,³ Sylvie Uffer, MD,³ Armand Bottani, MD,⁴ Leonidas Zografos, MD,² Carlo Rivolta, PhD¹

Purpose: To report the first case of choroidal schwannoma in a patient affected by *PTEN* hamartoma tumor syndrome (PHTS) and investigate the molecular involvement of the phosphatase and tensin homolog (*PTEN*) and neurofibromin 2 (*NF2*) genes in this rare intraocular tumor.

Design: Observational case report.

Participant: A 10-year-old girl diagnosed with PHTS.

Methods: The enucleated specimen underwent histologic, immunohistochemical, and transmission electronic microscopy. The expression of *PTEN* and *NF2* and their protein products were evaluated by reverse transcription-polymerase chain reaction and immunohistochemistry. Somatic mutations of *PTEN* and *NF2*, as well as allelic loss, were investigated by direct sequencing of DNA extracted from the tumor. *PTEN* epigenetic silencing was investigated by pyrosequencing.

Main Outcome Measures: Histopathologic and molecular characterization of a choroidal pigmented schwannoma.

Results: Histopathologic, immunohistochemical, and electron microscopic analysis demonstrated features consistent with a pigmented cellular schwannoma of the choroid. We found no loss of heterozygosity at the genomic level for the *PTEN* germline mutation and no promoter hypermethylation or other somatic intragenic mutations. However, we observed an approximate 40% reduction of *PTEN* expression at both the mRNA and the protein level, indicating that the tumor was nonetheless functionally deficient for *PTEN*. Although DNA sequencing of *NF2* failed to identify any pathologic variants, its expression was abolished within the tumor.

Conclusions: We report the first description of a pigmented choroidal schwannoma in the context of a PHTS. This rare tumor showed a unique combination of reduction of *PTEN* and absence of *NF2* expression.

Financial Disclosure(s): The author(s) have no proprietary or commercial interest in any materials discussed in this article. *Ophthalmology* 2012;119:857–864 © 2012 by the American Academy of Ophthalmology.



Schwannomas are nerve tumors originating exclusively from Schwann cells, which in a normal context are closely associated with myelinated and unmyelinated axons in the peripheral nerves. Schwannomas account for approximately 8% of all primary intracranial tumors, and they usually occur as solitary and sporadic lesions.¹ Both sporadic and familial schwannomas show loss of or mutation in the neurofibromin 2 (*NF2*) gene, encoding the protein merlin.^{2,3} Merlin shares sequences homology with the Ezrin-Radixin-Moesin protein family and acts as a tumor suppressor at the membrane-cytoskeleton interface and interferes with the transmission of mitogenic signals.⁴ Furthermore, experiments have shown that silencing of *NF2* in cultured Schwann cells increases cell proliferation, a key step in tumorigenesis.⁵ Schwannomas arising from the ciliary body of the eye and the choroid are rare forms of intraocular tumors that can clinically mimic amelanotic melanomas. To

the best of our knowledge, genetic alterations in these rare tumors have not been reported.

The *PTEN* hamartoma tumor syndrome (PHTS) is an autosomal dominant disorder caused by various mutations in the tumor-suppressor gene phosphatase and tensin homolog (*PTEN*), located at 10q23. The major diagnostic criteria for this syndrome are macrocephaly and breast and thyroid cancers, and minor criteria include lipomas, fibrocystic disease of the breast, hamartomatous intestinal polyps, and fibromas.^{6,7} The clinical spectrum of PHTS encompasses several syndromes with variable ocular involvement: Cowden syndrome, Bannayan-Riley-Ruvalcaba syndrome, and possibly Proteus syndrome. In Cowden syndrome, ophthalmic manifestations include trichilemmomas and cataracts.^{8,9} Conjunctival papilloma,¹⁰ retinal angioma,¹¹ and microphthalmia⁹ have also been reported as single cases in this syndrome. In Bannayan-Riley-Ruvalcaba syn-

drome, pseudopapilledema has been documented.¹² The ocular manifestations of Proteus syndrome, characterized by asymmetric skeletal overgrowth and palmar or plantar gyriform hypertrophy, are numerous and include epibulbar and posterior segment hamartomas,^{13,14} band keratopathy,¹⁵ retinal coloboma, nystagmus, strabismus, and cataract.^{14,16} Patients affected by PHTS provide a unique opportunity to examine the role of *PTEN* in human tumorigenesis and to study genotype–phenotype correlations.¹⁷ So far, only limited anomalies of the peripheral nervous system (mucocutaneous neuroma) have been described as clinical phenotypes of PHTS,¹⁸ although a more careful examination of the peripheral nervous system in patients with *PTEN* mutations is probably necessary.¹⁹

We report a female patient affected by PHTS who developed a unilateral choroidal schwannoma that led to the enucleation of her eye. The molecular involvement of *PTEN* in this rare intraocular tumor, described for the first time in the context of PHTS, and the possible contribution of the *NF2* tumor-suppressor gene in this condition are further investigated.

Materials and Methods

Clinical Analysis

The relevant clinical information was retrieved from the patient's files from Jules Gonin Eye Hospital. Institutional review board approval from Lausanne University was granted.

Histopathologic Analysis

The tumor was formalin-fixed, macroscopically processed, and dehydrated through graded alcohol followed by paraffin inclusion. Sections 5 μm in size were cut, and the following stains were performed: hematoxylin–eosin, periodic acid-Schiff, Alcian blue, Prussian blue, Masson Fontana, reticulin, and Masson trichrome.

Immunohistochemical Analysis

Immunohistochemistry was performed on formalin-fixed paraffin-embedded (FFPE) tissue sections representative of the choroidal schwannoma and the thyroid adenoma. After epitope retrieval at pH 6.0 or 9.0, endogenous peroxidase was blocked by 4% hydrogen peroxide for 10 minutes. The sections were incubated with several anti-human antibodies (anti-S100, rabbit polyclonal, Dako, Glostrup, Denmark; anti-Melan A, mouse monoclonal, Dako; anti-melanoma, mouse monoclonal, Diagnostic BioSystems, Pleasanton, CA; anti-collagen IV, mouse monoclonal, Dako; anti-glial fibrillary acidic protein, mouse monoclonal, Dako; anti-epithelial membrane antigen, mouse monoclonal, Dako; anti-muscle-actin, mouse monoclonal, Dako; anti-CD68, clone PGM1, mouse monoclonal, Dako; anti-Ki67, mouse monoclonal, Dako; anti-PTEN,

mouse monoclonal, Dako, dilution 1:100; anti-NF2-Merlin, rabbit polyclonal, Abcam [Cambridge, UK], dilution 1:200). A streptavidin/biotin detection method with 3,3'-diaminobenzidine tetrachloride or 3-amino 9-ethyl carbazole was used for signal detection (Dako Envision + System/HRP Dual Link).

Transmission Electron Microscopy

Fragments of tumor were postfixed in 2% tetroxide osmium in cacodylate sodium buffer and dehydrated through graded alcohol. The material was embedded in epoxy resin, and ultrathin cuts were performed. Transmission electron microscopy was performed using a Philips CM10 microscope (Amsterdam, The Netherlands).

Molecular Genetic Analysis

DNA and RNA were extracted from $3 \times 10\text{-}\mu\text{m}$ FFPE slices each using the RecoverAll Total Nucleic Acid Isolation Kit (Applied Biosystems, Inc., Carlsbad, CA). Genomic DNA was also extracted from peripheral blood leukocytes using the Nucleon Genomic DNA Extraction Kit (Tepnel Life Sciences PLC, Manchester, UK) according to the manufacturer's protocols. To circumvent problems due to partial DNA degradation in the fixed tissue, all the exons and proximal introns sequences of the 2 genes were amplified by short-range polymerase chain reaction (PCR) using the HotStar Taq DNA Polymerase (Qiagen, Venlo, The Netherlands) and extended cycling conditions (40 cycles). The thermal profile of the reactions was as follows: an initial denaturation step at 94°C for 15 minutes, followed by 40 cycles of denaturation at 94°C for 30 seconds, annealing according to primers' melting temperature for 30 seconds, and extension at 72°C for 1 minute, followed by a final extension step of 72°C for 10 minutes. The designed primers used for amplification of the coding region of *PTEN* are listed in Table 1 (available at <http://aaojournal.org>). The primers for the majority of *NF2* exons used were those described by Jacoby et al.²⁰ However, the primer pairs for exons 2, 3, 4, 5, 6, and 12, along with the forward exon 11 and 14 primers, were redesigned to increase the efficiency of the reaction (Table 2, available at <http://aaojournal.org>). Direct sequencing of the amplification products was performed by using the BigDye Terminator v1.1 Cycle Sequencing Kit (Applied Biosystems, Inc.).

PTEN promoter methylation analysis was carried out after bisulphite modification using the pyrosequencing technique, as described by Mirmohammadsadeh et al.²¹ Because most of the mRNA molecules isolated from FFPE tissues do not contain a poly(dA) sequence, random hexamers were chosen to perform cDNA synthesis with the SuperScript III First-Strand Synthesis System for reverse transcription (RT)-PCR (Invitrogen/Life Technologies, Inc., Grand Island, NY), according to the manufacturer's instructions.

PTEN and *NF2* mRNA expression levels were then evaluated by semiquantitative RT-PCR using as a reference gene for the normalization the 18S rRNA. The designed primers used for amplification of *PTEN*, *NF2*, and 18S cDNA are listed in Table 3 (available at <http://aaojournal.org>).

Figure 2. A, Low-power photomicrograph demonstrating a papillary and parapapillary choroidal mass accompanied by a small peritumoral retinal detachment (stain, hematoxylin–eosin). B, The tumor is composed of fascicles of spindle cells without Antoni B hypocellular areas. A thick-walled blood vessel can be observed in the right inferior corner of the picture (stain, hematoxylin–eosin; original magnification $\times 63$). C, In some areas foamy cells can also be identified (stain, hematoxylin–eosin; original magnification $\times 63$). D, Higher magnification demonstrates spindle cells without prominent nucleoli and moderate pleomorphism (stain, hematoxylin–eosin; original magnification $\times 126$). E, Reticulin stain showing a delicate pericellular fibrous network (original magnification $\times 126$).

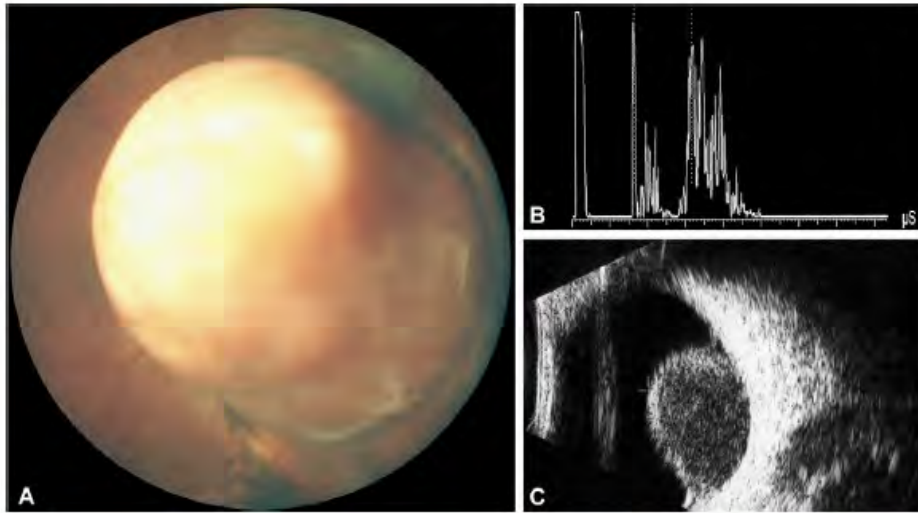
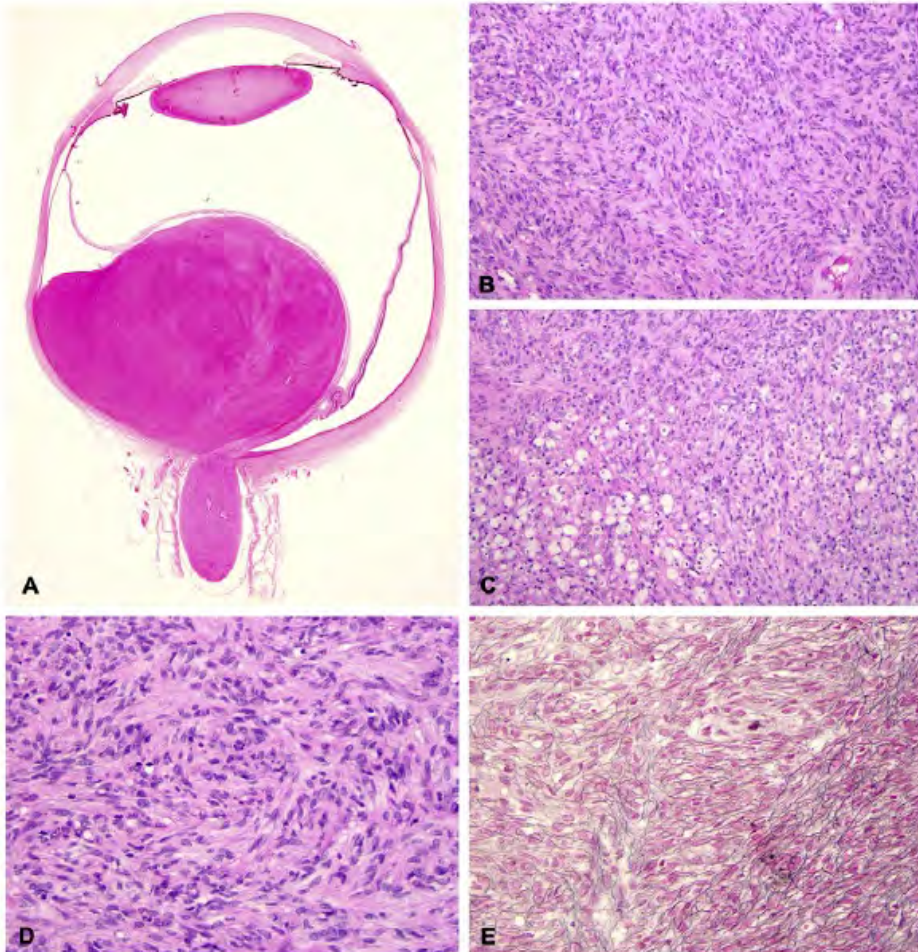


Figure 1. A, Fundus demonstrating a nonpigmented choroidal mass arising in the papillary and parapapillary area. B, A-scan ultrasonography showing moderate internal reflectivity and high attenuation. C, B-scan demonstrating a homogeneous choroidal mass measuring 10.4 mm.



Literature Review Strategy

A comprehensive literature review was performed using MEDLINE, EMBASE, and Web of Science with the keywords *PTEN*, or *Cowden syndrome*, or *Proteus syndrome* and *schwannoma*. Additional research was undertaken using Google with the keywords *PTEN* and *schwannoma* and *uvea*.

Results

Clinical Findings

A 10-year-old girl with a familial history of *PTEN* hamartoma tumor syndrome was referred to the Oncology Unit of Jules Gonin Eye Hospital because of decreased vision in the right eye for 1 month. A right leukocoria had been noticed 8 months earlier. Her medical history was significant for a thyroid adenoma. Right cortical dysplasia without mental retardation had been recently diagnosed. The patient, her sister, and her mother were macrocephalic. Her sister was born with a cyanotic heart disease (tricuspid valve atresia, pulmonary stenosis, and interauricular and interventricular septal defects) and later developed several vertebral haemangiomas.²² The mother had partial thyroidectomy for nodular hyperplasia and several breast cysts.

Best-corrected visual acuity of the right eye was limited to counting fingers and was 20/20 in the left eye. In slit-lamp examination, both anterior segments were unremarkable. Intraocular pressure was normal in both eyes. Fundus examination of the right eye revealed a right papillary nonpigmented choroidal mass extending nasally with localized retinal detachment (Fig 1A). A-scan ultrasonography showed a moderate internal reflectivity and high attenuation (Fig 1B). The tumor height measured 10.4 mm in B-scan ultrasonography, where it displayed a homogeneous aspect (Fig 1C). The differential diagnosis included an amelanotic melanoma, a schwannoma, and a leiomyoma. After a follow-up of 9 months, tumor height increased to 12.6 mm. Since a melanoma could not completely be ruled out and considering the risk of a glaucoma, an enucleation was performed.

Histopathology

The globe measured 22×21×22 mm with an optic nerve of 7 mm in length. Corneal diameter was 11 mm. After horizontal sectioning, a pale, slightly yellowish mass occupying more than two thirds of the vitreous cavity was found in the choroid. This mass was accompanied by a small retinal detachment.

Microscopically, the mass was composed by fascicles of spindle cells with mild nuclear pleomorphism (Fig 2). The nuclei had regular chromatin without prominent nucleoli (Fig 2D). The mitotic activity was low, and only occasional mitoses were identified (1–2/40 high-power field, 400×). No Antoni B hypocellular areas and no nuclear palisading (Verocay bodies) were found. In some areas, scattered cells with larger and clearer cytoplasm were observed (Fig 2C). The tumor was entirely situated within the choroid and in close contact with a short ciliary nerve. Although well demarcated, the tumor lacked a well-formed capsule. At the apex of the tumor, there were focal areas of retinal pigment epithelium atrophy and the overlying retina was displaying moderate atrophy, predominantly in the inner layers. Periodic acid-Schiff and reticulin stains revealed a fine and delicate fibrous network surrounding isolated cells or small clusters of spindle cells (Fig 2E). Masson Fontana stain was weakly positive in small granules within a few cells.

By immunohistochemistry, the spindle cells were diffusely expressing S100 protein (Fig 3A, available at <http://aaojournal.org>).

Some cells with foamy cytoplasm were also expressing S100 protein. Although no melanin granules could easily be identified in hematoxylin–eosin slides, more than 60% of the spindle cells expressed Melan A and demonstrated reactivity with melanoma antibody (Fig 3B, available at <http://aaojournal.org>). Type IV collagen was also identified around aggregates of spindle cells or isolated cells (Fig 3C, available at <http://aaojournal.org>). There was no expression of epithelial membrane antigen, glial fibrillary acidic protein, or muscle actin. The cells with larger and clearer cytoplasm were expressing CD68 (Fig 3D, available at <http://aaojournal.org>). The proliferation index (Ki67) was approximately 8%. The *PTEN* expression was identified in the cytoplasm of 60% of the cells (Fig 4B). In the thyroid adenoma, *PTEN* expression was lost in the follicular cells and conserved in the parafollicular cells (Fig 4C). Merlin was not expressed in the schwannoma (Fig 5B), in sharp contrast with nuclear and cytoplasmic staining in the thyroid adenoma (Fig 5C).

Transmission electronic microscopy revealed long and interdigitating processes partially covered by basement membrane material (Fig 6, available at <http://aaojournal.org>). No long-spaced collagen (Luse bodies) was found. Within the cytoplasm of the spindle cells, stage 2 to 4 melanosomes could be observed. On the basis of these findings, the diagnosis of a pigmented cellular choroidal schwannoma was established.

PTEN Molecular Analysis

A germline *PTEN* heterozygous missense mutation (c.406T>C, p.Cys136Arg)²³ had been previously identified on exon 5, immediately outside of the protein's phosphatase core motif, in both the mother and her 2 daughters.²² It was confirmed in the present experiments. DNA extracted from the tumor revealed no genomic loss of heterozygosity (LOH) for the germline mutation (Fig 7). Moreover, no other intragenic somatic mutations were present in all analyzed *PTEN* regions in the tumor sample compared with the blood from the patient.

Methylation analysis of 5 CpG islands within the *PTEN* promoter region (–1455 to –1231, with respect to the transcription start site) showed no epigenetic silencing of this gene in the tumor, compared with the patient's blood DNA. Gene silencing was not present, also in comparison with a schwannoma from another patient who did not carry any *PTEN* germline mutations, used as a negative control (data not shown).

Despite the absence of LOH and methylation-mediated epigenetic silencing, *PTEN* mRNA analysis revealed that the tumor expressed significantly reduced amounts of transcripts, both with respect to the non-*PTEN* schwannoma and to other normal or cancerous tissues (Fig 4A). This deficit was quantified to be approximately 40% by densitometry and corresponded approximately to the observed reduction of *PTEN* protein assessed by immunohistochemistry.

NF2 Molecular Analysis

Sequencing of all *NF2* exons and flanking introns did not reveal any pathologic variation within the tumor. We could only detect a novel heterozygous germline polymorphic variant on exon 6 (c.531T>C, p.Tyr177Tyr) in the DNA extracted from the patient's blood. This was confirmed to be present also in the DNA extracted from the tumor, again in a heterozygous state, indicating absence of LOH. *NF2* mRNA analysis by RT-PCR showed no detectable mRNA transcripts within the tumor (Fig 5A).

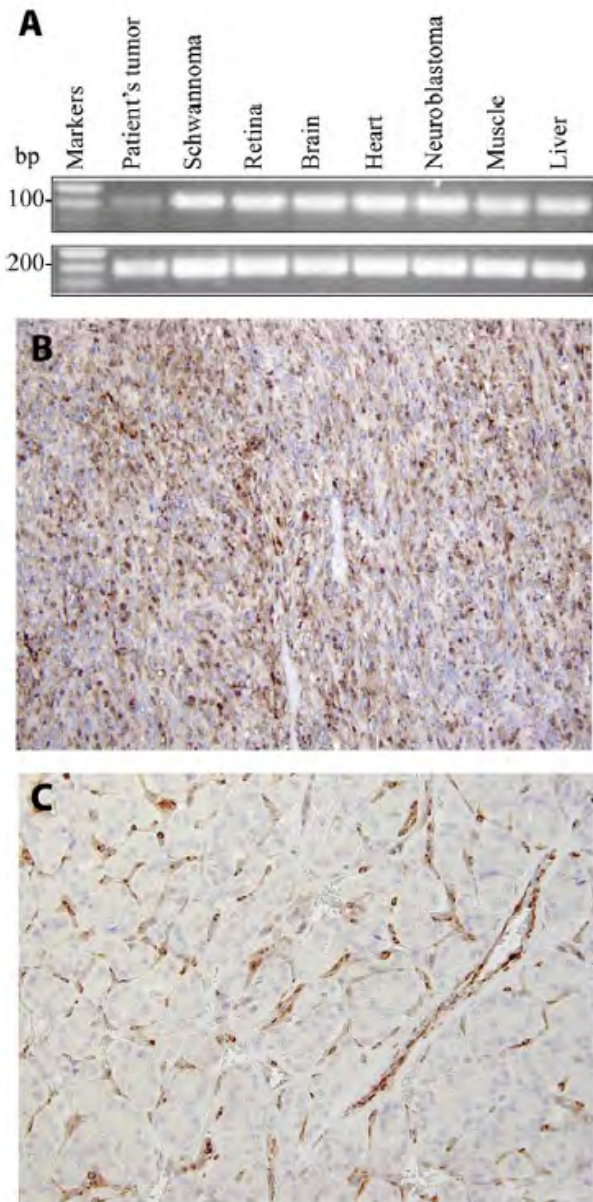


Figure 4. A, *PTEN* mRNA expression in the patient's tumor compared with other normal and cancerous tissue showed a reduction of ~40% in the patient's tumor compared with a schwannoma without *PTEN* germline mutation. B, *PTEN* expression in the patient's schwannoma; nuclear and cytoplasmic expression was found in approximately 60% of the tumor cells (original magnification, $\times 126$). C, *PTEN* expression in the thyroid adenoma: *PTEN* is highly expressed in the parafollicular C cells, but its expression is abolished in the follicular cells. bp = base pair.

Discussion

Schwannoma arising in the choroid are rare tumors, and the distinction from an amelanotic melanoma is difficult to establish clinically. Fluorescein angiography and ultrasonography provide little help in this situation. The age at

presentation varies between 9 and 74 years, with a mean age of approximately 35 years. Women tend to be more frequently affected (70%) in reported cases.²⁴⁻²⁷

The diagnosis of Schwannoma relies in our case on the light microscopic aspect of fascicles of spindle cells with bland-appearing nuclei, the presence of basement membrane surrounding the cells, and the electron microscopic aspect of multiples interdigitating processes.^{28,29} The ab-

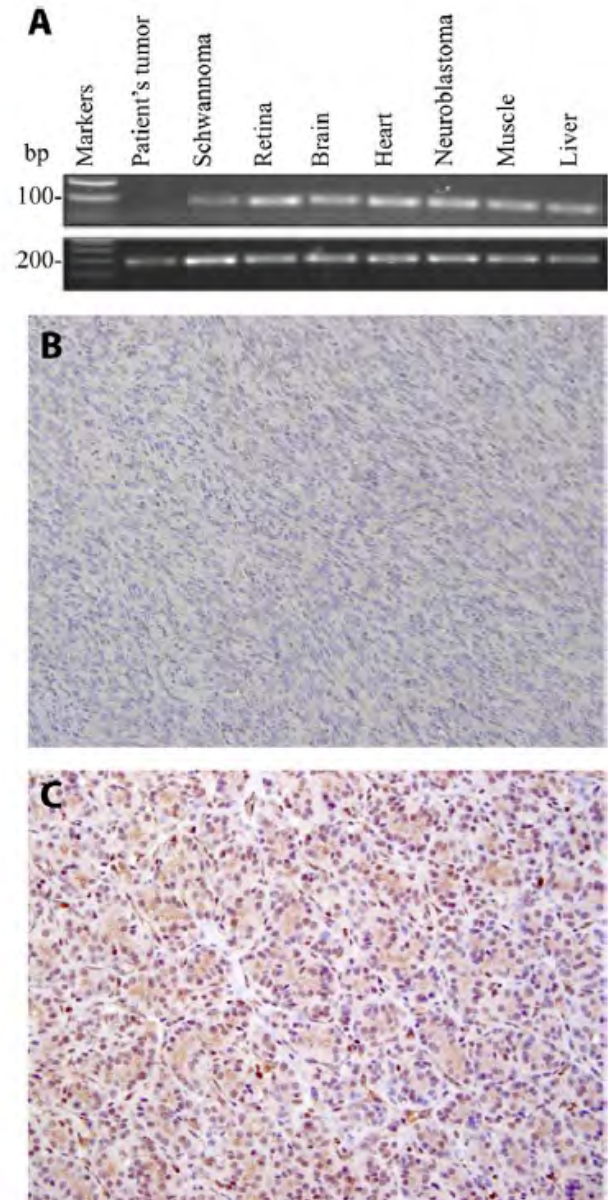


Figure 5. A, *NF2* mRNA expression was absent in the patient's tumor compared with other normal and cancerous tissues. B, *NF2* expression in the patient's schwannoma, confirming at the protein level the absence of *NF2* (original magnification, $\times 126$). C, *NF2* expression in the thyroid adenoma displaying a diffuse cytoplasmic and nuclear expression in the follicular cells (original magnification, $\times 126$). bp = base pair.

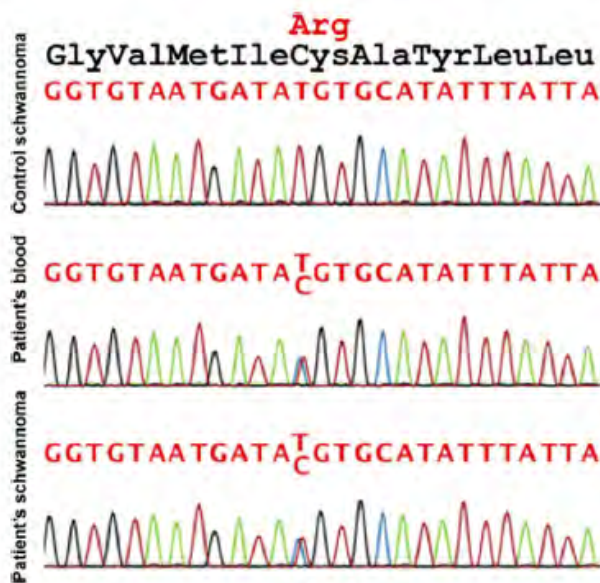


Figure 7. Electropherograms of part of *PTEN* exon 5 in a control Schwannoma and in the patient's blood and tumor. Sequencing analysis demonstrates that there is no loss of heterozygosity of the c.406T>C germline mutation in the patient's tumor.

sence of hypocellular areas (Antoni B), Verocay bodies, and the presence of scattered histiocytes are features commonly encountered in cellular schwannoma. Luse bodies are also less frequent in cellular schwannoma.³⁰ The combined expression of S100 protein and CD68 in foamy cells underscores their schwannian origin with phagocytic properties.³¹ Because no melanin could clearly be identified on the hematoxylin–eosin slides, the reactivity with melanocytic markers was surprising and confirmed by electron microscopy with the evidence of melanosomes. Pigmented schwannoma in the choroid are rare, and only 2 cases have so far been documented; in contrast with our case, pigmented cells could easily be seen in light microscopy.^{25,28} Of note, Carney complex has been associated with melanotic schwannoma, but in these cases, psammoma bodies and adipose-like cells are typically found within the schwannoma. The ability of melanin synthesis in Schwann cells and melanocytes probably reflects their neural crest origin.^{28,32}

In autosomal-dominant syndromes associated with germline mutations of tumor-suppressor genes, the neoplastic development usually occurs when a somatic event inactivates the nonmutated allele.³³ The best known example of this situation is represented by retinoblastoma. In the majority of these cases, the tumor results from the loss of 1 allele and the inactivation of the remaining allele by several different mechanisms leading to loss of gene expression.³⁴ *PTEN* inactivation occurs mainly by LOH,^{35,36} but also by the accumulation of somatic intragenic mutations and by hypermethylation of the promoter.^{37–39} In addition, it is now clear that *PTEN* may be inactivated by several different mechanisms, and that these can coexist within a single tumor type, despite the fact that specific tumors may have a predominant mechanism of inactivation.⁴⁰ Moreover, al-

though the precise molecular mechanism has yet to be elucidated, differential subcellular compartmentalization might also play a role in functional and restricted *PTEN* inactivation.⁴¹ Recent evidence from animal models suggests that subtle variations in *PTEN* expression not only lead to variations in tumor progression and aggressiveness but also play a role in the development of distinct tumor types.^{42–44}

Analysis of the role of *PTEN* in the tumorigenesis of sporadic vestibular schwannomas was previously performed.¹ In this work, no deficits in the expression of *PTEN* protein and no mutations of the gene were observed, suggesting the absence of a *PTEN*-associated tumor-suppressor role in sporadic vestibular schwannomas. However, evidence of reduction of *PTEN* expression, mediated by silencing the microRNA miR-21, was recently identified in these tumors.⁴⁵

Although we could not identify any Knudson's "second hit" at the genomic level, a contribution of *PTEN* in the tumorigenesis of this choroidal schwannoma is likely and based on its further inactivation in the tumor compared with normal cells carrying the germline mutation. In the tumor, *PTEN* was reduced by approximately 40% at both the mRNA and the protein levels compared with another tumor of the same cell type that was negative for *PTEN* mutations. This indicated that the tumor was nonetheless functionally deficient for *PTEN*.

Research performed so far has indicated that schwannomas are genetically heterogeneous tumors, and that their tumorigenesis is not solely dependent on only one gene.⁴⁶ It is possible that *PTEN* downregulation synergizes with effects conferred by other mutations that are contained within the tumor to increase proliferation and survival.⁴² This is suggested also by our analysis, indicating that in this rare choroidal schwannoma *PTEN* function is probably reduced but not completely abolished.

The development of ocular and periocular schwannomas has been associated with neurofibromatosis.^{47–50} Because the molecular genetics of both familial and sporadic schwannomas are partially explained by loss of function of *NF2*, it was likely that merlin could be a major component of the tumor analyzed in our patient. Specifically, although sequence analysis did not show any *NF2* variant that could be associated with the disease, we could demonstrate a complete deficit of merlin in this schwannoma but not in the control thyroid adenoma.

In conclusion, this study supports the existing knowledge that multiple genetic or epigenetic events may be necessary for choroidal schwannoma development and growth, probably led by *NF2* downregulation. In view of the rarity of uveal schwannoma and PHTS, as well as our data on reduced *PTEN* expression in the neoplasm analyzed, *PTEN* may also be a contributor to the genesis of this uncommon tumor.

References

1. Mawrin C, Kirches E, Boltze C, Dietzmann K. *PTEN* is not altered in sporadic vestibular schwannomas. *Histopathology* 2002;40:526–30.
2. Rouleau GA, Merel P, Lutchman M, et al. Alteration in a new gene encoding a putative membrane-organizing protein causes neuro-fibromatosis type 2. *Nature* 1993;363:515–21.

3. Trofatter JA, MacCollin MM, Rutter JL, et al. A novel moesin-, ezrin-, radixin-like gene is a candidate for the neurofibromatosis 2 tumor suppressor. *Cell* 1993;72:791–800.
4. Stamenkovic I, Yu Q, Merlin, a “magic” linker between extracellular cues and intracellular signaling pathways that regulate cell motility, proliferation, and survival. *Curr Protein Pept Sci* 2010;11:471–84.
5. Ahmad Z, Brown CM, Patel AK, et al. Merlin knockdown in human Schwann cells: clues to vestibular schwannoma tumorigenesis. *Otol Neurotol* 2010;31:460–6.
6. Hobert JA, Eng C. PTEN hamartoma tumor syndrome: an overview. *Genet Med* 2009;11:687–94.
7. Blumenthal GM, Dennis PA. PTEN hamartoma tumor syndromes. *Eur J Hum Genet* 2008;16:1289–300.
8. Starink TM, van der Veen JP, Arwert F, et al. The Cowden syndrome: a clinical and genetic study in 21 patients. *Clin Genet* 1986;29:222–33.
9. Vantomme N, Van Calenbergh F, Goffin J, et al. Lhermitte-Duclos disease is a clinical manifestation of Cowden's syndrome. *Surg Neurol* 2001;56:201–5.
10. Wells GB, Lasner TM, Yousem DM, Zager EL. Lhermitte-Duclos disease and Cowden's syndrome in an adolescent patient: case report. *J Neurosurg* 1994;81:133–6.
11. Gicquel JJ, Vabres P, Bonneau D, et al. Retinal angioma in a patient with Cowden disease. *Am J Ophthalmol* 2003;135:400–2.
12. Dvir M, Beer S, Aladjem M. Heredofamilial syndrome of mesodermal hamartomas, macrocephaly, and pseudopapilledema. *Pediatrics* 1988;81:287–90.
13. Burke JP, Bowell R, O'Doherty N. Proteus syndrome: ocular complications. *J Pediatr Ophthalmol Strabismus* 1988;25:99–102.
14. Bouzas EA, Krasnewich D, Koutroumanidis M, et al. Ophthalmologic examination in the diagnosis of Proteus syndrome. *Ophthalmology* 1993;100:334–8.
15. Sheard RM, Pope FM, Snead MP. A novel ophthalmic presentation of the Proteus syndrome. *Ophthalmology* 2002;109:1192–5.
16. De Becker I, Gajda DJ, Gilbert-Barnes E, Cohen MM Jr. Ocular manifestations in Proteus syndrome. *Am J Med Genet* 2000;92:350–2.
17. Lopiccolo J, Ballas MS, Dennis PA. PTEN hamartomatous tumor syndromes (PHTS): rare syndromes with great relevance to common cancers and targeted drug development. *Crit Rev Oncol Hematol* 2007;63:203–14.
18. Schaffer JV, Kamino H, Witkiewicz A, et al. Mucocutaneous neuromas: an underrecognized manifestation of PTEN hamartoma-tumor syndrome. *Arch Dermatol* 2006;142:625–32.
19. Gimm O, Attie-Bitach T, Lees JA, et al. Expression of the PTEN tumour suppressor protein during human development. *Hum Mol Genet* 2000;9:1633–9.
20. Jacoby LB, MacCollin M, Louis DN, et al. Exon scanning for mutation of the *NF2* gene in schwannomas. *Hum Mol Genet* 1994;3:413–9.
21. Mirmohammadsadegh A, Marini A, Nambiar S, et al. Epigenetic silencing of the *PTEN* gene in melanoma. *Cancer Res* 2006;66:6546–52.
22. Jenny B, Radovanovic I, Haeggeli CA, et al. Association of multiple vertebral hemangiomas and severe paraparesis in a patient with a PTEN hamartoma tumor syndrome: case report. *J Neurosurg* 2007;107(Suppl):307–13.
23. Kubo Y, Urano Y, Hida Y, et al. A novel *PTEN* mutation in a Japanese patient with Cowden disease. *Br J Dermatol* 2000;142:1100–5.
24. Lee SH, Hong JS, Choi JH, Chung WS. Choroidal schwannoma. *Acta Ophthalmol Scand* 2005;83:754–6.
25. Saavedra E, Singh AD, Sears JE, Ratliff NB. Plexiform pigmented schwannoma of the uvea. *Surv Ophthalmol* 2006;51:162–8.
26. Fan JT, Campbell RJ, Robertson DM. A survey of intraocular schwannoma with a case report. *Can J Ophthalmol* 1995;30:37–41.
27. Matsuo T, Notohara K. Choroidal schwannoma: immunohistochemical and electron-microscopic study. *Ophthalmologica* 2000;214:156–60.
28. Shields JA, Font RL, Eagle RC Jr, et al. Melanotic schwannoma of the choroid: immunohistochemistry and electron microscopic observations. *Ophthalmology* 1994;101:843–9.
29. Erlanson RA, Woodruff JM. Peripheral nerve sheath tumors: an electron microscopic study of 43 cases. *Cancer* 1982;49:273–87.
30. Kurtkaya-Yapici O, Scheithauer B, Woodruff JM. The pathobiologic spectrum of schwannomas. *Histol Histopathol* 2003;18:925–34.
31. Escalona-Zapata J, Diez Nau MD. The nature of macrophages (foam cells) in neurinomas: tissue culture study. *Acta Neuropathol* 1978;44:71–5.
32. Font RL, Truong LD. Melanotic schwannoma of soft tissues: electron-microscopic observations and review of literature. *Am J Surg Pathol* 1984;8:129–38.
33. Hottinger AF, Khakoo Y. Update on the management of familial central nervous system tumor syndromes. *Curr Neurol Neurosci Rep* 2007;7:200–7.
34. Harbour JW, Lai SL, Whang-Peng J, et al. Abnormalities in structure and expression of the human retinoblastoma gene in SCLC. *Science* 1988;241:353–7.
35. Kwabi-Addo B, Giri D, Schmidt K, et al. Haploinsufficiency of the *Pten* tumor suppressor gene promotes prostate cancer progression. *Proc Natl Acad Sci U S A* 2001;98:11563–8.
36. Sato N, Tsunoda H, Nishida M, et al. Loss of heterozygosity on 10q23.3 and mutation of the tumor suppressor gene *PTEN* in benign endometrial cyst of the ovary: possible sequence progression from benign endometrial cyst to endometrioid carcinoma and clear cell carcinoma of the ovary. *Cancer Res* 2000;60:7052–6.
37. Kurose K, Zhou XP, Araki T, Eng C. Biallelic inactivating mutations and an occult germline mutation of *PTEN* in primary cervical carcinomas. *Genes Chromosomes Cancer* 2000;29:166–72.
38. Goel A, Arnold CN, Niedzwiecki D, et al. Frequent inactivation of PTEN by promoter hypermethylation in microsatellite instability-high sporadic colorectal cancers. *Cancer Res* 2004;64:3014–21.
39. Garcia JM, Silva J, Pena C, et al. Promoter methylation of the *PTEN* gene is a common molecular change in breast cancer. *Genes Chromosomes Cancer* 2004;41:117–24.
40. Eng C. *PTEN*: one gene, many syndromes. *Hum Mutat* 2003;22:183–98.
41. Lian Z, Di Cristofano A. Class reunion: PTEN joins the nuclear crew. *Oncogene* 2005;24:7394–400.
42. Carracedo A, Alimonti A, Pandolfi PP. PTEN level in tumor suppression: how much is too little? *Cancer Res* 2011;71:629–33.
43. Alimonti A, Carracedo A, Clohessy JG, et al. Subtle variations in *Pten* dose determine cancer susceptibility. *Nat Genet* 2010;42:454–8.
44. Trotman LC, Niki M, Dotan ZA, et al. *Pten* dose dictates cancer progression in the prostate [report online]. *PLoS Biol* 2003;1:E59. Available at: <http://www.plosbiology.org/article/info%3Adoi%2F10.1371%2Fjournal.pbio.0000059>. Accessed September 26, 2011.
45. Cioffi JA, Yue WY, Mendolia-Loffredo S, et al. MicroRNA-21 overexpression contributes to vestibular schwannoma.

- noma cell proliferation and survival. *Otol Neurotol* 2010; 31:1455–62.
46. Sandberg AA, Stone JF. Benign peripheral nerve sheath tumors: neurofibromas, schwannomas, and perineuriomas. In: *The Genetics and Molecular Biology of Neural Tumors*. Totowa, NJ: Humana Press; 2008:6–19.
47. Bickler-Bluth ME, Custer PL, Smith ME. Neurilemoma as a presenting feature of neurofibromatosis. *Arch Ophthalmol* 1988;106:665–7.
48. Freedman SF, Elner VM, Donev I, et al. Intraocular neurilemmoma arising from the posterior ciliary nerve in neurofibromatosis: pathologic findings. *Ophthalmology* 1988; 95:1559–64.
49. Vannas S, Raitta C, Tarkkanen A. Neurilemmoma of the choroid in Recklinghausen's disease. *Acta Ophthalmol Suppl* 1974;123:126–33.
50. Maroon JC, Kennerdell JS, Abl A. The diagnosis and treatment of orbital tumors. *Clin Neurosurg* 1988;34:485–98.

Footnotes and Financial Disclosures

Originally received: May 12, 2011.

Final revision: August 30, 2011.

Accepted: September 29, 2011.

Available online: January 26, 2012.

Manuscript no. 2011-715.

¹ Department of Medical Genetics, University of Lausanne, Lausanne, Switzerland.

² Ophthalmology, Jules Gonin Eye Hospital, Lausanne, Switzerland.

³ Pathology, Jules Gonin Eye Hospital, Lausanne, Switzerland.

⁴ Service of Genetic Medicine, Geneva University Hospitals, Geneva, Switzerland.

*Drs. Venturini and Moulin contributed equally to this study.

Financial Disclosure(s):

The author(s) have no proprietary or commercial interest in any materials discussed in this article.

This study has been partially funded by the Swiss National Science Foundation (Grant 320000-121929, to CR).

Correspondence:

Alexandre P. Moulin, MD, Jules Gonin Eye Hospital, Avenue de France 15, 1004 Lausanne, Switzerland. E-mail: alexandre.moulin@fa2.ch.

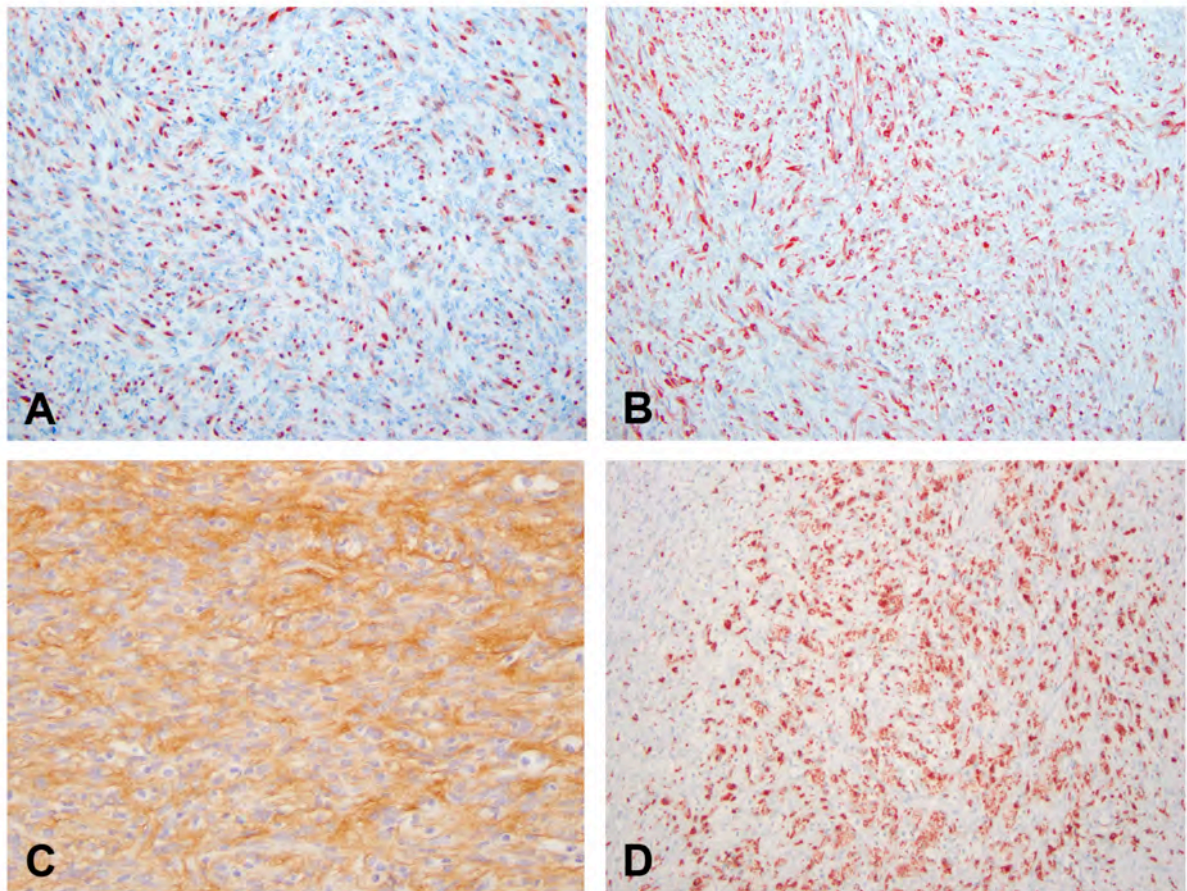


Figure 3.

A, S100 expression in the tumor cells (original magnification, x126). **B**, Some tumor cells express Melan A protein (original magnification, x126). **C**, Photomicrograph showing collagen IV decoration of a delicate fibrous network around isolated cells and small clusters of spindle cells (original magnification, x126). **D**, CD68 expression in cells with foamy cytoplasm (original magnification, x126).

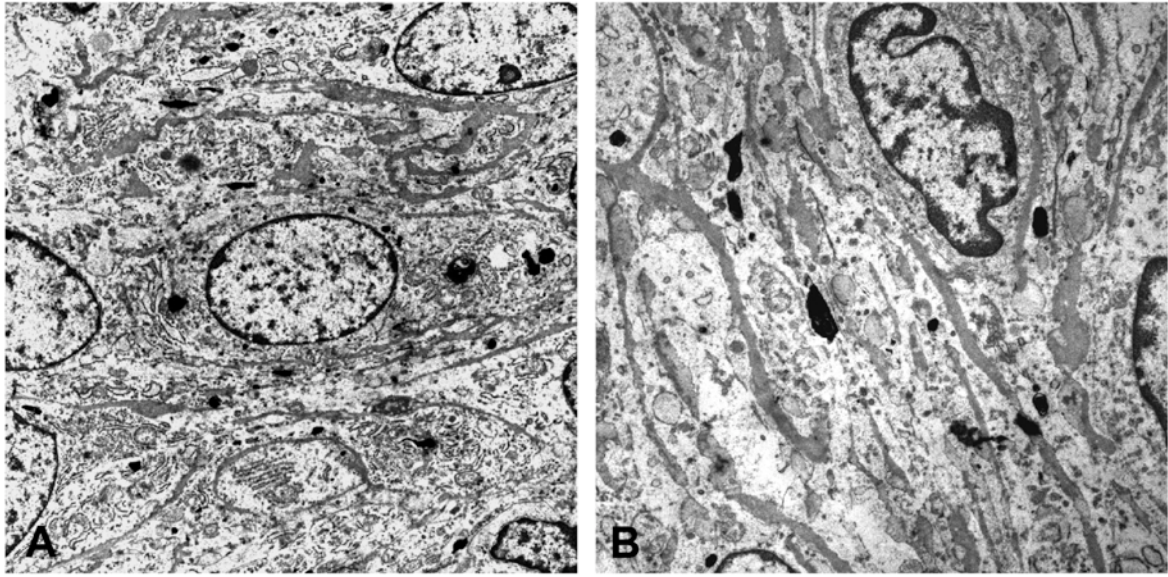


Figure 6.

A, Transmission electronic microscopy microphotograph demonstrating multiple interdigitating cell processes as well as thickened basement membrane material around the cells (original magnification, x 7200). **B,** Microphotograph showing thickened basement membrane material around the cells and stage 4 melanosomes (original magnification, x9700).

Table 1.Primers for polymerase chain reaction amplification of *PTEN* exons.

Targeted Exon	Sense primer	Antisense primer	Annealing temperature (°C)	Amplification product (bp)
Exon 1	GCAGCTTCTGCCATCTCTCT	CATCCGTCTACTCCCACGTT	60	200
Exon 2	GTTTGATTGCTGCATATTCAGAT	TGAAATAGAAAATCAAAGCATTCT	58	163
Exon 3	TTAATGGTGGCTTTTTGTTTGT	CTCTACCTCACTCTAACAAGCAGA	58	168
Exon 4	CTAAGTGCAAAAGATAAAGTTATATCA	ACAACATAGTACAGTACATTCATACCTAC	54	120
Exon 5 (I°)	CCTATTCTGAGGTATCTTTTTACCACA	ACACCAGTTCGTCCCTTTCCA	60	174
Exon 5 (II°)	GCTGGAAAGGGACGAACTGG	TCCAGGAAGAGGAAAGGAAAAAC	65	155
Exon 6	TGGCTACGACCCAGTTACCATAGCA	TGCAAGTCCGCCACTGAACA	54	235
Exon 7 (I°)	TACTGGTATGTATTTAACCATGCAG	ACACACAGGTAACGGCTGAG	58	139
Exon 7 (II°)	AGCCGTTACCTGTGTGGTGA	TGCCAGAGTAAGCAAAACACCTGC	65	200
Exon 8 (I°)	GTCATTCATTCTTTTTCTTTCT	CTGCACGCTCTATACTGCAAATG	60	169
Exon 8 (II°)	ACCAGGACCAGAGGAAACCT	ACAAGTCAACAACCCCAACA	60	227
Exon 9 (I°)	AGATGAGTCATATTTGTGGG	ATGATCAGGTTTCATTGTCAC	54	148
Exon 9 (II°)	CATCAACTTCTGTAACAC	ATGGTGTTTTATCCCTCTTG	51	165

bp: base pair.

Table 2.Redesigned primers for polymerase chain reaction amplification of *NF2* exons.

Targeted Exon	Sense primer	Antisense primer	Annealing temperature (°C)	Amplification product (bp)
Exon 2	TGTCCTTCCCCATTGGTTTG	CAGTTTCATCGAGTTCTAGCC	60	180
Exon 3	GGGTAGCACAGGAGGAAGTG	AACTCTGCAACCACTCCTGG	60	245
Exon 4	ATCAGCCTACACACCTCACT	ACCCAAATTAACGCCAGGA	60	194
Exon 5	AGAATCTCAATCGCCTGCTC	GATCCCACACTGTTTACTGG	58	254
Exon 6	TGTGACTATCTCCCTGGGT	CCAGCTCTCCCCTTTTCTT	58	358
Exon 11	CTTTGGGCCCTTGTGGCAC	-	60	268
Exon 12	CCATCTCAGTGTTCAAGGCA	CAGTCACCATCAGCCAAGGA	60	448
Exon 14	GTGCCCATTCCTCTGTG	-	60	253

Table 3.Primers for *PTEN*, *NF2* and 18S cDNA amplification.

Targeted sequence	Sense primer	Antisense primer	Annealing temperature (°C)	Amplification product (bp)
PTEN	TGAAGGCGTATACAGGAACAAT	CGGTGTCATAATGTCTTTCAGC	60	110
NF2	CGCCCATGAACCAATTC	GGCTGTCACCAATGAGGTTGA	60	70
18S	CGGCTACCACATCCAAGGAA	GCTGGAATTACCGCGGCT	60	187

Discussion

The focus of my thesis was to better understand the molecular mechanisms that are involved in the pathogenesis of retinitis pigmentosa (RP), one of the most common forms of inherited retinal degeneration. The most interesting aspect of this disease is certainly its wide heterogeneity both at the clinical and genetic level, which is not only due to different mutations in different genes, but also to different effects of the same mutation in different individuals, sometimes even within the same family.

In families with *PRPF31* mutations we often observe the presence of asymptomatic individuals who, despite being carriers of the mutation, do not develop any symptoms of the disease, even at a later age [1-4]. The vast majority of *PRPF31* mutations reported to date result in the degradation of the mutated allele by nonsense-mediated mRNA decay, suggesting that haploinsufficiency can explain the pathophysiological mechanism of the disease [5-8]. Asymptomatic individuals in *PRPF31* families have a higher amount of *PRPF31* wild type transcript with respect to their affected siblings, suggesting that this could prevent them from developing symptoms [9-10].

Penetrance of *PRPF31* mutations is known to be modulated by at least two penetrance factors, located on chromosome 19 in proximity of *PRPF31* itself and on chromosome 14, respectively [11-12]. They are most likely diffusible factors that act simultaneously on the transcription of both *PRPF31* alleles [12].

We identified the modifier of *PRPF31* penetrance located on chromosome 19q13.4 in a large family with several affected and asymptomatic sibships. The gene, *CNOT3*, has an inverse trend of expression with respect to that of *PRPF31*, being expressed poorly in asymptomatic compared to affected members of the same family [13]. Inhibition of *CNOT3* expression *in vitro* leads to increased *PRPF31* expression, suggesting that *CNOT3* may behave as a negative regulator of *PRPF31* expression [13]. Transcriptional regulation of *PRPF31* expression is mediated by the direct binding of *CNOT3* to the experimentally validated *PRPF31* promoter sequence [13]. Furthermore, polymorphic alleles on *CNOT3* genomic region (i.e. rs4806718) can explain the manifestation of the disease in three families with different *PRPF31* mutations, even if the association between rs4806718's C allele and the disease is not perfect [13] (Venturini, unpublished results). The not perfect genotype-phenotype correlation for the alleles on chromosome 19 was expected, since previous studies showed that they could not explain the manifestation of the disease

in all siblings of *PRPF31* families [11], and at least another factor on chromosome 14 should be involved in the regulation of *PRPF31* penetrance [12].

A link between rs4806718 alleles and *CNOT3* differential expression needs still to be proven with some functional evidences. However, given the presence of this SNP in a non-coding genomic region, it will not be straightforward.

Functional *PRPF31* promoter polymorphisms have been also investigated by others, but no association could be found to explain the variability in *PRPF31* expression [14].

The most likely scenario is that *PRPF31* expression level would be determined by several functional polymorphisms within the 19q13.4 region that may act in a cooperative manner.

CNOT3 involvement in the modulation of the penetrance of *PRPF31* mutations does not seem to be a mechanism refined to a single family, but to at least two other families with different *PRPF31* mutations (Venturini, unpublished results).

In all families we studied asymptomatic individuals have an increased expression not only of *PRPF31*, but also of all other splicing factors that we tested (Venturini, unpublished results). This is in agreement with the observation that *CNOT3* inhibition *in vitro* leads to a tendency of other splicing factors to be more highly expressed, although the most obvious effect is on *PRPF31* expression (Venturini, unpublished results). Our hypothesis is that there may be a direct effect of *CNOT3* only on *PRPF31* expression and what we observe at the level of other splicing factors is a stoichiometric response to the increased expression of one of the spliceosome components.

Overall, *PRPF31*-linked retinitis pigmentosa seems to be more complex than expected, since clinical manifestations would depend on several genetic interactions that would modulate the effect of *PRPF31* mutation.

Much remains to be assessed to fully understand the mechanisms that regulate *PRPF31* penetrance; our data show that *CNOT3* is the modifier on chromosome 19 of *PRPF31* penetrance, but other modifiers, including the one that lies on chromosome 14, should be considered.

Despite penetrance being a well-known concept in genetics, not much has been discovered about the molecular mechanisms that underlie incomplete penetrance in inherited human diseases; our research is one of the few examples in which a penetrance factor could be identified and its mechanism of action characterized.

Since haploinsufficiency is the cause of the disease in most *PRPF31* families, restoring the normal level of *PRPF31* transcript by subretinal injection of *PRPF31* wild-type cDNA could represent a promising therapeutic approach. Although we showed that *PRPF31* expression can be increased by inhibiting *CNOT3* expression, little has been so far elucidated on the overall effects of *CNOT3*

inhibition in human cells and tissues, thus further studies are required before thinking of a possible CNOT3-targeted therapeutic approach.

Following the same rationale of investigating molecular mechanisms that are responsible for clinical and genetic heterogeneity of retinitis pigmentosa, I have been studying a recessive form of the disease, where mutations in the same gene give rise to variable clinical manifestations. *FAM161A* mutations were recently identified in patients with recessive retinitis pigmentosa [15-16]. All reported mutations lead to loss-of-function of the encoded protein, but clinical manifestations of the disease may vary widely depending on the mutation. Patients with *FAM161A* mutations have been described as having a late-onset form of RP, described in a German cohort of patients [16], and an early-onset manifestation of the disease in Israeli and Palestinian individuals [15].

Prevalence of *FAM161A*-linked recessive RP is also different in individuals from different ethnicities, being in the German population comparable to the prevalence of most arRP genes [16], while, in the Israeli and Palestinian populations, *FAM161A* is the most frequently mutated gene in patients with arRP [15].

In a large cohort of North American arRP patients with mixed ethnicity, we found a prevalence of *FAM161A* mutations similar to that detected in Germany (<2%). Interestingly, one variant that had previously been reported as a founder mutation in the Israeli and Palestinian population (p.T452Sfx3) [15] is the only mutation that was found in patients from our cohort, and all except one of them reported Jewish ancestry.

Furthermore, from our study it emerged that there are many rare variants in *FAM161A*, which are reported in dbSNP with a minor allele frequency of less than 1%, that are frequently found in patients but not in controls, whose functional meaning is uncertain. In particular one of those variants (p.L378R), which is predicted to have a deleterious effect on the encoded protein and is affecting a highly conserved amino acid residue, has been frequently found in a heterozygous state in arRP patients both from our cohort and from the German one.

Growing evidences are highlighting that retinitis pigmentosa could be considered as an oligogenic disease in which several variants summed to the disease-causing mutation can modulate the phenotype of the disease. It would be interesting to see whether *FAM161A* p.L378R variant may behave as a modifier of recessive forms of retinitis pigmentosa; to investigate this hypothesis we are performing whole exome sequencing of all patients that harbour this variant in order to see if it would be frequently associated with other variants and if the phenotype within a family may be influenced by the presence of this variant.

In the last years there have been a rapid decrease in the cost of massively parallel sequencing together with an improvement of sequencing technologies, which enable today to interrogate the entire exome and even individual's genomes.

Exome sequencing is the most commonly used approach to unravel the genetic causes of inherited Mendelian diseases, as the costs of sequencing are contained and the information obtained correspond only to the coding fraction of the genome that is more easily interpretable.

On the other hand, it is increasingly evident in diseases such as retinitis pigmentosa that individuals in which we were unable to identify the genetic cause of the disease with standard diagnostic techniques and even with exome sequencing may harbour large structural rearrangements and/or variations in non-coding sequences of the genome.

Whole genome sequencing has the advantage, with respect to whole exome sequencing, of providing an overview of all variants and structural rearrangements in coding and non-coding portions of the genome, leading, nevertheless, to a huge increase in the amount of data to analyze, whose interpretability is not always easy.

Our experience with whole genome sequencing of unrelated patients with recessive retinitis pigmentosa shows that this approach can be effective in identifying disease-causing variants that might have otherwise failed to be detected with other screening methods (i.e. structural rearrangements larger than 1 kb) and that, starting from millions of variants per individual, we can get to a short list of candidates to be analysed.

The final goal, after having potentially identified a disease-causing variant, would be to prove at the functional level that the change is indeed responsible for the phenotype.

To test variations in genes with a tissue-specific expression it would be ideal to have access to the tissue where the disease develops. To date, blood is the most commonly used tissue from RP patients, because obviously we cannot have access to the retina of patients who are still alive.

The generation of induced pluripotent stem cells (iPSCs) from somatic human cells has opened the possibility to differentiate them into a wide range of tissue-specific lineages. Fibroblast-derived iPSCs have been already differentiated into photoreceptor and RPE cells and iPSCs have been also obtained from EBV-immortalised B-lymphocytes, or alternatively CD34+ blood cells [17-20].

A successful example of the advantage of differentiating retinal cells from fibroblast-derived iPSCs to functionally prove the effect of a mutation is represented by an Alu-element insertion in the gene *MAK*, which was found in a patient with recessive retinitis pigmentosa. In the retinal-like cells the mutation was in fact proven to prevent a retina-specific isoform to be expressed [21].

The same mutation, which was first identified in a patient with Jewish ancestry [21], was lately found in several other individuals with recessive RP who reported Jewish origin [22] (Venturini,

unpublished results); interestingly, all the ones we identified in our cohort share a common haplotype, suggestive of a founder mutation in the Jewish population. Since the majority of North American Jews belong to the Ashkenazi subpopulation, we are aiming to identify an Ashkenazi-specific haplotype in patients harbouring the mutation. If we could establish with certainty that the mutation is present only in Ashkenazi Jews with such a high prevalence this would be of clinical relevance to implement Ashkenazi carrier screening panels.

Finally, as a side project, I have been studying a rare form of cancer developed in the choroid of a young girl affected by PTEN hamartoma tumor syndrome, a genetic disorder caused by germline mutations of the tumor suppressor gene *PTEN*. For the first time we reported a choroidal tumor among the clinical manifestations of PHTS, which was made by glial cells of the peripheral nervous tissue [23].

Furthermore, this tumor showed a unique combination of PTEN reduction and NF2 absence [23], which is interesting considering that both proteins have been shown to be involved in the regulation of mTOR signalling pathway in human cancers [24]. This study has therefore highlighted the heterogeneity of this choroidal tumor, showing that genetic and/or epigenetic alterations in different genes may contribute to the tumor development and growth.

Overall, the work done during my thesis has helped to shed light on new molecular mechanisms that are involved in the pathogenesis of a common form of inherited retinal degeneration and of a rare tumor of the choroid and opens the perspective for further studies with the ultimate goal of developing molecular-targeted therapies.

References

1. Berson, E.L., et al., *Dominant retinitis pigmentosa with reduced penetrance*. Arch Ophthalmol, 1969. **81**(2): p. 226-34.
2. Berson, E.L. and E.A. Simonoff, *Dominant retinitis pigmentosa with reduced penetrance. Further studies of the electroretinogram*. Arch Ophthalmol, 1979. **97**(7): p. 1286-91.
3. Moore, A.T., et al., *Autosomal-Dominant Retinitis-Pigmentosa with Apparent Incomplete Penetrance - a Clinical, Electrophysiological, Psychophysical, and Molecular-Genetic Study*. British Journal of Ophthalmology, 1993. **77**(8): p. 473-479.
4. Jay, M., et al., *Nine generations of a family with autosomal dominant retinitis pigmentosa and evidence of variable expressivity from census records*. J Med Genet, 1992. **29**(12): p. 906-10.
5. Rio Frio, T., et al., *Premature termination codons in PRPF31 cause retinitis pigmentosa via haploinsufficiency due to nonsense-mediated mRNA decay*. J Clin Invest, 2008. **118**(4): p. 1519-31.
6. Audo, I., et al., *Prevalence and novelty of PRPF31 mutations in French autosomal dominant rod-cone dystrophy patients and a review of published reports*. BMC Med Genet, 2010. **11**: p. 145.
7. Sullivan, L.S., et al., *Genomic rearrangements of the PRPF31 gene account for 2.5% of autosomal dominant retinitis pigmentosa*. Invest Ophthalmol Vis Sci, 2006. **47**(10): p. 4579-88.
8. Abu-Safieh, L., et al., *A large deletion in the adRP gene PRPF31: evidence that haploinsufficiency is the cause of disease*. Mol Vis, 2006. **12**: p. 384-8.
9. Rivolta, C., et al., *Variation in retinitis pigmentosa-11 (PRPF31 or RP11) gene expression between symptomatic and asymptomatic patients with dominant RP11 mutations*. Hum Mutat, 2006. **27**(7): p. 644-53.
10. Vithana, E.N., et al., *Expression of PRPF31 mRNA in patients with autosomal dominant retinitis pigmentosa: a molecular clue for incomplete penetrance?* Invest Ophthalmol Vis Sci, 2003. **44**(10): p. 4204-9.
11. McGee, T.L., et al., *Evidence that the penetrance of mutations at the RP11 locus causing dominant retinitis pigmentosa is influenced by a gene linked to the homologous RP11 allele*. Am J Hum Genet, 1997. **61**(5): p. 1059-66.
12. Rio Frio, T., et al., *Two trans-acting eQTLs modulate the penetrance of PRPF31 mutations*. Hum Mol Genet, 2008. **17**(20): p. 3154-65.
13. Venturini, G., et al., *CNOT3 is a modifier of PRPF31 mutations in retinitis pigmentosa with incomplete penetrance*. PLoS Genet, 2012. **8**(11): p. e1003040.
14. Rose, A.M., et al., *Expression of PRPF31 and TFPT: regulation in health and retinal disease*. Hum Mol Genet, 2012. **21**(18): p. 4126-37.
15. Bandah-Rozenfeld, D., et al., *Homozygosity mapping reveals null mutations in FAM161A as a cause of autosomal-recessive retinitis pigmentosa*. Am J Hum Genet, 2010. **87**(3): p. 382-91.
16. Langmann, T., et al., *Nonsense mutations in FAM161A cause RP28-associated recessive retinitis pigmentosa*. Am J Hum Genet, 2010. **87**(3): p. 376-81.
17. Mellough, C.B., et al., *Efficient stage-specific differentiation of human pluripotent stem cells toward retinal photoreceptor cells*. Stem Cells, 2012. **30**(4): p. 673-86.
18. Choi, S.M., et al., *Reprogramming of EBV-immortalized B-lymphocyte cell lines into induced pluripotent stem cells*. Blood, 2011. **118**(7): p. 1801-5.
19. Carr, A.J., et al., *Protective effects of human iPS-derived retinal pigment epithelium cell transplantation in the retinal dystrophic rat*. PLoS One, 2009. **4**(12): p. e8152.

20. Mack, A.A., et al., *Generation of induced pluripotent stem cells from CD34+ cells across blood drawn from multiple donors with non-integrating episomal vectors*. PLoS One, 2011. **6**(11): p. e27956.
21. Tucker, B.A., et al., *Exome sequencing and analysis of induced pluripotent stem cells identify the cilia-related gene male germ cell-associated kinase (MAK) as a cause of retinitis pigmentosa*. Proc Natl Acad Sci U S A, 2011. **108**(34): p. E569-76.
22. Stone, E.M., et al., *Autosomal recessive retinitis pigmentosa caused by mutations in the MAK gene*. Invest Ophthalmol Vis Sci, 2011. **52**(13): p. 9665-73.
23. Venturini, G., et al., *Clinicopathologic and molecular analysis of a choroidal pigmented schwannoma in the context of a PTEN hamartoma tumor syndrome*. Ophthalmology, 2012. **119**(4): p. 857-64.
24. Menon, S. and B.D. Manning, *Common corruption of the mTOR signaling network in human tumors*. Oncogene, 2008. **27 Suppl 2**: p. S43-51.

Other collaborations

1. Rose A.M., Shah A.Z., **Venturini G.**, Rivolta C., Bhattacharya S.S.
Dominant *PRPF31* mutations are hypostatic to a recessive *CNOT3* polymorphism in retinitis pigmentosa.
Submitted to *Annals of Human Genetics*.
2. **Venturini G.**, Moulin A.P.
PTEN involvement in eye embryology and pathology.
Book chapter accepted for publication by *Nova Science Publishers*.
3. Nishiguchi K.M., Tearle R.G., Yangfan L., Oh E.C., Miyake N., Benaglio P., Harper S., Koskiniemi H., **Venturini G.**, the European Retinal Disease Consortium, Nakamura M., Mineo K., Ueno S., Yasuma T., Beckmann J.S., Ikegawa S., Matsumoto N., Terasaki H., Berson E.L., Katsanis N. and Rivolta C.
Whole genome sequencing in 16 unrelated patients with retinitis pigmentosa identifies pathogenic DNA structural rearrangements and *NEK2* as a novel disease gene.
Submitted to *PNAS*.
4. Azzedine H., Zavadakova P., Planté-Bordeneuve V., Vaz Patto M., Pinto N., Bartesaghi L., Zenker J., Poirot O., Bernard-Marissal N., Arnaud E., Cartoni R., Title A., **Venturini G.**, Médard J.J., Schöls L., Claeys K., Stendel C., Roos A., Weis J., Dubourg O., Leal Loureiro J., Stevanin G., Said G., Amato A., Baraban J., LeGuern E., Senderek J., Rivolta C. and Chrast R.
PLEKHG5 deficiency leads to an intermediate form of autosomal recessive Charcot-Marie-Tooth disease.
Published in *Human Molecular Genetics*, 17 June 2013.

Abbreviations

Ab	Antibody
ACTB	Beta-actin
adRP	Autosomal dominant retinitis pigmentosa
AF	Affected individuals
AJ	Ashkenazi Jews
AMD	Age-related macular degeneration
ARPE-19	Human retinal pigment epithelial cell line
arRP	Autosomal recessive retinitis pigmentosa
AS	Asymptomatic individuals
BCA	Bicinchoninic acid
bFGF	Basic fibroblast-derived growth factor
bp	Base pair
BRR2	Small nuclear ribonucleoprotein 200kDa (U5)
BSA	Bovine serum albumin
cDNA	Complementary DNA
CEPH	Centre d'etude du polymorphisme humain
cGMP	Cyclic guanosine monophosphate
ChIP	Chromatin immunoprecipitation
CLRN1	Clarin-1
CNOT2	CCR4-NOT Transcription Complex, Subunit 2
CNOT3	CCR4-NOT Transcription Complex, Subunit 3
CNTF	Ciliary neurotrophic factor
CRX	Cone-rod homeobox protein
DA	Dark adaptation
dbSNP	Short genetic variations database
del	Deletion
DHA	Docosahezaenoic acid
DHDDS	Dehydrodolichyl diphosphate synthase
DHFR	Dihydrofolate reductase
DMSO	Dimethyl sulfoxide
DNA	Deoxyribonucleic acid
DNase	Deoxyribonuclease
dNTP	Deoxyribonucleotide triphosphate
e.g.	Exempli gratia
EBV	Epstein Barr virus
EDTA	Ethylenediaminetetraacetic acid
ERG	Electroretinogram
EST	Expressed sequence tag
EYS	Eyes shut homolog (Drosophila)
FAM161A	Family with sequence similarity 161, member A
FECH	Ferrochelatase

FFPE	Formalin-fixed paraffin-embedded
GAPDH	Glyceraldehyde 3-phosphate dehydrogenase
GCL	Ganglion cell layer
HRP	Horseradish peroxidase
hrs	Hours
Hz	Hertz
i.e.	Id est
IBD	Identical by descent
IgG	Immunoglobulin G
ILT7	Leukocyte immunoglobulin-like receptor subfamily A member 4
INL	Inner nuclear layer
IP	Immunoprecipitation
IPL	Inner plexiform layer
ipRGCs	Intrinsically photosensitive retinal ganglion cells
iPSCs	Induced pluripotent stem cells
IRB	Institutional review board
IU	International units
kb	Kilobase
kDa	Kilodalton
LCA	Leber congenital amaurosis
LCL	Lymphoblastoid cell line
LCR	Leukocyte receptor cluster
LENG1	Leukocyte receptor cluster, member 1
LILRB3	Leukocyte immunoglobulin-like receptor, subfamily B, member 3
LOH	Loss of heterozygosity
MAF	Minor allele frequency
MAK	Male germ cell-associated kinase
Mb	Megabase
MBOAT7	Membrane bound O-acyltransferase domain containing 7
MDH1	Malate dehydrogenase 1, NAD
miRNA	microRNA
ml	Milliliter
mRNA	Messenger RNA
mTOR	Mammalian target of rapamycin
mV	Millivolt
μl	Microliter
μM	Micromolar
μV	Microvolt
NA	Not available
NALP2	NLR family, pyrin domain containing 2
NCBI	National center for biotechnology information
NDUFA3	NADH dehydrogenase (ubiquinone) 1 alpha subcomplex, 3
NF2	Neurofibromin 2
NFL	Nerve fiber layer
ng	Nanogram

NGS	Next generation sequencing
nM	Nanomolar
NMD	Nonsense mediated mRNA decay
nmol	Nanomole
NRL	Neural retina-specific leucine zipper protein
OD	Oculus dexter
ONL	Outer nuclear layer
OPL	Outer plexiform layer
OS	Oculus sinister
PAP-1	Retinitis pigmentosa 9 (autosomal dominant)
PBS	Phosphate buffered saline
PCDH15	Protocadherin-15
PCR	Polymerase chain reaction
PHTS	PTEN hamartoma tumor syndrome
pmol	Picomole
pre-mRNA	Precursor mRNA
PRPF3	PRP3 pre-mRNA processing factor 3 homolog (S. Cerevisiae)
PRPF31	PRP31 pre-mRNA processing factor 31 homolog (S. Cerevisiae)
PRPF6	PRP6 pre-mRNA processing factor 6 homolog (S. Cerevisiae)
PRPF8	PRP8 pre-mRNA processing factor 8 homolog (S. Cerevisiae)
PTEN	Phosphatase and tensin homolog
qPCR	Quantitative real time polymerase chain reaction
RACE	Rapid amplification of cDNA ends
RDS	Peripherin
RetNet	Retinal information network
RHO	Rhodopsin
RIPA	Radio immuno precipitation assay
RNA	Ribonucleic acid
RNAi	RNA interference
RNase	Ribonuclease
ROM1	Rod outer segment membrane protein 1
RP	Retinitis pigmentosa
RP1	Retinitis Pigmentosa 1 (Autosomal Dominant)
RPE	Retinal pigment epithelium
RPE65	Retinal pigment epithelium-specific 65 kDa protein
RPGR	X-linked retinitis pigmentosa GTPase regulator
RPMI	Roswell Park Memorial Institute
RPS9	40S ribosomal protein S9
RT-PCR	Reverse transcription polymerase chain reaction
SDS-PAGE	Sodium dodecyl sulphate - polyacrylamide gel electrophoresis
siRNA	Small interfering RNA
SNP	Single-nucleotide polymorphism
snRNP	Small nuclear ribonuclear particles
SPATA7	Spermatogenesis associated 7
SPTA1	Spectrin

TFPT	TCF3 (E2A) Fusion Partner (In Childhood Leukemia)
TBS	Tris-buffered saline
TE	Tris-EDTA
TSEN34	tRNA splicing endonuclease 34 homolog (<i>S. Cerevisiae</i>)
U snRNA	Small nuclear uridine-rich RNA
U.S.	United States
USH2A	Usherin
UTR	Untranslated region
WES	Whole exome sequencing
WGS	Whole genome sequencing

